

DECENTRALIZED CONTROL OF NETWORKS OF UNCERTAIN DYNAMICAL
SYSTEMS

By

JUSTIN RICHARD KLOTZ

A DISSERTATION PRESENTED TO THE GRADUATE SCHOOL
OF THE UNIVERSITY OF FLORIDA IN PARTIAL FULFILLMENT
OF THE REQUIREMENTS FOR THE DEGREE OF
DOCTOR OF PHILOSOPHY

UNIVERSITY OF FLORIDA

2015

© 2015 Justin Richard Klotz

To my parents, *Rick* and *Karen*, my sister, *Heather*, and my friends, for their boundless support and encouragement

ACKNOWLEDGMENTS

I would like to express my sincere gratitude to Dr. Warren E. Dixon, whose advice and motivation were essential to my academic success. As my advisor, he has guided my research and encouraged the creativity that helped shape this dissertation. As a mentor, he has helped me choose the direction of my career and develop professionally. I would also like to extend gratitude to my committee members Dr. Prabir Barooah, Dr. Carl Crane, and Dr. John Shea for their valuable recommendations and insights. I am also thankful to my family and friends for their enduring support and to my coworkers in the Nonlinear Controls and Robotics laboratory for our fruitful collaboration.

TABLE OF CONTENTS

	<u>page</u>
ACKNOWLEDGMENTS	4
LIST OF TABLES	8
LIST OF FIGURES	9
LIST OF ABBREVIATIONS	11
ABSTRACT	12
CHAPTER	
1 INTRODUCTION	14
1.1 Motivation	14
1.2 Literature Review	18
1.3 Contributions	22
1.4 Preliminaries	25
2 ASYMPTOTIC SYNCHRONIZATION OF A LEADER-FOLLOWER NETWORK SUBJECT TO UNCERTAIN DISTURBANCES	26
2.1 Problem Formulation	26
2.1.1 Dynamic Models and Properties	26
2.1.2 Control Objective	28
2.2 Controller Development	30
2.3 Convergence Analysis	33
2.4 Simulation	38
2.5 Extension to Formation Control	43
2.5.1 Modified Error Signal	43
2.5.2 Simulation	44
2.6 Concluding Remarks	49
3 ROBUST CONTAINMENT CONTROL IN A LEADER-FOLLOWER NETWORK OF UNCERTAIN EULER-LAGRANGE SYSTEMS	50
3.1 Problem Formulation	50
3.1.1 Notation for a Multi-Leader Network	50
3.1.2 Dynamic Models and Properties	51
3.1.3 Control Objective	53
3.2 Controller Development	54
3.3 Convergence Analysis	58
3.4 Simulation	63
3.5 Concluding Remarks	67

4	SYNCHRONIZATION OF UNCERTAIN EULER-LAGRANGE SYSTEMS WITH UNCERTAIN TIME-VARYING COMMUNICATION DELAYS	68
4.1	Problem Formulation	69
4.1.1	Dynamic Models and Properties	69
4.1.2	Control Objective	71
4.2	Controller Development	71
4.2.1	Communication-Delayed Control	71
4.2.2	Motivating Example	73
4.3	Closed-loop Error System	75
4.4	Convergence Analysis	78
4.5	Simulation	91
4.6	Concluding Remarks	96
5	DECENTRALIZED SYNCHRONIZATION OF UNCERTAIN NONLINEAR SYSTEMS WITH A REPUTATION ALGORITHM	98
5.1	Problem Formulation	98
5.1.1	Network Properties	98
5.1.2	Dynamic Models and Properties	99
5.1.3	Neighbor Communication and Sensing	100
5.1.4	Control Objective	101
5.2	Controller Development	101
5.2.1	Error System	101
5.2.2	Decentralized Controller	102
5.2.3	Reputation Algorithm	102
5.2.4	Edge Weight Updates	104
5.3	Closed-loop Error System	105
5.4	Convergence Analysis	107
5.5	Satisfaction of Sufficient Conditions	112
5.5.1	A Lower Bound on the Solution of the CALE	112
5.5.2	An Upper Bound on the Solution of the CALE	113
5.5.3	Computation of Sufficient Conditions	115
5.6	Simulation	116
5.7	Concluding Remarks	122
6	CONCLUSIONS AND FUTURE WORK	124
6.1	Conclusions	124
6.2	Future Work	127
APPENDIX		
A	Proof that P is Nonnegative (CH 2)	129
B	Proof of Supporting Lemma (CH 3)	131
C	Demonstration of Supporting Inequality (CH 4)	132

D	Demonstration of Reputation Bound (CH 5)	134
E	Proof of Supporting Lemma (CH 5)	135
F	Proof of Supporting Lemma (CH 5)	137
	REFERENCES	138
	BIOGRAPHICAL SKETCH	145

LIST OF TABLES

<u>Table</u>	<u>page</u>
2-1 Simulation parameters.	41
2-2 Controller performance comparison.	43
2-3 Disturbance and formation position parameters.	48
3-1 Leader initial positions in surge (x), sway (y), and heave (z).	64
3-2 Follower initial positions in surge (x), sway (y), and heave (z).	65
4-1 Disturbance parameters.	92
4-2 Communication delay and delay estimate parameters for each communication link.	93
4-3 Tuned gains and associated costs for (a) feedback without self-delay, (b) only feedback with self-delay, and (c) a mixture of feedback with self-delay and without self-delay.	94
5-1 Parameters in dynamics.	119
5-2 Steady-state RMS leader-tracking performance.	119

LIST OF FIGURES

<u>Figure</u>	<u>page</u>
2-1 Network communication topology.	40
2-2 Joint 1 leader-tracking error using (a) [1], (b) [2, Section IV], and (c) the proposed controller.	41
2-3 Joint 2 leader-tracking error using (a) [1], (b) [2, Section IV], and (c) the proposed controller.	42
2-4 Joint 1 control effort using (a) [1], (b) [2, Section IV], and (c) the proposed controller.	42
2-5 Joint 2 control effort using (a) [1], (b) [2, Section IV], and (c) the proposed controller.	43
2-6 Network communication topology.	47
2-7 Agent trajectories in surge and sway.	48
2-8 Error in convergence to the formation positions in the dimensions surge, sway and yaw.	49
3-1 Network communication topology of leader (“L”) and follower (“F”) AUVs.	64
3-2 [Top view] Follower AUV trajectories in the surge (x) and sway (y) dimensions.	65
3-3 [Front view] Follower AUV trajectories in the surge (x) and heave (z) dimensions.	66
3-4 Euclidean norms of the follower AUV control efforts.	66
4-1 Network communication topology.	74
4-2 Leader-tracking error under communication-delayed control using (a) only feedback without self-delay, (b) only feedback with exact self-delay, and (c) only feedback with inexact self-delay.	75
4-3 Network communication topology.	92
4-4 Leader-tracking error under communication-delayed closed-loop control using only feedback without self-delay ($\kappa_1 = 1, \kappa_2 = 0$).	95
4-5 Leader-tracking error under communication-delayed closed-loop control using only feedback with self-delay ($\kappa_1 = 0, \kappa_2 = 1$).	95
4-6 Leader-tracking error under communication-delayed closed-loop control using a mixture of feedback without self-delay and feedback with inexact self-delay ($\kappa_1 = 0.69, \kappa_2 = 0.31$).	96

5-1	Network communication topology.	119
5-2	Leader-tracking error.	120
5-3	Trust measurements.	120
5-4	Neighbor reputations.	121
5-5	Dynamically updated consensus (adjacency) weights.	121
5-6	Neighbor reputations produced by the alternative reputation algorithm in (5–21).122	

LIST OF ABBREVIATIONS

a.e.	almost everywhere
AUV	autonomous underwater vehicle
CALE	continuous algebraic Lyapunov Equation
IMU	inertial measurement unit
LK	Lyapunov-Krasovskii
LOS	line-of-sight
PD	proportional-derivative
RHS	right-hand side
RISE	Robust Integral of the Sign of the Error
RMS	root-mean-square
SLAM	simultaneous localization and mapping
UAV	unmanned aerial vehicle
UUB	uniformly ultimately bounded

Abstract of Dissertation Presented to the Graduate School
of the University of Florida in Partial Fulfillment of the
Requirements for the Degree of Doctor of Philosophy

DECENTRALIZED CONTROL OF NETWORKS OF UNCERTAIN DYNAMICAL
SYSTEMS

By

Justin Richard Klotz

May 2015

Chair: Warren E. Dixon

Major: Mechanical Engineering

Multi-agent networks, such as teams of robotic systems, benefit from the ability to interact and sense the environment in a collaborative manner. Networks containing agents operating under decentralized control policies, wherein only information from neighboring agents is used to internally make decisions, benefit from autonomy: each agent is encoded with a local objective and has no need to maintain contact with a network coordinator. Such an interaction structure reduces the communication bandwidth and the associated computational requirements in comparison to centralized control schemes, wherein a single network coordinator computes a control policy for each agent based on communicated information. However, the development of decentralized control policies should address the deleterious effects accompanied by the decentralized network structure, such as cascading effects caused by exogenous disturbances, model uncertainty, communication delays, and reduced situational awareness.

Chapter 1 motivates the current challenges in the field of decentralized control, provides a comprehensive review of relevant literature, and discusses the contributions of this dissertation. Chapter 2 details the development of a novel, decentralized control policy which provides asymptotic convergence of the states of a leader-follower network of autonomous agents despite the effects of uncertain nonlinear dynamics and unknown

exogenous disturbances. This robust control structure is extended in Chapter 3 for containment control, a strategy which uses multiple leaders to guide a group of autonomous agents. Chapter 4 investigates the effects of communication delay in the decentralized leader-follower framework and develops a novel decentralized controller which uses estimates of the heterogeneous, time-varying communication delays to mitigate the effects of the delay and provide more robust stability criteria. Chapter 5 investigates the issue of reduced situational awareness by considering a scenario in which communication is unreliable. A novel, reputation-based decentralized controller is developed which prioritizes feedback from network neighbors based on past communication integrity. Sufficient conditions for the successful completion of the control objective are given in each chapter to facilitate the implementation of the developed control strategies.

CHAPTER 1 INTRODUCTION

1.1 Motivation

Decentralized control refers to the cooperation of multiple agents in a network to accomplish a collective task. Instead of a single control system performing a task, multiple potentially lower cost systems can be coordinated to achieve a network-wide goal. The networked agents generally represent autonomous robotic systems, such as mobile ground robots, unmanned aerial vehicles (UAVs), autonomous underwater vehicles (AUVs), and spacecraft, and interact via communication and/or sensing. Some applications of decentralized control are cooperative target tracking, cooperative surveillance, search-and-rescue missions, collective satellite interferometry, coordinated control of infrastructure systems, industrial process control, highway automation, and flying in formation to reduce drag (cf. [3–6]).

Compared to centralized control, in which a central agent communicates with all other systems to compute control policies, decentralized control is characterized by local interactions, in which agents autonomously coordinate with only a subset of the network to accomplish a network-wide task. The distribution of control policy generation yields the benefits of mitigated computational and bandwidth demand, robustness to communication link failure, greater flexibility, and robustness to unexpected agent failure. However, decentralized control suffers from a greater vulnerability to deleterious phenomena, such as disturbances in agent dynamics, communication delay, and imperfect communication, the effects of which can cascade through a network and cause mission performance degradation or failure. In addition, as opposed to centralized control, in which a central agent can vet any agent in comparison with the rest of the network, decentralized control exhibits less situational awareness in the sense that an agent is only exposed to the actions of its neighbors. Thus, there are fewer ways to vet communicated information in a decentralized control framework, which motivates

the development of decentralized methods which evaluate a level of trust for network neighbors. The focus of this work is the development of controllers which demonstrate robustness to phenomena such as disturbances, communication delay, and imperfect communication.

A common framework for decentralized control is synchronization, wherein agents cooperate to drive their states towards that of a network leader which has a time-varying trajectory (cf. [1–3, 7–17]). The network leader can be a preset time-varying trajectory, called a virtual leader, or a physical system which the “follower” systems interact with via sensing or communication. For example, a task which requires an expensive sensor in a search and rescue mission can be accomplished by endowing just one system with the expensive sensor and instructing the other systems to cooperatively interact with the autonomous “leader.” Alternatively, a team of autonomous vehicles performing reconnaissance can be directed by a “leader” vehicle piloted by a human and thereby assist the pilot in mission completion. This control objective is made more practical by limiting interaction with the leader to only a subset of the follower systems; e.g., it may be the case that only a few follower UAVs in the front of a flying formation may see the leader vehicle.

Synchronization is typically achieved using a composite error system that penalizes both state dissimilarity between neighbors and the dissimilarity between a follower agent and the leader, if that connection exists, so that neighbors are cooperatively driven towards the state of the leader. However, the ability to achieve synchronization may be affected by exogenous disturbances in the agents’ dynamics. For example, a gust of wind may throw a UAV off course, which may consequently cause a wave of disruption to percolate through the network. Additionally, synchronization of physical systems leads to additional challenges in the sense that the trajectories of neighboring agents are less predictable due to heterogeneity and parametric uncertainty. Thus, decentralized control designers should consider the possibility of unmodeled disturbances and model

uncertainty during the design of robust controllers so that mission completion can still be achieved. Chapter 2 uses this leader-follower framework to develop a novel decentralized controller which achieves network synchronization despite the presence of unmodeled, exogenous input disturbances in the follower agents' dynamics and model uncertainty. An extension to the synchronization framework is also provided in Chapter 2 for the similar task of formation control, which is a convenient control approach when spatial distribution of the follower agents is necessary. Specifically, formation control entails the convergence of follower agents' states to a geometric configuration specified with respect to the leader state while only communicating in a decentralized manner.

Containment control (cf. [18–27]) is another common framework for decentralized control and represents a generalization of the synchronization problem that allows for a collection of leaders. For example, containment control is useful in applications where a team of autonomous vehicles is directed by multiple pilots or for networks of autonomous systems where only a subset of the systems is equipped with expensive sensing hardware. The typical objective in the containment control framework is to regulate the states of the networked systems to the convex hull spanned by the leaders' states, where the convex hull is used because it facilitates a convenient description of the demarcation of where the follower systems should be with respect to the leaders. By using an error signal which augments the one typically used for synchronization to include the contributions from other leaders, it can be shown that regulation of that error signal implies convergence to a trajectory which is a linear combination of the leaders' trajectories that depends on follower connections, leader connections, and the relative weighting of network connections. The developments in Chapter 2 are extended for the containment control framework in Chapter 3 to develop a controller which provides disturbance rejection for the setting of decentralized control with multiple leaders.

Communication delay, also known as broadcast, coupling or transmission delay, is a phenomenon in which inter-agent interaction is delayed during information exchange.

Even a small communication delay, such as that caused by information processing or a communication protocol, can cause networked autonomous systems to become unstable (cf. [4]): analysis is motivated to ensure stability. Furthermore, synchronization with a time-varying leader trajectory and limited leader connectivity presents a challenging issue: if an agent is not aware of the leader's state, it must depend on the delayed state of neighboring follower agent(s) between itself and the leader, i.e., the effect of a change in the leader's state may not affect a follower agent until the time duration of multiple communication delays has passed.

Chapter 4 presents the development of a novel controller which mitigates the effects of communication delay by combining two types of delay-affected feedback. The delayed version of the typical neighborhood error signal is augmented with feedback terms which compare a neighbor's delayed state with the agent's own state manually delayed by an estimate of the delay duration. This approach is demonstrated in simulation to provide improved tracking performance and less sensitive stability criteria compared to other contemporary decentralized control types.

There are multiple methods for an autonomous vehicle to determine its position, orientation, and velocity, including using GPS, an inertial measurement unit (IMU), and simultaneous localization and mapping (SLAM). However, self-localization may produce inaccurate results. For example, a UAV might poorly estimate its own state as a result of corruption of an IMU, GPS spoofing, GPS jamming (and subsequent use of a less accurate IMU), inaccurate onboard SLAM due to a lack of landscape features, or IMU/GPS/SLAM measurement noise. In addition, heterogeneity in the hardware of the robotic platforms can naturally lead to disparity in the accuracy of agents' estimates of their own states. Thus, if communication is used in a team of autonomous systems to share state information, care should be taken when using a neighbor's communicated state in a control policy, especially in the context of decentralized interactions.

Another method to obtain information about agents in the network is neighbor sensing, e.g., use of a camera or radar. Neighbor sensing can provide the relative position of neighboring vehicles; however, it is very reliant on a direct line-of-sight (LOS) between the vehicles. For example, ground vehicles may temporarily lose LOS when navigating around buildings or other obstructions. In addition, agents may need to distribute neighbor sensing time between multiple neighbors. For example, if a ground vehicle can observe two neighboring vehicles in dissimilar locations with a camera but cannot observe both neighbors at the same time due to a narrow camera field of view, the camera may need to rotate continuously to share observation time between the two neighbors. Chapter 5 considers a decentralized network control scenario in which agents use both communication and neighbor sensing to interact. Communication is assumed to be continuously available, but have possible inaccuracies due to poor self localization. The sensor measurements are assumed to provide accurate relative position information, but only occur intermittently. Because the sensor measurements are modeled as intermittent, and therefore may not be frequent enough to be implemented in closed-loop control, they are used to vet communicated information so that an agent can rely more on information from more reliable neighbors. A trust algorithm is developed in which each agent quantitatively evaluates the trust of each neighbor based on the discrepancy between communicated and sensed information. The trust values are used in a reputation algorithm, in which agents communicate about a mutually shared neighbor to collaboratively obtain a reputation. Each agent's contribution to the reputation algorithm is weighted by that neighbor's own reputation. The result of the reputation algorithm is used to update consensus weights which affect the relative weighting in use of a neighbor's communicated information compared to other neighbors', if an agent has multiple neighbors.

1.2 Literature Review

A review of relevant literature is provided in the following.

Chapter 2: Asymptotic Synchronization of a Leader-Follower Network Subject to Uncertain Disturbances: Results such as [3, 8, 10–12, 16] achieve decentralized synchronization; however, all the agents are able to communicate with the network leader so that the developed controllers for each agent exploit explicit knowledge of the desired goal. This communication framework lacks the flexibility associated with general leader-follower networks. Synchronization results which model the leader connectivity as limited to a subset of follower agents have typically focused on networks of linear dynamical systems (cf. [7, 15]); however, these results are limited by the strict assumption of linear dynamics. Recent results such as [9] and [14] investigate the more general problem where agents' trajectories are described by nonlinear dynamics; specifically, the results in [9] and [14] focus on Euler-Lagrange systems, where Euler-Lagrange dynamics are used for the broad applicability to many engineering systems. However, both [9] and [14] develop controllers which assume exact knowledge of the agent dynamics so that a feedback linearization approach can be used to compensate for the nonlinear dynamics. Motivated to improve robustness, results such as [1, 2, 28] consider uncertainty in the nonlinear agent dynamics. In [28], a continuous controller is proposed to yield asymptotic synchronization in the presence of parametric uncertainty. In addition to parametric uncertainty, the results in [1, 2] also consider exogenous disturbances. The result in [1] uses a neural network-based adaptive synchronization method and the result in [2] exploits a sliding mode-based approach. The continuous controller in [1] yields a uniformly ultimately bounded (UUB) result, whereas [2] achieves exponential synchronization through the use of a discontinuous controller.

Chapter 3: Robust Containment Control in a Leader-Follower Network of Uncertain Euler-Lagrange Systems: Containment control is investigated in [18] and [20] for static leaders and in [19] for a combination of static and dynamic leaders. Containment controllers for dynamic leaders and followers with linear dynamics are developed in [21–24]. A controller designed for the containment of social networks

with linear opinion dynamics represented with fractional order calculus is developed in [25]. Results in [26] and [27] develop a model knowledge-dependent and model-free containment controller, respectively, for the case of dynamic leaders and Euler-Lagrange dynamics. However, none of the previous results analyze the case where follower systems are affected by an exogenous, unknown disturbance, which has the capability of cascading and disrupting the performance of the entire network from a single source.

Chapter 4: Synchronization of Uncertain Euler-Lagrange Systems with Uncertain Time-Varying Communication Delays: Controllers developed in [29–38] are designed to provide convergence for a network of communication-delayed autonomous synchronizing agents without the presence of a network leader. As demonstrated in [29], asymptotic convergence towards a fixed consensus point is achievable, despite the effects of the communication delay, for synchronization without a leader. The communication-delayed synchronization problem is generalized in [3, 39–41] to include a network leader, wherein every follower agent interacts with the leader agent. As illustrated in [3], asymptotic convergence towards the leader trajectory is achievable for synchronizing agents with full leader connectivity, despite the effects of communication delay. The controllers in [42–44] are developed to address the more challenging problem of communication-delayed synchronization with limited leader connectivity. The work in [42] is developed for follower agents with single integrator dynamics, undelayed state communication and uniformly delayed communication of control effort. The controller in [43] is designed for follower agents with single integrator dynamics and uniformly delayed state communication. However, an analysis which considers single integrator dynamics does not account for the potentially destabilizing state drift that can be caused by drift dynamics, which are present in many engineering systems, during the period of communication delay. Synchronization with uniformly delayed state communication is investigated in [44] for follower agents with nonlinear dynamics; however, the development assumes that the follower agents' dynamics are

globally Lipschitz, which is restrictive and excludes many physical systems. Because globally Lipschitz nonlinear dynamics can be uniformly upper-bounded by a linear expression, the result in [44] develops a convergence analysis which does not account for general nonlinearities. Hence, the developments in [42–44] do not directly apply to networks with agents which have general nonlinear dynamics. A new strategy is required for demonstrating convergence in synchronization of a network of agents with general nonlinear dynamics, delayed communication, and limited connectivity to a time-varying leader trajectory.

Chapter 5: Decentralized Synchronization of Uncertain Nonlinear Systems with a Reputation Algorithm: The recent results in [45–47] propose reputation algorithms for networked agents performing decentralized control; however, no convergence analysis is given to guarantee achievement of the control objective with regard to the physical states of the networked systems. One of the difficulties in performing a convergence analysis for a reputation algorithm combined with a decentralized controller is that consensus weight updates can cause discontinuities in the control policy, making the network a switched system, and requiring a dwell-time between updates to the consensus weights (cf. [48]). Furthermore, because consensus weights generally take any value between 0 and 1, there are an infinite number of possible consensus weight combinations in the network, which makes a switched system-based approach difficult: a common Lyapunov function or bounds on a candidate switched Lyapunov function may be difficult to obtain. The insightful work in [48] develops conditions for convergence for a network of agents with single integrator dynamics performing decentralized control with a reputation algorithm. However, the reputation algorithm in [48] inherently requires the control objective to be convergence of all agents' states to a fixed point, which is more restrictive than the general leader-synchronization problem. Additionally, the work in [48] relies on the existence of a dwell-time between consensus weight updates, but an approach to compute a sufficient dwell-time is not discussed. The development in [49]

avoids the effects of discontinuities by updating consensus weights smoothly in time based on continuously updated trust values in a network of agents with single integrator dynamics. However, the effects on the performance of the dynamical systems due to varying the consensus weights in time is not addressed. Additionally, the controller in [49] only provides network convergence of the agents' states to a single point, which is a function of the trust values, initial conditions of the agents' states, and the network configuration.

1.3 Contributions

The contributions of the developments in this work are described below.

Chapter 2: Asymptotic Synchronization of a Leader-Follower Network Subject to Uncertain Disturbances: This chapter investigates the synchronization of networked systems consisting of a single leader and an arbitrary number of followers, where at least one follower is connected to the leader. The networked systems are modeled by nonlinear, heterogeneous, and uncertain Euler-Lagrange dynamics which are affected by additive unmodeled disturbances. Notions from the Robust Integral of the Sign of the Error (RISE) controller are used to develop a novel, robust decentralized controller based on state feedback from neighbors. The most comparable results to the current result are [1] and [2]. In contrast to the discontinuous result in [2], the developed decentralized controller is continuous and still obtains asymptotic synchronization despite the effects of uncertain dynamics and exogenous disturbances. In contrast to the result in [1], the developed approach yields asymptotic synchronization with neighboring states and the time-varying state of the leader, despite the effects of uncertain dynamics and exogenous disturbances. A Lyapunov-based analysis is provided that proves asymptotic synchronization of each agent's state. A simulation of a network of second order Euler-Lagrange systems is provided that demonstrates the practical implications of achieving an asymptotic result using a continuous controller in comparison with the results in [1] and [2, Section IV].

Chapter 3: Robust Containment Control in a Leader-Follower Network of Uncertain Euler-Lagrange Systems: Compared to the most similar work in [27], the development in this chapter does not require communication of an acceleration signal from leader agents and demonstrates compensation of unknown input disturbances. Furthermore, whereas the convergence analysis in [27] is temporally divided into an estimation segment and a subsequent Lyapunov-based convergence analysis for showing network containment, which relies on the assumption of boundedness of the dynamics until estimate equivalence is reached, the present work yields asymptotic network containment throughout the entire state trajectory. The contribution of this chapter is the development of a continuous, decentralized controller which provides asymptotic containment control in a network of dynamic leaders and followers with uncertain nonlinear Euler-Lagrange dynamics, despite the effects of exogenous disturbances, where at least one of the followers interacts with at least one leader and the follower network is connected.

Chapter 4: Synchronization of Uncertain Euler-Lagrange Systems with Uncertain Time-Varying Communication Delays: This chapter considers the problem of synchronization of a leader-follower network of agents with heterogeneous dynamics described by nonlinear Euler-Lagrange equations of motion affected by an unknown, time-varying, exogenous input disturbance. The leader agent has a time-varying trajectory and is assumed to interact with at least one follower agent. The agents are delayed in communicating state information and do not communicate control effort information. The communication delay is assumed to be uncertain, heterogeneous, time-varying and bounded. Motivated by recent results (cf. [35, 50]) which demonstrate that approximate knowledge of delay can be incorporated into a controller for improved performance, an estimate of the communication delay is used to provide feedback of an estimated recent tracking error in a novel controller. A detailed Lyapunov-based convergence analysis using Lyapunov-Krasovskii (LK) functionals is provided to develop

sufficient conditions for uniformly ultimately bounded convergence to the leader state for each follower agent. Simulation results are provided to demonstrate the performance of the developed controller compared to other delay-affected decentralized control techniques.

Chapter 5: Decentralized Synchronization of Uncertain Nonlinear Systems with a Reputation Algorithm: This chapter develops novel decentralized trust, reputation and control algorithms for synchronization to a time-varying leader trajectory for a network of autonomous agents with nonlinear second-order dynamics. The networked agents are modeled to interact via communication and sensing in a directed topology, where communication of state information is continuously available, but possibly inaccurate, and sensing is intermittent, but provides accurate relative state information. The collaborative reputation algorithm is updated using trust measurements and is used to update consensus weights which provide relative importance in the use of a neighbor's communicated information compared to other neighbors', if an agent has multiple neighbors. An associated convergence analysis and sufficient gain conditions are provided for the developed trust, reputation and control algorithms. Based on the convergence analysis, this work discusses a novel method to compute a sufficient minimum dwell-time for the switched network system. The sufficient minimum dwell-time is developed by bounding eigenvalues of the solution to the continuous algebraic Lyapunov Equation (CALE) over a bounded, but uncountably infinite set of Hurwitz matrices. To the author's knowledge, the development of a dwell-time for a network of autonomous agents with an infinite possible number of feedback structures (i.e., consensus weight combinations) has not been addressed. Simulation results are provided to demonstrate the performance of the developed trust, reputation, and control algorithms and network topology-dependent dwell-time.

1.4 Preliminaries

Graph theory is used to describe the information exchange between agents in a network. Consider a network consisting of a single leader and $\mathcal{F} \in \mathbb{Z}_{>0}$ follower agents. The communication topology of the followers is characterized by a fixed graph, $\mathcal{G}_{\mathcal{F}} = \{\mathcal{V}_{\mathcal{F}}, \mathcal{E}_{\mathcal{F}}\}$, which has a non-empty finite set of nodes $\mathcal{V}_{\mathcal{F}} = \{1, \dots, \mathcal{F}\}$ and a set of edges $\mathcal{E}_{\mathcal{F}} \subseteq \mathcal{V}_{\mathcal{F}} \times \mathcal{V}_{\mathcal{F}}$. An edge $(j, i) \in \mathcal{E}_{\mathcal{F}}$ exists if agent $i \in \mathcal{V}_{\mathcal{F}}$ receives information from agent $j \in \mathcal{V}_{\mathcal{F}}$. The set of neighboring follower agents which provide information to agent $i \in \mathcal{V}_{\mathcal{F}}$ is defined as $\mathcal{N}_{\mathcal{F}i} \triangleq \{j \in \mathcal{V}_{\mathcal{F}} \mid (j, i) \in \mathcal{E}_{\mathcal{F}}\}$. An adjacency matrix $A = [a_{ij}] \in \mathbb{R}^{\mathcal{F} \times \mathcal{F}}$ weights the network connections and is defined such that $a_{ij} > 0$ if $(j, i) \in \mathcal{E}_{\mathcal{F}}$ and $a_{ij} = 0$ otherwise. It is assumed that the graph is simple, i.e., $(i, i) \notin \mathcal{E}_{\mathcal{F}}$, and thus $a_{ii} = 0$ for all $i \in \mathcal{V}_{\mathcal{F}}$. The Laplacian matrix $\mathcal{L}_{\mathcal{F}} \in \mathbb{R}^{\mathcal{F} \times \mathcal{F}}$ of graph $\mathcal{G}_{\mathcal{F}}$ is defined as $\mathcal{L}_{\mathcal{F}} \triangleq D - A$, where $D \triangleq \text{diag}\{D_1, \dots, D_{\mathcal{F}}\} \in \mathbb{R}^{\mathcal{F} \times \mathcal{F}}$ is the degree matrix with $D_i \triangleq \sum_{j \in \mathcal{N}_{\mathcal{F}i}} a_{ij}$. The graph which includes a single leader agent is constructed as $\mathcal{G} = \{\mathcal{V}_{\mathcal{F}} \cup \{L\}, \mathcal{E}_{\mathcal{F}} \cup \mathcal{E}_L\}$, where L denotes the leader agent and the edge (L, i) belongs to \mathcal{E}_L if the follower agent $i \in \mathcal{V}_{\mathcal{F}}$ receives information from the leader. The leader-included neighbor set is defined as $\bar{\mathcal{N}}_{\mathcal{F}i} \triangleq \{j \in \mathcal{V}_{\mathcal{F}} \cup \{L\} \mid (j, i) \in \mathcal{E}_{\mathcal{F}} \cup \mathcal{E}_L\}$. The leader-connectivity (i.e., pinning) matrix $B \in \mathbb{R}^{\mathcal{F} \times \mathcal{F}}$ is defined as the diagonal matrix $B \triangleq \text{diag}\{b_1, \dots, b_{\mathcal{F}}\}$, where $b_i > 0$ if $(L, i) \in \mathcal{E}_L$ and $b_i = 0$ otherwise.

Throughout the following developments, the notations $|\cdot|$, $\|\cdot\|$, $\|\cdot\|_{\infty}$ and $\|\cdot\|_F$ are used to denote set cardinality for a set argument, the Euclidean norm, the infinity norm, and the Frobenius norm, respectively. Additionally, Π is used to denote the Cartesian product; for example, $\Pi_{k=1}^3 \mathbb{R}$ denotes $\mathbb{R} \times \mathbb{R} \times \mathbb{R}$. The operators $\underline{\lambda}(\cdot)$ and $\bar{\lambda}(\cdot)$ are used to denote the minimum and maximum eigenvalues, respectively. The operator \otimes is used to denote the Kronecker product. Finally, the symbols $\mathbf{0}$ and $\mathbf{1}$ are used to respectively denote a vector of zeros or ones of the indicated dimension, and I denotes the identity matrix of the indicated dimension.

CHAPTER 2
ASYMPTOTIC SYNCHRONIZATION OF A LEADER-FOLLOWER NETWORK
SUBJECT TO UNCERTAIN DISTURBANCES

This chapter investigates the synchronization of a network of Euler-Lagrange systems with leader tracking. The Euler-Lagrange systems are heterogeneous and uncertain and contain bounded, exogenous disturbances. The network leader has a time-varying trajectory which is known to only a subset of the follower agents. Concepts from the Robust Integral Sign of the Error (RISE) control method are used to develop a novel, decentralized control policy which guarantees semi-global asymptotic synchronization. The contribution to the current literature is the development of a *continuous*, decentralized controller which achieves asymptotic synchronization of a leader-follower network of agents with uncertain dynamics affected by exogenous disturbances. To the author's knowledge, prior to this development, this had only been accomplished with a discontinuous decentralized controller. Notions from nonsmooth analysis and a Lyapunov-based convergence analysis are used to demonstrate the theoretical result. An extension to the developed control algorithm is given for the problem of decentralized formation control, wherein follower agents converge to a geometric configuration specified with respect to the leader.

2.1 Problem Formulation

2.1.1 Dynamic Models and Properties

Consider a network of one leader and \mathcal{F} follower agents which have dynamics described by the heterogeneous Euler-Lagrange equations of motion

$$M_L(q_L) \ddot{q}_L + C_L(q_L, \dot{q}_L) \dot{q}_L + F_L(\dot{q}_L) + G_L(q_L) = u_L \quad (2-1)$$

$$M_i(q_i) \ddot{q}_i + C_i(q_i, \dot{q}_i) \dot{q}_i + F_i(\dot{q}_i) + G_i(q_i) + d_i(t) = u_i, \quad i \in \mathcal{F}. \quad (2-2)$$

The terms in (2-1) and (2-2) are defined such that $q_j \in \mathbb{R}^m$ ($j \in \mathcal{V}_{\mathcal{F}} \cup \{L\}$) is the generalized configuration coordinate, $M_j : \mathbb{R}^m \rightarrow \mathbb{R}^{m \times m}$ is the inertia matrix, $C_j :$

$\mathbb{R}^m \times \mathbb{R}^m \rightarrow \mathbb{R}^{m \times m}$ is the Coriolis/centrifugal matrix, $F_j : \mathbb{R}^m \rightarrow \mathbb{R}^m$ is the friction term, $G_j : \mathbb{R}^m \rightarrow \mathbb{R}^m$ is the vector of gravitational torques, $u_j \in \mathbb{R}^m$ is the vector of control inputs, $d_i : \mathbb{R}_{\geq 0} \rightarrow \mathbb{R}^m$ ($i \in \mathcal{V}_{\mathcal{F}}$) is a time-varying nonlinear exogenous disturbance, and $t \in \mathbb{R}_{\geq 0}$ is the elapsed time.

The following assumptions are used in the subsequent analysis.

Assumption 2.1. The inertia matrix M_j is symmetric, positive definite, and satisfies $\underline{m}_j \|\xi\|^2 \leq \xi^T M_j(\psi) \xi \leq \bar{m}_j \|\xi\|^2$ for all $\xi, \psi \in \mathbb{R}^m$ and $j \in \mathcal{V}_{\mathcal{F}} \cup \{L\}$, where $\underline{m}_j, \bar{m}_j \in \mathbb{R}$ are positive known constants [51].

Assumption 2.2. The functions M_j, C_j, F_j, G_j are second-order differentiable for all $j \in \mathcal{V}_{\mathcal{F}} \cup \{L\}$ such that their second derivatives are bounded if $q_j^{(k)} \in \mathcal{L}_{\infty}$, $k = 0, 1, 2, 3$ [52].

Assumption 2.3. [51] For each follower agent $i \in \mathcal{V}_{\mathcal{F}}$, the time-varying disturbance term is sufficiently smooth such that it and its first two time derivatives, $d_i, \dot{d}_i, \ddot{d}_i$, are bounded by known¹ constants.

Assumption 2.4. The leader configuration coordinate, q_L , is sufficiently smooth such that $q_L \in \mathcal{C}^2$; additionally, the leader configuration coordinate and its first two time derivatives are bounded such that $q_L, \dot{q}_L, \ddot{q}_L \in \mathcal{L}_{\infty}$.

Assumption 2.5. The follower graph $\mathcal{G}_{\mathcal{F}}$ is undirected and connected and at least one follower agent is connected to the leader.

The equation of motion for the follower agents may be written as

$$M\ddot{Q}_{\mathcal{F}} + C\dot{Q}_{\mathcal{F}} + F + G + d = u, \quad (2-3)$$

¹ Following the developments in [53] and [54], Assumption 2.3 can be relaxed such that the bounding constants can be unknown.

where

$$\begin{aligned}
Q_{\mathcal{F}} &\triangleq [q_1^T, \dots, q_{\mathcal{F}}^T]^T \in \mathbb{R}^{\mathcal{F}m} \\
M &\triangleq \text{diag} \{M_1, \dots, M_{\mathcal{F}}\} \in \mathbb{R}^{\mathcal{F}m \times \mathcal{F}m} \\
C &\triangleq \text{diag} \{C_1, \dots, C_{\mathcal{F}}\} \in \mathbb{R}^{\mathcal{F}m \times \mathcal{F}m} \\
F &\triangleq [F_1^T, \dots, F_{\mathcal{F}}^T]^T \in \mathbb{R}^{\mathcal{F}m} \\
G &\triangleq [G_1^T, \dots, G_{\mathcal{F}}^T]^T \in \mathbb{R}^{\mathcal{F}m} \\
d &\triangleq [d_1^T, \dots, d_{\mathcal{F}}^T]^T \in \mathbb{R}^{\mathcal{F}m} \\
u &\triangleq [u_1^T, \dots, u_{\mathcal{F}}^T]^T \in \mathbb{R}^{\mathcal{F}m}.
\end{aligned}$$

For convenience in the subsequent analysis, the leader dynamics are represented as

$$M_{\emptyset} \ddot{Q}_L + C_{\emptyset} \dot{Q}_L + F_{\emptyset} + G_{\emptyset} = u_{\emptyset}, \quad (2-4)$$

where $Q_L \triangleq \mathbf{1}_{\mathcal{F}} \otimes q_L \in \mathbb{R}^{\mathcal{F}m}$, $M_{\emptyset} \triangleq I_{\mathcal{F}} \otimes M_L \in \mathbb{R}^{\mathcal{F}m \times \mathcal{F}m}$, $C_{\emptyset} \triangleq I_{\mathcal{F}} \otimes C_L \in \mathbb{R}^{\mathcal{F}m \times \mathcal{F}m}$, $F_{\emptyset} \triangleq \mathbf{1}_{\mathcal{F}} \otimes F_L \in \mathbb{R}^{\mathcal{F}m}$, $G_{\emptyset} \triangleq \mathbf{1}_{\mathcal{F}} \otimes G_L \in \mathbb{R}^{\mathcal{F}m}$, and $u_{\emptyset} \triangleq \mathbf{1}_{\mathcal{F}} \otimes u_L \in \mathbb{R}^{\mathcal{F}m}$.

Note that because the graph $\mathcal{G}_{\mathcal{F}}$ is undirected and connected and at least one follower agent is connected to the leader by Assumption 2.5, the matrix $\mathcal{L}_{\mathcal{F}} + B$ is positive definite and symmetric [55]. The customarily used Laplacian matrix is positive semi-definite for a connected undirected graph; however, the matrix $\mathcal{L}_{\mathcal{F}}$, also known as the ‘‘Dirichlet’’ or ‘‘Grounded’’ Laplacian matrix, is designed such that $\mathcal{L}_{\mathcal{F}} + B$ is positive definite given Assumption 2.5 [55].

2.1.2 Control Objective

The objective is to design a continuous controller which ensures that all follower agents asymptotically track the state of the leader agent with only neighbor feedback such that $\limsup_{t \rightarrow \infty} \|q_L - q_i\| = 0$ for all $i \in \mathcal{V}_{\mathcal{F}}$, despite model uncertainties and bounded exogenous system disturbances. Moreover, the subsequent control design is

based on the constraint that only the generalized configuration coordinate and its first derivative are measurable.

To quantify the control objective, a local neighborhood position tracking error, $e_{1,i} \in \mathbb{R}^m$, is defined as [9]

$$e_{1,i} \triangleq \sum_{j \in \mathcal{N}_{\mathcal{F}i}} a_{ij} (q_j - q_i) + b_i (q_L - q_i). \quad (2-5)$$

The error signal in (2-5) includes the summation $\sum_{j \in \mathcal{N}_{\mathcal{F}i}} a_{ij} (q_j - q_i)$ to penalize state dissimilarity between neighbors and the proportional term $b_i (q_L - q_i)$ to penalize state dissimilarity between a follower agent and the leader, if that connection exists. The ability to emphasize either follower agent synchronization or leader tracking is rendered by assigning $a_{ij} = k_a$ if $(j, i) \in \mathcal{E}_{\mathcal{F}}$ and $b_i = k_b$ if $(L, i) \in \mathcal{E}_{\mathcal{F}}$, where $k_a, k_b \in \mathbb{R}$ are constant positive gains. Thus, if a control application dictates the need for close similarity in follower agents' states while approaching the leader trajectory, the gain k_a may be selected such that $k_a \gg k_b$. Alternatively, the gain k_b may be selected such that $k_b \gg k_a$ if quick convergence to the leader state is desired and similarity in follower agents' states is not as important.

An auxiliary tracking error, denoted by $e_{2,i} \in \mathbb{R}^m$, is defined as

$$e_{2,i} \triangleq \dot{e}_{1,i} + \alpha_{1,i} e_{1,i}, \quad (2-6)$$

where $\alpha_{1,i} \in \mathbb{R}$ denotes a constant positive gain. The error systems in (2-5) and (2-6) may be represented as

$$E_1 = ((\mathcal{L}_{\mathcal{F}} + B) \otimes I_m) (Q_L - Q_{\mathcal{F}}), \quad (2-7)$$

$$E_2 = \dot{E}_1 + \Lambda_1 E_1, \quad (2-8)$$

where $E_1 \triangleq [e_{1,1}^T, \dots, e_{1,\mathcal{F}}^T]^T \in \mathbb{R}^{\mathcal{F}m}$, $E_2 \triangleq [e_{2,1}^T, \dots, e_{2,\mathcal{F}}^T]^T \in \mathbb{R}^{\mathcal{F}m}$, and $\Lambda_1 \triangleq \text{diag}(\alpha_{1,1}, \dots, \alpha_{1,\mathcal{F}}) \otimes I_m \in \mathbb{R}^{\mathcal{F}m \times \mathcal{F}m}$. Another auxiliary error signal, $R \in \mathbb{R}^{\mathcal{F}m}$, is

defined as

$$R \triangleq ((\mathcal{L}_{\mathcal{F}} + B)^{-1} \otimes I_m) \left(\dot{E}_2 + \Lambda_2 E_2 \right), \quad (2-9)$$

where $\Lambda_2 \triangleq \text{diag}(\alpha_{2,1}, \dots, \alpha_{2,\mathcal{F}}) \otimes I_m \in \mathbb{R}^{\mathcal{F}m \times \mathcal{F}m}$ and $\alpha_{2,i} \in \mathbb{R}$ is a constant positive gain.

The introduction of R facilitates the subsequent convergence analysis; however, it is not measurable because it depends on the second derivative of the generalized configuration coordinate, and hence, is not used in the subsequently developed controller.

2.2 Controller Development

The open-loop tracking error system is developed by multiplying (2-9) by M and utilizing (2-3), (2-4) and (2-7)-(2-9) to obtain

$$MR = -u + d + S_1 + S_2, \quad (2-10)$$

where the auxiliary functions $S_1 : \Pi_{k=1}^6 \mathbb{R}^{\mathcal{F}m} \rightarrow \mathbb{R}^{\mathcal{F}m}$ and $S_2 : \mathbb{R}^{\mathcal{F}m} \times \mathbb{R}^{\mathcal{F}m} \rightarrow \mathbb{R}^{\mathcal{F}m}$ are defined as

$$\begin{aligned} S_1 \triangleq & M(Q_{\mathcal{F}}) M_{\emptyset}^{-1} u_{\emptyset} - M(Q_L) M_{\emptyset}^{-1} u_{\emptyset} - M(Q_{\mathcal{F}}) f_L(Q_L, \dot{Q}_L) + M(Q_L) f_L(Q_L, \dot{Q}_L) \\ & + f(Q_{\mathcal{F}}, \dot{Q}_{\mathcal{F}}) - f(Q_L, \dot{Q}_L) + M(Q_{\mathcal{F}}) ((\mathcal{L}_{\mathcal{F}} + B)^{-1} \otimes I_m) (-\Lambda_1^2 E_1 + (\Lambda_1 + \Lambda_2) E_2), \end{aligned}$$

$$S_2 \triangleq M(Q_L) M_{\emptyset}^{-1} u_{\emptyset} - M(Q_L) f_L(Q_L, \dot{Q}_L) + f(Q_L, \dot{Q}_L),$$

where the functional dependency of M is given for clarity, and the auxiliary functions

$f_L : \mathbb{R}^{\mathcal{F}m} \times \mathbb{R}^{\mathcal{F}m} \rightarrow \mathbb{R}^{\mathcal{F}m}$ and $f : \mathbb{R}^{\mathcal{F}m} \times \mathbb{R}^{\mathcal{F}m} \rightarrow \mathbb{R}^{\mathcal{F}m}$ are defined as

$$f_L \triangleq M_{\emptyset}^{-1} \left(C_{\emptyset} \dot{Q}_L + F_{\emptyset} + G_{\emptyset} \right), \quad (2-11)$$

$$f \triangleq C \dot{Q}_{\mathcal{F}} + F + G. \quad (2-12)$$

The RISE-based (cf. [56], [57]) control input is designed for agent $i \in \mathcal{V}_{\mathcal{F}}$ as

$$u_i \triangleq (k_i + 1) (e_{2,i} - e_{2,i}(0)) + \nu_i, \quad (2-13)$$

where $\nu_i \in \mathbb{R}^m$ is the generalized solution to the differential equation

$$\begin{aligned}\dot{\nu}_i &= (k_i + 1) \alpha_{2,i} e_{2,i} + b_i \chi_i \operatorname{sgn}(e_{2,i}) \\ &\quad + \sum_{j \in \mathcal{N}_{\mathcal{F}_i}} a_{ij} (\chi_i \operatorname{sgn}(e_{2,i}) - \chi_j \operatorname{sgn}(e_{2,j})), \\ \nu_i(0) &= \nu_{i0},\end{aligned}\tag{2-14}$$

where $\nu_{i0} \in \mathbb{R}^m$ is an initial condition, $k_i, \chi_i \in \mathbb{R}$ are constant positive gains, and $\operatorname{sgn}(\cdot)$ is defined $\forall \xi = \begin{bmatrix} \xi_1 & \xi_2 & \dots & \xi_l \end{bmatrix}^T \in \mathbb{R}^l$ as $\operatorname{sgn}(\xi) \triangleq \begin{bmatrix} \operatorname{sgn}(\xi_1) & \operatorname{sgn}(\xi_2) & \dots & \operatorname{sgn}(\xi_l) \end{bmatrix}^T$. Note that the continuous controller in (2-13) is decentralized: only local communication is required to compute the controller. The following development exploits the fact that the time derivative of (2-13) is

$$\begin{aligned}\dot{u}_i &= (k_i + 1) (\dot{e}_{2,i} + \alpha_{2,i} e_{2,i}) + b_i \chi_i \operatorname{sgn}(e_{2,i}) \\ &\quad + \sum_{j \in \mathcal{N}_{\mathcal{F}_i}} a_{ij} (\chi_i \operatorname{sgn}(e_{2,i}) - \chi_j \operatorname{sgn}(e_{2,j})),\end{aligned}\tag{2-15}$$

which allows the $\operatorname{sgn}(\cdot)$ terms to cancel disturbance terms in the Lyapunov-based convergence analysis that have a linear state bound, similar to sliding mode-based results.

After substituting (2-15) into (2-10), the closed-loop error system can be expressed as

$$\begin{aligned}M\dot{R} &= -\frac{1}{2}\dot{M}R + \tilde{N} + \left((\mathcal{L}_{\mathcal{F}} + B)^T \otimes I_m \right) N_d - \left((\mathcal{L}_{\mathcal{F}} + B)^T \otimes I_m \right) E_2 \\ &\quad - \left((\mathcal{L}_{\mathcal{F}} + B) \otimes I_m \right) \beta \operatorname{sgn}(E_2) - (K_s + I_{\mathcal{F}m}) \left(\dot{E}_2 + \Lambda_2 E_2 \right),\end{aligned}\tag{2-16}$$

where (2-15) is expressed in block form as

$$\dot{u} = (K_s + I_{\mathcal{F}m}) \left(\dot{E}_2 + \Lambda_2 E_2 \right) + \left((\mathcal{L}_{\mathcal{F}} + B) \otimes I_m \right) \beta \operatorname{sgn}(E_2),$$

with $K_s \triangleq \text{diag}(k_1, \dots, k_{\mathcal{F}}) \otimes I_m$ and $\beta \triangleq \text{diag}(\chi_1, \dots, \chi_{\mathcal{F}}) \otimes I_m$. In (2–16), the unmeasurable/uncertain auxiliary functions \tilde{N} and N_d are defined as

$$\tilde{N} \triangleq -\frac{1}{2}\dot{M}R + \dot{S}_1 + \left((\mathcal{L}_{\mathcal{F}} + B)^T \otimes I_m \right) E_2, \quad (2-17)$$

$$N_d \triangleq \left((\mathcal{L}_{\mathcal{F}} + B)^{-T} \otimes I_m \right) \left(\dot{d} + \dot{S}_2 \right). \quad (2-18)$$

The auxiliary terms in (2–17) and (2–18) are segregated such that after utilizing (2–7)-(2–9), Properties 2.1-2.2, Assumptions 2.3-2.4, the Mean Value Theorem, and the relations $Q_L - Q_{\mathcal{F}} = \left((\mathcal{L}_{\mathcal{F}} + B)^{-1} \otimes I_m \right) E_1$, $\dot{E}_1 = E_2 - \Lambda_1 E_1$, and $\dot{E}_2 = \left((\mathcal{L}_{\mathcal{F}} + B) \otimes I_m \right) R - \Lambda_2 E_2$, the following upper bounds are satisfied

$$\left\| \tilde{N} \right\| \leq \rho(\|Z\|) \|Z\|, \quad (2-19)$$

$$\sup_{t \in [0, \infty)} |N_{d_l}| \leq \zeta_{a_l}, \quad l = 1, 2, \dots, \mathcal{F}m, \quad (2-20)$$

$$\sup_{t \in [0, \infty)} \left| \dot{N}_{d_l} \right| \leq \zeta_{b_l}, \quad l = 1, 2, \dots, \mathcal{F}m, \quad (2-21)$$

where $\rho : \mathbb{R}_{\geq 0} \rightarrow \mathbb{R}$ is a strictly increasing, radially unbounded function (cf. [58, Lemma 3]); N_{d_l} and \dot{N}_{d_l} denote the l^{th} element of N_d and \dot{N}_d , respectively, the elements of $\zeta_a \in \mathbb{R}^{\mathcal{F}m}$ and $\zeta_b \in \mathbb{R}^{\mathcal{F}m}$ denote some known upper bounds on the corresponding elements in N_d and \dot{N}_d , respectively, and $Z \in \mathbb{R}^{3\mathcal{F}m}$ is the composite error vector

$$Z \triangleq \begin{bmatrix} E_1^T & E_2^T & R^T \end{bmatrix}^T. \quad (2-22)$$

Thus, the terms which arise from the exogenous disturbance and dynamics are segregated by those which can be upper-bounded by a function of the state (after use of the Mean Value Theorem) and those which can be upper-bounded by a constant. This separation clarifies how these different terms are handled robustly by the different feedback terms in the controller. Specifically, compensation for the terms in \tilde{N} is achieved by using the proportional and derivative feedback terms and compensation for the terms in N_d is achieved by using the RISE-based feedback terms. The terms N_d and \dot{N}_d do

not need to be known exactly to determine the corresponding sufficient upper bounds in ζ_a and ζ_b ; however, obtaining numerical values for ζ_a and ζ_b involves a priori upper bounds related to the leader trajectory, the leader and followers' dynamics, and the exogenous disturbances. For example, a leader's future trajectory may be unknown, but practical limitations on leader behavior can guide in selecting appropriate upper bounds. Additionally, developing upper bounds for the parametrically uncertain dynamics is straightforward since the uncertain coefficients (e.g. mass and friction coefficients) can easily be upper-bounded. See results such as [53] and [54] for an extension to the controller for systems where the sufficient bounding constants in (2–20) and (2–21) cannot be determined.

For clarity in the definitions of the sufficient gain conditions in the following convergence analysis, let the constant vectors $\varsigma_{ai}, \varsigma_{bi} \in \mathbb{R}^m$, $i \in \mathcal{V}_{\mathcal{F}}$, be defined such that $\zeta_a = \begin{bmatrix} \varsigma_{a1}^T & \varsigma_{a2}^T & \dots & \varsigma_{a\mathcal{F}}^T \end{bmatrix}^T$ and $\zeta_b = \begin{bmatrix} \varsigma_{b1}^T & \varsigma_{b2}^T & \dots & \varsigma_{b\mathcal{F}}^T \end{bmatrix}^T$. Furthermore, let the auxiliary bounding constant $\psi \in \mathbb{R}$ be defined as

$$\psi \triangleq \min \left\{ \underline{\lambda}(\Lambda_1) - \frac{1}{2}, \underline{\lambda}(\Lambda_2) - \frac{1}{2}, \underline{\lambda}(\mathcal{L}_{\mathcal{F}} + B) \right\}.$$

2.3 Convergence Analysis

To simplify the development of the subsequent theorem statement and associated proof, various expressions and upper bounds are presented.

An auxiliary function $P \in \mathbb{R}$ is used in the following convergence analysis as a means to develop sufficient gain conditions that enable the controller to compensate for the disturbance terms given in N_d ; P is defined as the generalized solution to the differential equation

$$\dot{P} = - \left(\dot{E}_2 + \Lambda_2 E_2 \right)^T (N_d - \beta \operatorname{sgn}(E_2)), \quad (2-23)$$

$$P(0) = \sum_{l=1}^{\mathcal{F}m} \beta_{l,l} |E_{2l}(0)| - E_2^T(0) N_d(0),$$

where $\beta_{l,l}$ denotes the l^{th} diagonal element of β and E_{2_l} denotes the l^{th} element of the vector E_2 . Provided the sufficient conditions in (2–29) are satisfied, then $P \geq 0$ (see Appendix A), and can be included in the subsequently defined positive definite function V_L . The inclusion of P enables the development of sufficient gain conditions that ensure asymptotic tracking by the continuous controller, despite the effects of additive exogenous disturbances.

Remark 2.1. Because the derivative of the closed-loop tracking error system in (2–16) is discontinuous, the existence of Filippov solutions to the developed differential equations is established. Let the composite vector $w \in \mathbb{R}^{4\mathcal{F}m+1}$ be defined as $w \triangleq \begin{bmatrix} Z^T & \nu^T & \sqrt{P} \end{bmatrix}^T$, where $\nu \triangleq \begin{bmatrix} \nu_1^T & \nu_2^T & \dots & \nu_{\mathcal{F}}^T \end{bmatrix}^T$. The existence of Filippov solutions can be established for the closed-loop dynamical system $\dot{w} = K[h_1](w, t)$, where $h_1 : \mathbb{R}^{4\mathcal{F}m+1} \times \mathbb{R}_{\geq 0} \rightarrow \mathbb{R}^{4\mathcal{F}m+1}$ is defined as the right-hand side (RHS) of \dot{w} and $K[h_1](\sigma, t) \triangleq \cap_{\delta>0} \cap_{\mu(S_m)=0} \overline{\text{co}} h_1(B_\delta(\sigma) \setminus S_m, t)$, where $\delta \in \mathbb{R}$, $\cap_{\mu(S_m)=0}$ denotes an intersection over sets S_m of Lebesgue measure zero, $\overline{\text{co}}$ denotes convex closure, and $B_\delta(\sigma) \triangleq \{\varrho \in \mathbb{R}^{4\mathcal{F}m+1} \mid \|\sigma - \varrho\| < \delta\}$ [59–61].

Let $V_L : \mathcal{D} \rightarrow \mathbb{R}$ be a continuously differentiable, positive definite function defined as

$$V_L(y, t) \triangleq \frac{1}{2}E_1^T E_1 + \frac{1}{2}E_2^T E_2 + \frac{1}{2}R^T M R + P, \quad (2-24)$$

where $y \in \mathbb{R}^{3\mathcal{F}m+1}$ is defined as

$$y \triangleq \begin{bmatrix} Z^T & \sqrt{P} \end{bmatrix}^T, \quad (2-25)$$

and the domain \mathcal{D} is the open and connected set $\mathcal{D} \triangleq \left\{ \varrho \in \mathbb{R}^{3\mathcal{F}m+1} \mid \|\varrho\| < \inf \left(\rho^{-1} \left(\left[2\sqrt{\psi \lambda} (K_s ((\mathcal{L}_{\mathcal{F}} + B) \otimes I_m)), \infty \right) \right) \right) \right\}$. The expression in (2–24) satisfies the inequalities

$$\lambda_1 \|y\|^2 \leq V_L(y, t) \leq \lambda_2 \|y\|^2, \quad (2-26)$$

where $\lambda_1 \triangleq \frac{1}{2} \min \left\{ 1, \min_{i \in \mathcal{V}_{\mathcal{F}}} (m_i) \right\}$, and $\lambda_2 \triangleq \max \left\{ 1, \frac{1}{2} \sum_{i \in \mathcal{V}_{\mathcal{F}}} \bar{m}_i \right\}$. Let the set of stabilizing initial conditions $S_{\mathcal{D}} \subset \mathcal{D}$ be defined as

$$S_{\mathcal{D}} \triangleq \left\{ \varrho \in \mathcal{D} \mid \|\varrho\| < \sqrt{\frac{\lambda_1}{\lambda_2}} \inf \left(\rho^{-1} \left(\left[2\sqrt{\psi \underline{\lambda}} (K_s ((\mathcal{L}_{\mathcal{F}} + B) \otimes I_m)), \infty \right) \right) \right) \right\}. \quad (2-27)$$

Theorem 2.1. *For each follower agent $i \in \mathcal{V}_{\mathcal{F}}$, the controller given in (2-13) and (2-14) ensures that all system signals are bounded under closed-loop operation and that the position tracking error is semi-globally regulated in the sense that*

$$\|q_L - q_i\| \rightarrow 0 \text{ as } t \rightarrow \infty \quad \forall i \in \mathcal{V}_{\mathcal{F}}$$

(and thus $\|q_i - q_j\| \rightarrow 0 \quad \forall i, j \in \mathcal{V}_{\mathcal{F}}, i \neq j$), provided that k_i introduced in (2-13) is selected sufficiently large such that $y(0) \in S_{\mathcal{D}}$, Assumptions 2.1-2.5 are satisfied, and the parameters $\alpha_{1,i}, \alpha_{2,i}, \chi_i$ are selected according to the sufficient conditions

$$\alpha_{1,i} > \frac{1}{2}, \quad \alpha_{2,i} > \frac{1}{2}, \quad (2-28)$$

$$\chi_i > \|\varsigma_{ai}\|_{\infty} + \frac{1}{\alpha_{2,i}} \|\varsigma_{bi}\|_{\infty}, \quad (2-29)$$

where χ_i was introduced in (2-14).

Proof. Under Filippov's framework, a Filippov solution y can be established for the closed-loop system $\dot{y} = h_2(y, t)$ if $y(0) \in S_{\mathcal{D}}$, where $h_2 : \mathbb{R}^{3\mathcal{F}m+1} \times \mathbb{R}_{\geq 0} \rightarrow \mathbb{R}^{3\mathcal{F}m+1}$ denotes the RHS of the closed-loop error signals. The time derivative of (2-24) exists almost everywhere (a.e.), i.e., for almost all $t \in [0, \infty)$, and $\dot{V}_L \stackrel{a.e.}{\in} \check{V}_L$ where

$$\check{V}_L = \bigcap_{\xi \in \partial V_L(y,t)} \xi^T K \begin{bmatrix} \dot{E}_1^T & \dot{E}_2^T & \dot{R}^T & \frac{1}{2} P^{-\frac{1}{2}} \dot{P} & 1 \end{bmatrix}^T,$$

where ∂V_L is the generalized gradient of V_L [62]. Because V_L is continuously differentiable,

$$\check{V}_L \subseteq \nabla V_L K \begin{bmatrix} \dot{E}_1^T & \dot{E}_2^T & \dot{R}^T & \frac{1}{2} P^{-\frac{1}{2}} \dot{P} & 1 \end{bmatrix}^T, \quad (2-30)$$

where

$$\nabla V_L \triangleq \begin{bmatrix} E_1^T & E_2^T & R^T M & 2P^{\frac{1}{2}} & \frac{1}{2}R^T \dot{M}R \end{bmatrix}.$$

Using the calculus for $K[\cdot]$ from [60], substituting (2–8), (2–9), (2–16), and (2–23) into (2–30), using the fact that the matrix $\mathcal{L}_{\mathcal{F}} + B$ is symmetric, and canceling common terms yields

$$\begin{aligned} \dot{V}_L \subseteq & E_1^T (E_2 - \Lambda_1 E_1) + E_2^T (((\mathcal{L}_{\mathcal{F}} + B) \otimes I_m) R - \Lambda_2 E_2) \\ & + R^T \left(\tilde{N} + ((\mathcal{L}_{\mathcal{F}} + B)^T \otimes I_m) N_d - ((\mathcal{L}_{\mathcal{F}} + B)^T \otimes I_m) E_2 \right) \\ & + R^T \left(-(K_s + I_{\mathcal{F}m}) ((\mathcal{L}_{\mathcal{F}} + B) \otimes I_m) R - ((\mathcal{L}_{\mathcal{F}} + B) \otimes I_m) \beta K [\text{sgn}(E_2)] \right) \\ & - \left(\dot{E}_2 + \Lambda_2 E_2 \right)^T (N_d - \beta K [\text{sgn}(E_2)]), \end{aligned} \quad (2-31)$$

where $K[\text{sgn}(E_2)] = \text{SGN}(E_2)$ such that $\text{SGN}(E_{2_i}) = 1$ if $E_{2_i} > 0$, $\text{SGN}(E_{2_i}) = -1$ if $E_{2_i} < 0$, and $\text{SGN}(E_{2_i}) = [-1, 1]$ if $E_{2_i} = 0$ [60]. Using the upper bound in (2–19) and applying the Raleigh-Ritz theorem, (2–31) can be upper-bounded as

$$\begin{aligned} \dot{V}_L \stackrel{\text{a.e.}}{\leq} & \|E_1\| \|E_2\| - \underline{\lambda}(\Lambda_1) \|E_1\|^2 - \underline{\lambda}(\Lambda_2) \|E_2\|^2 + \|R\| \rho(\|Z\|) \|Z\| \\ & - \underline{\lambda}(\mathcal{L}_{\mathcal{F}} + B) \|R\|^2 - \underline{\lambda}(K_s ((\mathcal{L}_{\mathcal{F}} + B) \otimes I_m)) \|R\|^2, \end{aligned} \quad (2-32)$$

where the set in (2–31) reduces to the scalar inequality in (2–32) since the RHS is continuous a.e.; i.e., the RHS is continuous except for the Lebesgue negligible set of times when $R^T ((\mathcal{L}_{\mathcal{F}} + B) \otimes I_m) \beta K [\text{sgn}(E_2)] - R^T ((\mathcal{L}_{\mathcal{F}} + B) \otimes I_m) \beta K [\text{sgn}(E_2)] \neq \{0\}$.²

² The set of times $\Gamma \triangleq \left\{ t \in \mathbb{R}_{\geq 0} \mid R^T ((\mathcal{L}_{\mathcal{F}} + B) \otimes I_m) \beta K [\text{sgn}(E_2)] - R^T ((\mathcal{L}_{\mathcal{F}} + B) \otimes I_m) \beta K [\text{sgn}(E_2)] \neq \{0\} \right\}$ is equal to the set of times $\Phi = \cup_{l=1,2,\dots,\mathcal{F}m} \Phi_l$, where $\Phi_l \triangleq \{t \in \mathbb{R}_{\geq 0} \mid E_{2_l} = 0 \wedge R_l \neq 0\}$. Due to the structure of R in (2–9), Φ_l may be reexpressed as $\Phi_l = \left\{ t \in \mathbb{R}_{\geq 0} \mid E_{2_l} = 0 \wedge \dot{E}_{2_l} \neq 0 \right\}$. Since $E_2 : \mathbb{R}_{\geq 0} \rightarrow \mathbb{R}^{\mathcal{F}m}$ is continuously differentiable, it can be shown that Φ_l is Lebesgue measure zero [58]. Because a finite union of sets of Lebesgue measure zero is itself Lebesgue measure zero, Φ has Lebesgue measure zero. Hence, Γ is Lebesgue negligible.

Young's inequality gives $\|E_1\| \|E_2\| \leq \frac{1}{2} \|E_1\|^2 + \frac{1}{2} \|E_2\|^2$, which allows for (2–32) to be upper-bounded as

$$\begin{aligned} \dot{V}_L \stackrel{a.e.}{\leq} & \frac{1}{2} \|E_1\|^2 + \frac{1}{2} \|E_2\|^2 - \underline{\lambda}(\Lambda_1) \|E_1\|^2 - \underline{\lambda}(\Lambda_2) \|E_2\|^2 + \|R\| \rho(\|Z\|) \|Z\| \\ & - \underline{\lambda}(\mathcal{L}_{\mathcal{F}} + B) \|R\|^2 - \underline{\lambda}(K_s((\mathcal{L}_{\mathcal{F}} + B) \otimes I_m)) \|R\|^2. \end{aligned} \quad (2-33)$$

Using the gain condition in (2–28), (2–33) is upper-bounded by

$$\dot{V}_L \stackrel{a.e.}{\leq} -\psi \|Z\|^2 - \underline{\lambda}(K_s((\mathcal{L}_{\mathcal{F}} + B) \otimes I_m)) \|R\|^2 + \rho(\|Z\|) \|R\| \|Z\|. \quad (2-34)$$

Completing the squares for terms in (2–34) yields

$$\dot{V}_L \stackrel{a.e.}{\leq} - \left(\psi - \frac{\rho^2(\|Z\|)}{4 \underline{\lambda}(K_s((\mathcal{L}_{\mathcal{F}} + B) \otimes I_m))} \right) \|Z\|^2. \quad (2-35)$$

Provided the control gains k_i are selected sufficiently large such that $y(0) \in \mathcal{S}_{\mathcal{D}}$, the expression in (2–35) can be further upper-bounded by

$$\dot{V}_L \stackrel{a.e.}{\leq} -c \|Z\|^2 \quad (2-36)$$

for all $y \in \mathcal{D}$, for some positive constant $c \in \mathbb{R}$.

The inequalities in (2–26) and (2–36) can be used to show that $V_L \in \mathcal{L}_{\infty}$. Thus, $E_1, E_2, R \in \mathcal{L}_{\infty}$. The closed-loop error system can be used to conclude that the remaining signals are bounded. From (2–36), [61, Corollary 1] can be invoked to show that $c \|Z\|^2 \rightarrow 0$ as $t \rightarrow \infty \forall y(0) \in \mathcal{S}_{\mathcal{D}}$. Based on the definition of Z in (2–22), $\|E_1\| \rightarrow 0$ as $t \rightarrow \infty \forall y(0) \in \mathcal{S}_{\mathcal{D}}$. Noting the definition of E_1 in (2–7) and the fact that $((\mathcal{L} + B) \otimes I_m)$ is full rank, it is clear that $\|Q_L - Q_{\mathcal{F}}\| \rightarrow 0$ as $t \rightarrow \infty$ if and only if $\|E_1\| \rightarrow 0$ as $t \rightarrow \infty$. Thus, $\|q_L - q_i\| \rightarrow 0$ as $t \rightarrow \infty \forall i \in \mathcal{V}_{\mathcal{F}}, \forall y(0) \in \mathcal{S}_{\mathcal{D}}$. It logically follows that $\|q_i - q_j\| \rightarrow 0$ as $t \rightarrow \infty \forall i, j \in \mathcal{V}_{\mathcal{F}}, i \neq j, \forall y(0) \in \mathcal{S}_{\mathcal{D}}$. \square

Note that the region of attraction in (2–27) can be made arbitrarily large to include any initial conditions by adjusting the control gains k_i (i.e., a semi-global result). The decentralized controller shown in (2–13) and (2–14) is decentralized in the sense that

only local feedback is necessary to compute the controller. However, because the constant gain k_i must be selected based on sufficient conditions involving the matrix $\mathcal{L}_{\mathcal{F}} + B$, which contains information regarding the configuration of the entire network, this gain is selected in a centralized manner before the control law is implemented.

2.4 Simulation

Simulations were performed with multiple decentralized control methods for a network of robotic manipulators to compare the performance of the developed method with other related decentralized control methods. The developed control policy is compared with the adaptive control policy in [1] and the sliding mode-based control policy in [2, Section IV]. Simulation results are presented for the synchronization of four follower agents to a leader's state trajectory in the network shown in Fig. 2-1. Similar to [1] and [2, Section IV], each follower is modeled as a two-link robotic manipulator (a typical example of an Euler-Lagrange system) with the two-dimensional dynamics

$$u_i = \begin{bmatrix} p_{1,i} + 2p_{3,i}c_{2,i} & p_{2,i} + p_{3,i}c_{2,i} \\ p_{2,i} + p_{3,i}c_{2,i} & p_{2,i} \end{bmatrix} \ddot{q}_i + \begin{bmatrix} -p_{3,i}s_{2,i}\dot{q}_{2,i} & -p_{3,i}s_{2,i}(\dot{q}_{1,i} + \dot{q}_{2,i}) \\ p_{3,i}s_{2,i}\dot{q}_{1,i} & 0 \end{bmatrix} \dot{q} + \begin{bmatrix} f_{d1,i} & 0 \\ 0 & f_{d2,i} \end{bmatrix} \begin{bmatrix} \dot{q}_1 \\ \dot{q}_2 \end{bmatrix} + d_i,$$

where $q = \begin{bmatrix} q_1 \\ q_2 \end{bmatrix} \in \mathbb{R}^2$ denotes the joint angles, $c_{2,i} \triangleq \cos(q_{2,i})$, and $s_{2,i} \triangleq \sin(q_{2,i})$. The constant unknown parameters $p_{1,i}, p_{2,i}, p_{3,i}, f_{d1,i}, f_{d2,i} \in \mathbb{R}$ differ for each manipulator. The virtual leader is defined by the trajectory $q_L = \begin{bmatrix} 2 \sin(2t) \\ \cos(3t) \end{bmatrix}$, where the first and second entries are the desired trajectories for the first and second joint angles, respectively. The time-varying disturbance term has the form $d_i = \begin{bmatrix} a_i \sin(b_i t) \\ c_i \sin(d_i t) \end{bmatrix}$, where the constants $a_i, b_i, c_i, d_i \in \mathbb{R}$ differ for each manipulator. The model parameters for each manipulator are shown in Table 2-1.

The control gains for each method were selected based on convergence rate, residual error, and magnitude of control authority. The gains were obtained for each controller by qualitatively determining an appropriate range for each gain and then running 10,000 simulations with random gain sampling within those ranges in attempt to minimize

$$J = \sum_{i=1}^4 \sum_{j=1}^2 \text{rms}_{[2,10]}(q_{L,j} - q_{i,j}) \quad (2-37)$$

(with $a_{ij} = 1$ if $(j, i) \in \mathcal{E}_{\mathcal{F}}$ and $b_i = 4$ if $(L, i) \in \mathcal{E}_L$) while satisfying bounds on the control input such that the entry-wise inequality $u_k(t) \leq \begin{bmatrix} 500 \\ 150 \end{bmatrix}$, $k = 1, 2, 3, 4$, $\forall t \in [0.2, 10]$ is satisfied, where $\text{rms}_{[2,10]}(\cdot)$ denotes the root-mean-square (RMS) of the argument's sampled trajectory over the time interval $[2, 10]$. Beginning the RMS error at two seconds encourages high convergence rate and low residual error, while monitoring the control input only after 0.2 seconds accommodates for a possibly high initial control input. The cost function in (2-37) was chosen based on the synchronization goal that $\|q_L - q_i\|$ goes to zero.

Fig. 2-2 and 2-3 demonstrate that asymptotic synchronization of the follower agents and tracking of the leader trajectory are qualitatively achieved for the developed controller, despite the exogenous disturbances. Fig. 2-4 and 2-5 illustrate the effects of the control methods used to obtain synchronization: the controller in [2, Section IV] utilizes a high frequency, discontinuous, sliding-mode based control signal, whereas the developed controller is continuous and exhibits lower frequency content.

As shown in Fig. 2-2 and 2-3, asymptotic synchronization is qualitatively achieved more slowly for the control method in [2, Section IV], despite the fact that it is based on sliding-mode control concepts. This is due to the magnitude of the control signal being produced and the way the simulation trials are vetted. Observe from Fig. 2-4 that the control effort for [2, Section IV] is near to violating the entry-wise inequality $u_k(t) \leq$

$\begin{bmatrix} 500 \\ 150 \end{bmatrix}$; larger gains lead the control signal to violating this condition. In conclusion, it qualitatively appears that the control method in [2, Section IV] needs a higher control magnitude in addition to its high frequency content to achieve synchronization at a similar rate compared to the developed control method.

As shown in Fig. 2-2 - 2-5, the neural network-based adaptive controller given in [1] stabilizes the system using a continuous controller which produces a control signal of moderate magnitude, but maintains a residual error. This behavior agrees with the theoretical result in [1]: the controller achieves bounded convergence.

Table 2-2 provides a quantitative comparison of the controllers, where J is introduced in (2-37). Compared to the methods in [1] and [2, Section IV], the proposed controller provides significantly improved tracking performance with a continuous control signal of a relatively low magnitude.

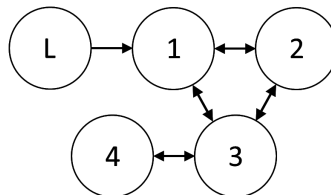


Figure 2-1. Network communication topology.

Table 2-1. Simulation parameters.

	Robot 1	Robot 2	Robot 3	Robot 4
$p_{1,i}$	3.7	3.5	3.2	3.0
$p_{2,i}$	0.22	0.20	0.18	0.17
$p_{3,i}$	0.19	0.25	0.23	0.21
$f_{d1,i}$	5.3	5.1	5.2	5.4
$f_{d2,i}$	1.1	1.3	1.0	1.2
a_i	2.0	4.0	3.0	5.0
b_i	1.0	2.0	3.0	5.0
c_i	1.0	3.0	4.0	2.0
d_i	4.0	3.0	1.0	2.0

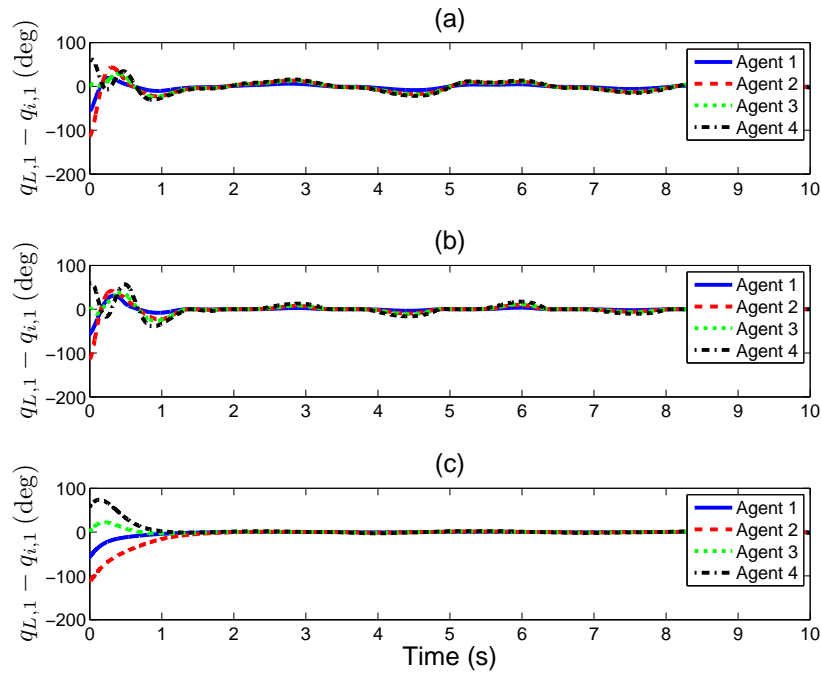


Figure 2-2. Joint 1 leader-tracking error using (a) [1], (b) [2, Section IV], and (c) the proposed controller.

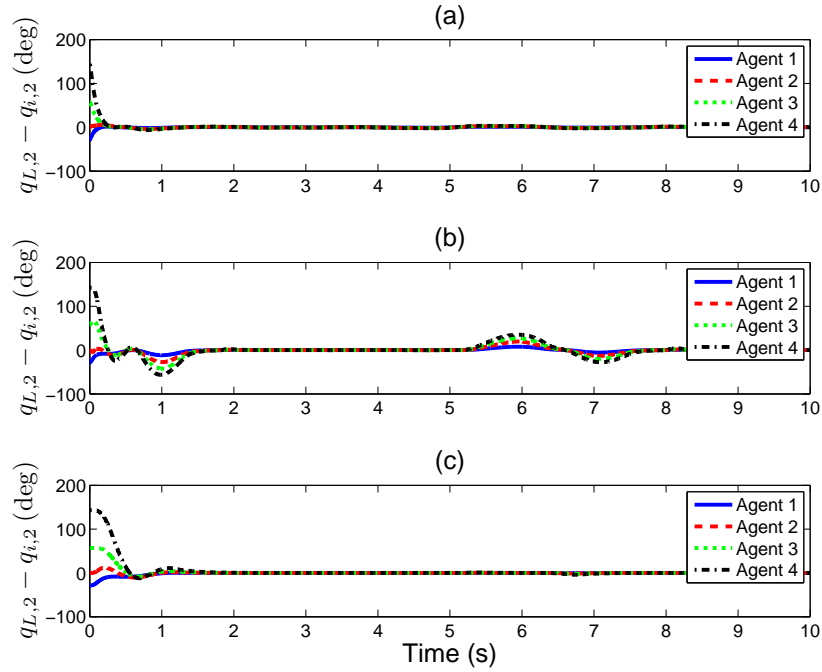


Figure 2-3. Joint 2 leader-tracking error using (a) [1], (b) [2, Section IV], and (c) the proposed controller.

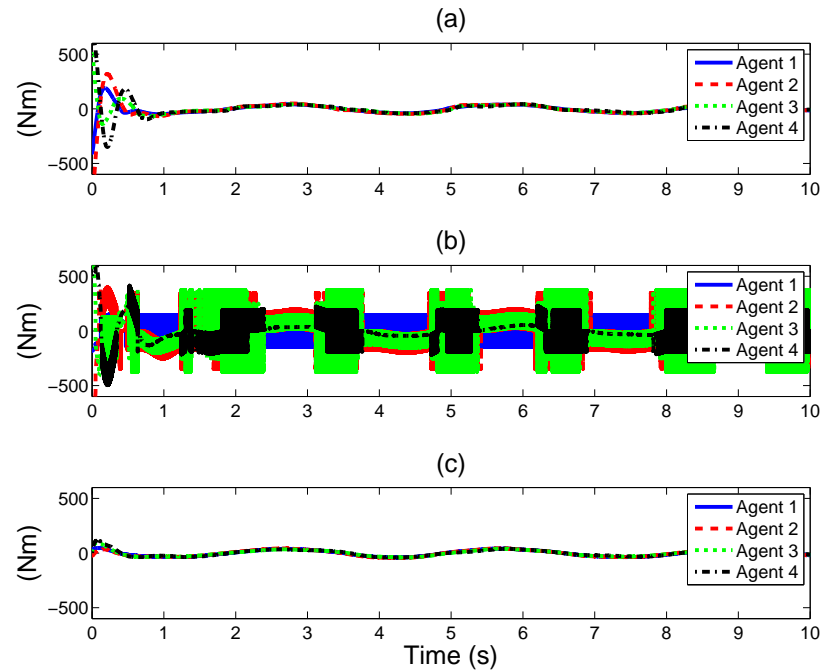


Figure 2-4. Joint 1 control effort using (a) [1], (b) [2, Section IV], and (c) the proposed controller.

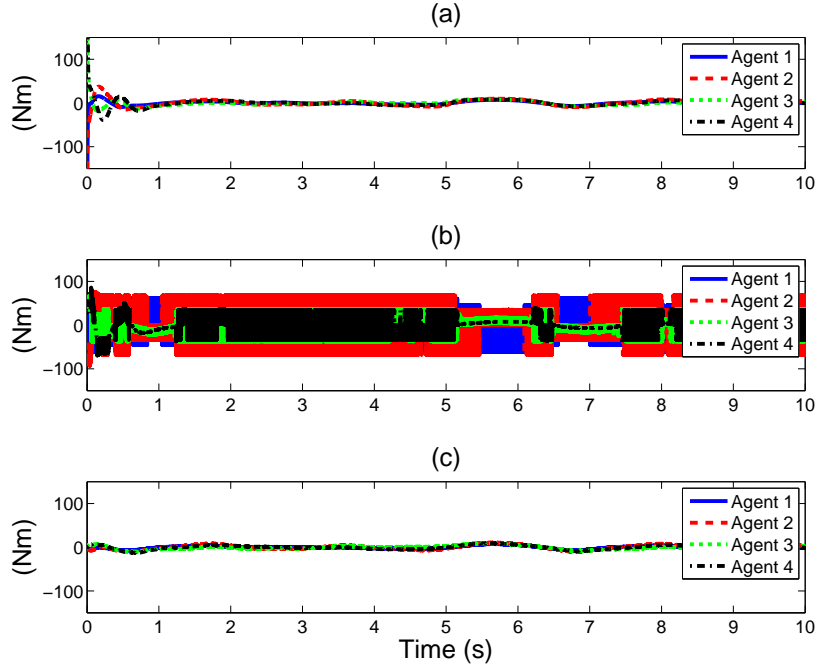


Figure 2-5. Joint 2 control effort using (a) [1], (b) [2, Section IV], and (c) the proposed controller.

Table 2-2. Controller performance comparison.

Method	$\max_{t \in [0, 2, 10]} \max_{i \in \mathcal{V}_{\mathcal{F}}} \ u_i\ $ (Nm)	J
[1]	352	0.638
[2, Section IV]	500	0.569
Proposed	73.4	0.0863

2.5 Extension to Formation Control

2.5.1 Modified Error Signal

Driving the neighborhood-based error signal in (2–5) to zero for each follower agent provides network synchronization such that the state of every agent converges to the state of the leader; for example, power networks supported by generators need to maintain synchronization of the generator phase angles to avoid damage of the electrical infrastructure system. However, for some applications, it may be desirable to drive the states of the follower agents to a configuration that is spatially oriented with

respect to the leader, such as the spatial arrangement shown in Fig. 2-6. This goal, often called “flocking” or “formation control”, can be accomplished by a simple extension of the synchronization framework. The control objective for formation control can be cast as $\lim_{t \rightarrow \infty} \|q_L - q_i + q_{diL}\| = 0$, where the vector $q_{diL} \in \mathbb{R}^m$ is a desired relative position of agent $i \in \mathcal{V}_{\mathcal{F}}$ with respect to the leader. A new neighborhood-based error signal, denoted as $e_{F1,i} \in \mathbb{R}^m$, can be designed to accomplish formation control by a modification of (2-5) as

$$e_{F1,i} \triangleq \sum_{j \in \mathcal{N}_{\mathcal{F}i}} a_{ij} ((q_j - q_{djL}) - (q_i - q_{diL})) + b_i (q_L - (q_i - q_{diL})), \quad (2-38)$$

which is implementable provided that each agent is encoded with the relative position information q_{diL} , $q_{diL} - q_{djL}$ for each neighbor $j \in \mathcal{N}_{\mathcal{F}i}$ prior to control implementation. Similar to the definition of E_1 , the network stack of the error signal $e_{F1,i}$ can be written as

$$\begin{aligned} E_{F1} &\triangleq [e_{F1,1}^T, \dots, e_{F1,\mathcal{F}}^T]^T \\ &= ((\mathcal{L}_{\mathcal{F}} + B) \otimes I_m) (Q_L - Q_{\mathcal{F}} + Q_d), \end{aligned}$$

where $Q_d \triangleq [q_{d1L}^T, \dots, q_{d\mathcal{F}L}^T]^T$ is the stack of desired relative positions. Provided that each desired relative position q_{diL} is constant, the controller in (2-13) can be shown to achieve the control objective $\lim_{t \rightarrow \infty} \|q_L - q_i + q_{diL}\| = 0$ with the error signal modification $e_{2,i} = \dot{e}_{F1,i} + \alpha_{1,i} e_{F1,i}$ despite the effects of modeling uncertainties and unknown disturbances using the convergence analysis given for the synchronization problem in this chapter. A similar approach can be used to demonstrate achievement of the formation control objective if the desired relative positions are time-varying using sufficient conditions on boundedness and smoothness of the relative position vectors' trajectories and their first, second and third derivatives.

2.5.2 Simulation

To demonstrate the utility of the error signal in (2-38) in achieving formation control, a numerical simulation is performed using ship dynamics detailed in [63].

Following [63], the experimentally verified model of the equations of motion of the surface ship “CyberShip II” can be written as

$$M_i \dot{\vartheta}_i + C_i(\vartheta_i) \vartheta_i + D_i(\vartheta_i) \dot{\vartheta}_i + d_i(t) = u_{\vartheta_i}, \quad (2-39)$$

where $M_i \in \mathbb{R}^{3 \times 3}$ denotes the ship’s inertia matrix, $C_i : \mathbb{R}^3 \rightarrow \mathbb{R}^{3 \times 3}$ denotes the Coriolis and centrifugal matrix, $D_i : \mathbb{R}^3 \rightarrow \mathbb{R}^{3 \times 3}$ denotes the nonlinear damping matrix, $d_i : \mathbb{R} \rightarrow \mathbb{R}^3$ denotes a time-varying exogenous disturbance, $u_{\vartheta_i} \in \mathbb{R}^3$ is the control effort, and the vector $\vartheta_i \triangleq [u_i, v_i, \dot{\psi}_i]^T$ contains the body-fixed linear velocities in surge ($u_i \in \mathbb{R}$) and sway ($v_i \in \mathbb{R}$) and the yaw (heading) angle rate $\dot{\psi}_i \in \mathbb{R}$. CyberShip II is a scaled replica of a supply ship and is fully actuated with two main propellers, two aft rudders, and one bow thruster; more information, including the units of all coordinates and parameters, can be seen in [63]. The matrices M_i, C_i, D_i are identified in [63] and written compactly in [64] as

$$M_i = \begin{bmatrix} 25.8 & 0 & 0 \\ 0 & 33.8 & 1.01 \\ 0 & 1.01 & 2.76 \end{bmatrix},$$

$$C_i = \begin{bmatrix} 0 & 0 & -33.8v_i - 1.01\dot{\psi}_i \\ 0 & 0 & 25.8u_i \\ 33.8v_i + 1.01\dot{\psi}_i & -25.8u_i & 0 \end{bmatrix},$$

$$D_i = \begin{bmatrix} 1.33 |u_i| + 5.87u_i^2 + 0.72 & 0 & 0 \\ 0 & 36.5 |v_i| + 0.805 |\dot{\psi}_i| + 0.890 & 0.845 |v_i| + 3.45 |\dot{\psi}_i| + 7.25 \\ 0 & 3.96 |v_i| - 0.130 |\dot{\psi}_i| + 0.0313 & 0.080 |v_i| + 0.75 |\dot{\psi}_i| + 1.90 \end{bmatrix}.$$

Using a local earth-fixed coordinate frame, the model in (2-39) can be transformed to the coordinates $q_i = [x_i, y_i, \psi_i]^T$ containing surge position ($x_i \in \mathbb{R}$), sway position ($y_i \in \mathbb{R}$),

and yaw angle ψ_i as

$$M'_i(q_i) \ddot{q}_i + C'_i(q_i, \dot{q}_i) \dot{q}_i + D'_i(q_i, \dot{q}_i) \dot{q}_i + d'_i = u'_i \quad (2-40)$$

with the kinematic transformations

$$\begin{aligned} M'_i &= J_i^{-T} M_i J_i^{-T} \\ C'_i &= J_i^{-T} \left[C_i - M_i J_i^{-1} \dot{J}_i \right] J_i^{-1} \\ D'_i &= J_i^{-T} D_i J_i^{-1} \\ d'_i &= J_i^{-T} d_i \end{aligned}$$

where $u'_i \in \mathbb{R}^3$ and the rotation matrix J provides the kinematic relationship $\dot{q}_i = J_i(q_i) \vartheta_i$ as

$$J_i = \begin{bmatrix} \cos(\psi_i) & -\sin(\psi_i) & 0 \\ \sin(\psi_i) & \cos(\psi_i) & 0 \\ 0 & 0 & 1 \end{bmatrix}.$$

Thus, the ship's dynamics can be transformed to a model with the same structure as (2-2), where u'_i is used to command the formation control in terms of surge, sway and yaw. The simulation is performed with four follower agents in the communication topology shown in Fig. 2-6, where each follower agent is modeled with the dynamics for the ship CyberShip II given in (2-40). Each surface ship is affected by disturbances (e.g., waves) as $d'_i = [a_{1,i} \sin(t), a_{2,i} \sin(t), 0]^T$, where the constants $a_1, a_2 \in \mathbb{R}$ are shown in Table 2-3. The desired formation of the surface ships with respect to the leader is encoded with the constant vectors q_{diL} , which are given in Table 2-3. The initial positions of the follower agents are not coincident with the initial desired positions and are described in Table 2-3. The initial velocities for each follower agent $i \in \mathcal{V}_F$ are set as $\dot{q}_i(0) = [0, 0, 0]^T$. The leader trajectory traces an ellipse with the trajectories $u_L = 10 \cos\left(\frac{1}{40}(2\pi t)\right)$, $v_L = 5 \sin\left(\frac{1}{40}(2\pi t)\right)$, $\psi_L = \tan^{-1}\left(\frac{v_L}{u_L}\right)$. The control gains for each

follower agent are selected as $k_i = \begin{bmatrix} 400 & 0 & 0 \\ 0 & 300 & 0 \\ 0 & 0 & 150 \end{bmatrix}$, $\chi_i = 100$, $\alpha_{1,i} = 3$, and $\alpha_{2,i} = 3$

for all $i \in \mathcal{V}_{\mathcal{F}}$.

Fig. 2-7 depicts the trajectories of the leader and follower agents in surge and sway as the follower agents converge to the desired formation positions relative to the network leader. The agent positions and desired positions at 0, 15, and 30 seconds are denoted by markers, where the leader position is represented by an asterisk, the follower agent positions are represented by squares, and the desired formation positions of the follower agents are represented by circles. Fig. 2-8 depicts the error in convergence of the follower agent states to the state of the leader offset by the constant desired relative position in terms of surge, sway and yaw. As shown in Fig. 2-7 and 2-8, the follower surface ships quickly converge to the formation positions specified by the leader position and the desired relative positions of the agents, despite limited connectivity to the leader, model uncertainty and exogenous disturbances.

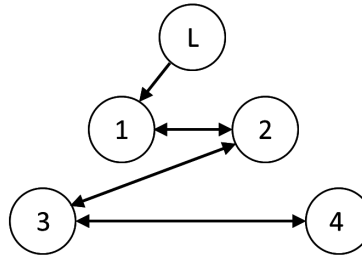


Figure 2-6. Network communication topology.

Table 2-3. Disturbance and formation position parameters.

	Robot 1	Robot 2	Robot 3	Robot 4
$a_{1,i}$	0.5	1.1	0.7	0.2
$a_{2,i}$	0.9	-0.5	-0.8	0.4
q_{diL}	$\begin{bmatrix} -2 \\ -2 \\ 0 \end{bmatrix}$	$\begin{bmatrix} 2 \\ -2 \\ 0 \end{bmatrix}$	$\begin{bmatrix} -4 \\ -4 \\ 0 \end{bmatrix}$	$\begin{bmatrix} 4 \\ -4 \\ 0 \end{bmatrix}$
$q_i(0)$	$\begin{bmatrix} 10 \\ -11 \\ 5.7 \end{bmatrix}$	$\begin{bmatrix} 17 \\ 1 \\ 8.6 \end{bmatrix}$	$\begin{bmatrix} 8 \\ 2 \\ -5.7 \end{bmatrix}$	$\begin{bmatrix} 7 \\ -9 \\ -11 \end{bmatrix}$

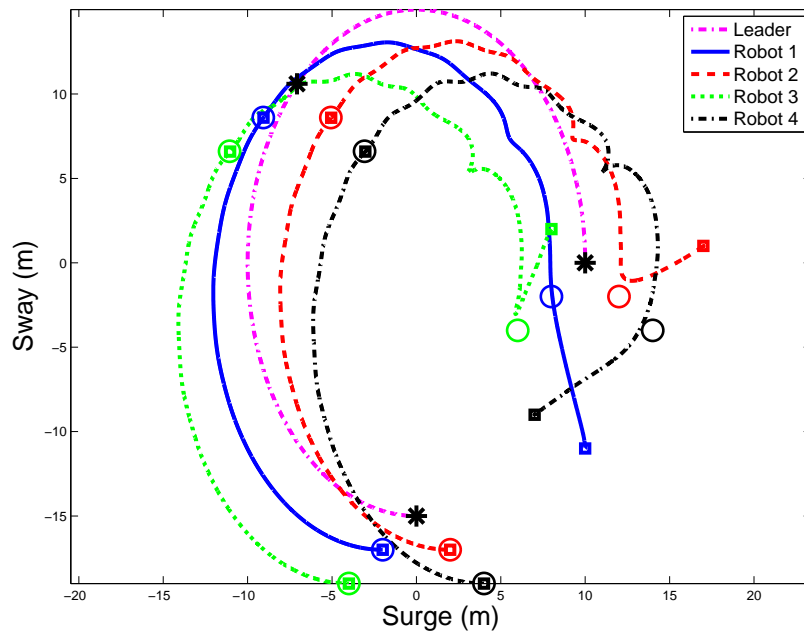


Figure 2-7. Agent trajectories in surge and sway.

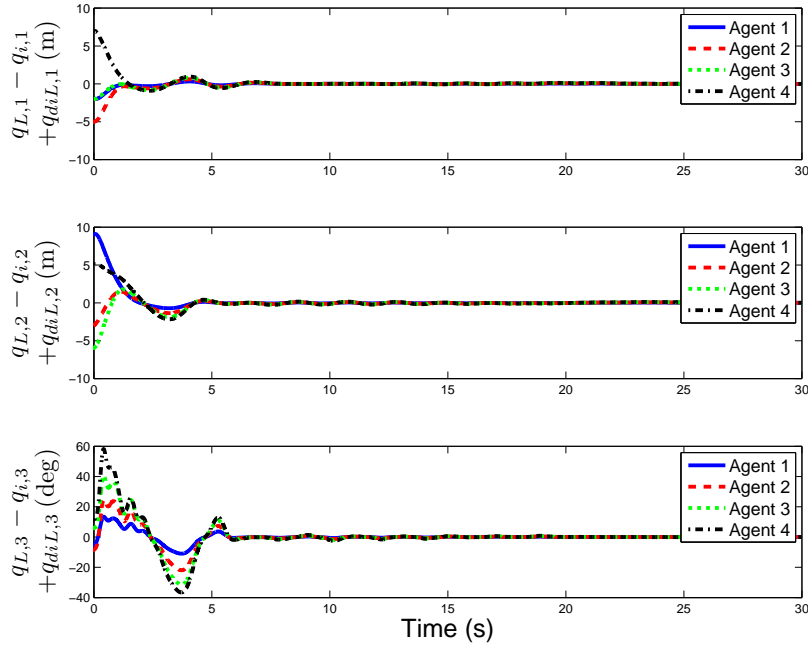


Figure 2-8. Error in convergence to the formation positions in the dimensions surge, sway and yaw.

2.6 Concluding Remarks

A decentralized RISE-based controller was developed which ensures semi-global asymptotic synchronization of networked followers' states towards a leader's time-varying state using a continuous control input, despite model uncertainty and exogenous disturbances, where the leader and follower agents have uncertain and heterogeneous Euler-Lagrange dynamics. The graph of the networked follower agents is assumed to be connected and at least one follower agent receives information from the leader. Simulation results are provided for the proposed decentralized controller to demonstrate its performance compared to other prominent related decentralized controllers. An extension to the developed error signal is provided for the application of formation control, wherein follower agents converge to a geometric formation specified with respect to the leader. Numerical simulation results are provided for the problem of formation control of a decentralized network of surface ships to demonstrate the performance of the developed controller when applied to formation control.

CHAPTER 3 ROBUST CONTAINMENT CONTROL IN A LEADER-FOLLOWER NETWORK OF UNCERTAIN EULER-LAGRANGE SYSTEMS

The previous chapter presented a controller development for the asymptotic synchronization of a network of follower agents to the trajectory of a single leader. This chapter extends the decentralized controller for single-leader synchronization to the problem of tracking multiple leaders by a network of follower agents. Tracking of multiple leaders is generally referred to as containment control, wherein follower agents can communicate with multiple leaders; for example, containment control is useful in applications where a team of autonomous vehicles is directed by multiple pilots or for networks of autonomous systems where only a subset of the systems is equipped with expensive sensing hardware. The typical objective of containment control is to drive the states of the follower agents to the convex hull of the leaders' states, where each follower agents' trajectory converges to a linear combination of the leaders' trajectories which depends on the structure of the follower network, leader connections, and the weights in the decentralized error signals. This result is facilitated by a lemma which relates a neighborhood-based error signal to containment of the follower agents within the dynamic convex hull spanned by the leaders' states.

3.1 Problem Formulation

3.1.1 Notation for a Multi-Leader Network

Some additional notation is introduced to facilitate the description of multiple leaders' interaction within a network. Consider a network of $L \in \mathbb{Z}_{>0}$ leader agents and $\mathcal{F} \in \mathbb{Z}_{>0}$ follower agents. Communication of the follower agents is described with a fixed undirected graph, $\mathcal{G}_{\mathcal{F}} = \{\mathcal{V}_{\mathcal{F}}, \mathcal{E}_{\mathcal{F}}\}$, where $\mathcal{V}_{\mathcal{F}} \triangleq \{L + 1, \dots, L + \mathcal{F}\}$ is the set of follower nodes and $\mathcal{E}_{\mathcal{F}} \subseteq \mathcal{V}_{\mathcal{F}} \times \mathcal{V}_{\mathcal{F}}$ is the corresponding edge set. An undirected edge (j, i) (and also (i, j)) is an element of $\mathcal{E}_{\mathcal{F}}$ if agents $i, j \in \mathcal{V}_{\mathcal{F}}$ communicate information with each other; without loss of generality, the graph is considered to be simple, i.e., $(i, i) \notin \mathcal{E}_{\mathcal{F}} \forall i \in \mathcal{V}_{\mathcal{F}}$. The follower agent neighbor set $\mathcal{N}_{\mathcal{F}i} \triangleq \{j \in \mathcal{V}_{\mathcal{F}} \mid (j, i) \in \mathcal{E}_{\mathcal{F}}\}$ is the

set of follower agents that transmit information to agent i . The connections in $\mathcal{G}_{\mathcal{F}}$ are succinctly described with the adjacency matrix $\mathcal{A}_{\mathcal{F}} = [a_{ij}] \in \mathbb{R}^{\mathcal{F} \times \mathcal{F}}$, where $a_{ij} > 0$ if $(j, i) \in \mathcal{E}_{\mathcal{F}}$ and $a_{ij} = 0$ otherwise. The Laplacian matrix $\mathcal{L}_{\mathcal{F}} = [p_{ij}] \in \mathbb{R}^{\mathcal{F} \times \mathcal{F}}$ associated with graph $\mathcal{G}_{\mathcal{F}}$ is constructed such that $p_{ii} = \sum_{j \in \mathcal{N}_{\mathcal{F}i}} a_{ij}$ and $p_{ij} = -a_{ij}$ if $i \neq j$. The directed graph $\mathcal{G} = \{\mathcal{V}_{\mathcal{F}} \cup \mathcal{V}_L, \mathcal{E}_{\mathcal{F}} \cup \mathcal{E}_L\}$ containing both the leader and follower agents is a supergraph of $\mathcal{G}_{\mathcal{F}}$ constructed by appending an edge $(l, i) \in \mathcal{E}_L$ to $\mathcal{G}_{\mathcal{F}}$ if leader agent $l \in \mathcal{V}_L$ communicates information to follower agent $i \in \mathcal{V}_{\mathcal{F}}$, where $\mathcal{V}_L \triangleq \{1, \dots, L\}$ is the leader node set and $\mathcal{E}_L \subseteq \mathcal{V}_L \times \mathcal{V}_{\mathcal{F}}$ is the set of leader-follower edges. The adjacency matrix $\mathcal{A} = [a_{ij}] \in \mathbb{R}^{(L+\mathcal{F}) \times (L+\mathcal{F})}$ for graph \mathcal{G} is similarly defined such that $a_{ij} > 0$ if $(j, i) \in \mathcal{E}_{\mathcal{F}} \cup \mathcal{E}_L$ and $a_{ij} = 0$ otherwise. Let the diagonal leader-connectivity matrix $B = [b_{ij}] \in \mathbb{R}^{\mathcal{F} \times \mathcal{F}}$ be defined such that $b_{ii} = \sum_{l \in \mathcal{V}_L} a_{il}$. The Laplacian matrix for graph \mathcal{G} can be constructed similarly to $\mathcal{L}_{\mathcal{F}}$ and can be represented as $\mathcal{L} = \begin{bmatrix} \mathbf{0}_{L \times L} & \mathbf{0}_{L \times \mathcal{F}} \\ \mathcal{L}_L & \mathcal{L}_{\mathcal{F}} + B \end{bmatrix}$, where $\mathcal{L}_L \in \mathbb{R}^{\mathcal{F} \times L}$.

3.1.2 Dynamic Models and Properties

The dynamics of each follower agent $i \in \mathcal{V}_{\mathcal{F}}$ are described by the nonidentical Euler-Lagrange equations of motion

$$M_i(q_i) \ddot{q}_i + C_i(q_i, \dot{q}_i) \dot{q}_i + F_i(\dot{q}_i) + G_i(q_i) + d_i = u_i, \quad (3-1)$$

where $q_i \in \mathbb{R}^m$ is the generalized configuration coordinate, $M_i : \mathbb{R}^m \rightarrow \mathbb{R}^{m \times m}$ is the inertia matrix, $C_i : \mathbb{R}^m \times \mathbb{R}^m \rightarrow \mathbb{R}^{m \times m}$ is the Coriolis/centrifugal matrix, $F_i : \mathbb{R}^m \rightarrow \mathbb{R}^m$ represents friction, $G_i : \mathbb{R}^m \rightarrow \mathbb{R}^m$ represents gravitational effects, $u_i \in \mathbb{R}^m$ represents the vector of control inputs, and $d_i : \mathbb{R}_{\geq 0} \rightarrow \mathbb{R}^m$ is a time-varying nonlinear exogenous disturbance. Functional dependency will be omitted in the remainder of the chapter where the meaning is clear from context. The following assumption is characteristic of physical systems with dynamics described by Euler-Lagrange equations of motion.

Assumption 3.1. For each follower agent $i \in \mathcal{V}_F$, the inertia matrix is positive definite and symmetric, and there exist positive constants $\underline{m}, \bar{m} \in \mathbb{R}$ such that the inertia matrix satisfies the inequalities $\underline{m} \|\xi\|^2 \leq \xi^T M_i(\psi) \xi \leq \bar{m} \|\xi\|^2$ for all $\xi, \psi \in \mathbb{R}^m$ and $i \in \mathcal{V}_F$.

The following assumptions concerning the smoothness of dynamics and network connectivity are used in the subsequent controller performance analysis.

Assumption 3.2. [52] For each follower agent $i \in \mathcal{V}_F$, the functions M_i, C_i, F_i, G_i are second order differentiable such that the second time derivative is bounded provided $q_i^{(k)} \in \mathcal{L}_\infty, k = 0, \dots, 3$.

Assumption 3.3. [51] For each follower agent $i \in \mathcal{V}_F$, the time-varying disturbance term is sufficiently smooth such that it and its first two time derivatives, $d_i, \dot{d}_i, \ddot{d}_i$, are bounded by known¹ constants.

Assumption 3.4. Each time-varying leader configuration coordinate, $q_l : \mathbb{R}_{\geq 0} \rightarrow \mathbb{R}^m$ ($l \in \mathcal{V}_L$), is sufficiently smooth such that $q_l \in \mathcal{C}^2$; additionally, each leader configuration coordinate and its first two time derivatives are bounded such that $q_l, \dot{q}_l, \ddot{q}_l \in \mathcal{L}_\infty$.

Assumption 3.5. For each follower agent $i \in \mathcal{V}_F$, there exists a directed path from a leader $l \in \mathcal{V}_L$ to i .

Note that, similar to Chapter 2, the matrix $\mathcal{L}_F + B$ is positive definite by Assumption 3.5 and [18, Lemma 4.1]. For convenience, the follower agents' dynamics are stacked as

$$M\ddot{Q}_F + C\dot{Q}_F + F + G + d = u, \quad (3-2)$$

where $M \triangleq \text{diag}(M_{L+1}, \dots, M_{L+F}) \in \mathbb{R}^{\mathcal{F}m \times \mathcal{F}m}$, $Q_F \triangleq \begin{bmatrix} q_{L+1}^T & \dots & q_{L+F}^T \end{bmatrix}^T \in \mathbb{R}^{\mathcal{F}m}$, $C \triangleq \text{diag}(C_{L+1}, \dots, C_{L+F}) \in \mathbb{R}^{\mathcal{F}m \times \mathcal{F}m}$, $F \triangleq \begin{bmatrix} F_{L+1}^T & \dots & F_{L+F}^T \end{bmatrix}^T \in \mathbb{R}^{\mathcal{F}m}$,

¹ Following the developments in [53] and [54], Assumption 3.3 can be relaxed such that the bounding constants can be unknown.

$$G \triangleq \left[G_{L+1}^T, \dots, G_{L+\mathcal{F}}^T \right]^T \in \mathbb{R}^{\mathcal{F}m}, d \triangleq \left[d_{L+1}^T, \dots, d_{L+\mathcal{F}}^T \right]^T \in \mathbb{R}^{\mathcal{F}m}, \text{ and}$$

$$u \triangleq \left[u_{L+1}^T, \dots, u_{L+\mathcal{F}}^T \right]^T \in \mathbb{R}^{\mathcal{F}m}.$$

3.1.3 Control Objective

The objective is to design a continuous controller for the follower agent dynamics in (3–1) which drives the states of all follower agents to the (possibly time-varying) convex hull spanned by the leader agents' states despite exogenous input disturbances and modeling uncertainties. Furthermore, only the configuration coordinate and its first time derivative are assumed to be measurable for the leader and follower agents. An error signal, $e_{1,i} \in \mathbb{R}^m$ ($i \in \mathcal{V}_{\mathcal{F}}$), is developed to quantify the neighborhood tracking error as

$$e_{1,i} \triangleq \sum_{j \in \mathcal{V}_{\mathcal{F}} \cup \mathcal{V}_L} a_{ij} (q_i - q_j), \quad (3-3)$$

which includes the state difference between neighboring follower agents and neighboring leader agents, if those connections exist. Note that there is no restriction on an edge weight a_{ij} for an existing connection $(j, i) \in \mathcal{E}$ other than that the weight is positive and $a_{ij} = a_{ji} \forall i, j \in \mathcal{V}_{\mathcal{F}}$. Therefore, the control can emphasize a connection (j, i) by increasing a_{ij} if it is desired for agent $i \in \mathcal{V}_{\mathcal{F}}$ to maintain close similarity to agent $j \in \mathcal{V}_{\mathcal{F}} \cup \mathcal{V}_L$. An auxiliary tracking error, $e_{2,i} \in \mathbb{R}^m$, is designed as

$$e_{2,i} \triangleq \dot{e}_{1,i} + \alpha_{1,i} e_{1,i},$$

where $\alpha_{1,i} \in \mathbb{R}_{>0}$ is a constant gain. By stacking the follower agents' error signals $e_{1,i}$ and $e_{2,i}$ as $E_1 \triangleq [e_{1,L+1}^T, \dots, e_{1,L+\mathcal{F}}^T]^T \in \mathbb{R}^{\mathcal{F}m}$ and $E_2 \triangleq [e_{2,L+1}^T, \dots, e_{2,L+\mathcal{F}}^T]^T \in \mathbb{R}^{\mathcal{F}m}$, the network error dynamics can be written as

$$E_1 = ((\mathcal{L}_{\mathcal{F}} + B) \otimes I_m) Q_{\mathcal{F}} + (\mathcal{L}_L \otimes I_m) Q_L, \quad (3-4)$$

$$E_2 = \dot{E}_1 + \Lambda_1 E_1, \quad (3-5)$$

where $Q_L \triangleq \begin{bmatrix} q_1^T & \dots & q_L^T \end{bmatrix}^T \in \mathbb{R}^{Lm}$ is the stack of leader agent states, and $\Lambda_1 \triangleq \text{diag}(\alpha_{1,L+1}, \dots, \alpha_{1,L+\mathcal{F}}) \otimes I_m \in \mathbb{R}^{\mathcal{F}m \times \mathcal{F}m}$ is a diagonal matrix of gains. An auxiliary error signal, $R \in \mathbb{R}^{\mathcal{F}m}$, is designed as

$$R \triangleq ((\mathcal{L}_{\mathcal{F}} + B)^{-1} \otimes I_m) \left(\dot{E}_2 + \Lambda_2 E_2 \right), \quad (3-6)$$

where $\Lambda_2 \triangleq \text{diag}(\alpha_{2,L+1}, \dots, \alpha_{2,L+\mathcal{F}}) \otimes I_m \in \mathbb{R}^{\mathcal{F}m \times \mathcal{F}m}$ is a diagonal matrix containing the gains $\alpha_{2,i} \in \mathbb{R}_{>0}$. The auxiliary error signal R is not used in the subsequently designed controller since it depends on the second derivative of the configuration coordinate and is only introduced to facilitate an expression for the closed-loop error system.

Similar to [24], the error system in (3-3) is designed such that $\|E_1\| \rightarrow 0$ implies that the Euclidean distance from q_i to the convex hull formed by the leader agents also asymptotically converges to zero for all $i \in \mathcal{V}_{\mathcal{F}}$. This implication is stated in the following lemma, which is used in the subsequent development.

Lemma 3.1. *If Assumption 3.5 is satisfied, then $\|E_1\| \rightarrow 0$ implies that*

$$d(q_i, \text{Conv} \{q_l \mid l \in \mathcal{V}_L\}) \rightarrow 0 \quad \forall i \in \mathcal{V}_{\mathcal{F}},$$

where $\text{Conv} \{\cdot\}$ denotes the convex hull of the set of points in its argument and the distance $d(p, S)$ between a point p and a set S is defined as $\inf_{s \in S} \|p - s\|$ for all $p \in \mathbb{R}^n$ and $S \subset \mathbb{R}^n$.

Proof. See Appendix B. □

3.2 Controller Development

An open-loop error system is designed by pre-multiplying the auxiliary tracking error R in (3-6) by M and using (3-2), (3-4) and (3-5) as

$$MR = u - d + S_1 + S_2, \quad (3-7)$$

where the functions $S_1 : \Pi_{k=1}^7 \mathbb{R}^{\mathcal{F}m} \rightarrow \mathbb{R}^{\mathcal{F}m}$ and $S_2 \Pi_{k=1}^3 \mathbb{R}^{\mathcal{F}m} \rightarrow \mathbb{R}^{\mathcal{F}m}$ are defined as

$$\begin{aligned}
S_1 \triangleq & M(Q_{\mathcal{F}}) ((\mathcal{L}_{\mathcal{F}} + B)^{-1} \otimes I_m) ((\Lambda_1 + \Lambda_2) E_2 - \Lambda_1^2 E_1) - C(Q_{\mathcal{F}}, \dot{Q}_{\mathcal{F}}) \dot{Q}_{\mathcal{F}} \\
& - F(\dot{Q}_{\mathcal{F}}) - G(Q_{\mathcal{F}}) + M(Q_{\mathcal{F}}) ((\mathcal{L}_{\mathcal{F}} + B)^{-1} \mathcal{L}_L \otimes I_m) \ddot{Q}_L \\
& + F\left(\left(\left(\left(\mathcal{L}_{\mathcal{F}} + B\right)^{-1} \mathcal{L}_L\right) \otimes I_m\right) \dot{Q}_L\right) + G\left(\left(\left(\left(\mathcal{L}_{\mathcal{F}} + B\right)^{-1} \mathcal{L}_L\right) \otimes I_m\right) Q_L\right) \\
& + C\left(\left(\left(\left(\mathcal{L}_{\mathcal{F}} + B\right)^{-1} \mathcal{L}_L\right) \otimes I_m\right) Q_L, \left(\left(\left(\mathcal{L}_{\mathcal{F}} + B\right)^{-1} \mathcal{L}_L\right) \otimes I_m\right) \dot{Q}_L\right) \\
& \cdot \left(\left(\left(\mathcal{L}_{\mathcal{F}} + B\right)^{-1} \mathcal{L}_L\right) \otimes I_m\right) \dot{Q}_L \\
& - M\left(\left(\left(\left(\mathcal{L}_{\mathcal{F}} + B\right)^{-1} \mathcal{L}_L\right) \otimes I_m\right) Q_L\right) \left(\left(\mathcal{L}_{\mathcal{F}} + B\right)^{-1} \mathcal{L}_L \otimes I_m\right) \ddot{Q}_L, \\
S_2 \triangleq & -C\left(\left(\left(\left(\mathcal{L}_{\mathcal{F}} + B\right)^{-1} \mathcal{L}_L\right) \otimes I_m\right) Q_L, \left(\left(\left(\mathcal{L}_{\mathcal{F}} + B\right)^{-1} \mathcal{L}_L\right) \otimes I_m\right) \dot{Q}_L\right) \\
& \times \left(\left(\left(\mathcal{L}_{\mathcal{F}} + B\right)^{-1} \mathcal{L}_L\right) \otimes I_m\right) \dot{Q}_L - F\left(\left(\left(\left(\mathcal{L}_{\mathcal{F}} + B\right)^{-1} \mathcal{L}_L\right) \otimes I_m\right) \dot{Q}_L\right) \\
& - G\left(\left(\left(\left(\mathcal{L}_{\mathcal{F}} + B\right)^{-1} \mathcal{L}_L\right) \otimes I_m\right) Q_L\right) \\
& + M\left(\left(\left(\left(\mathcal{L}_{\mathcal{F}} + B\right)^{-1} \mathcal{L}_L\right) \otimes I_m\right) Q_L\right) \left(\left(\mathcal{L}_{\mathcal{F}} + B\right)^{-1} \mathcal{L}_L \otimes I_m\right) \ddot{Q}_L.
\end{aligned}$$

Terms in (3–7) are organized so that, after a Mean Value Theorem-based approach (cf. [58, Lemma 5]), $\|S_1\|$ can be upper-bounded by a function of the errors signals E_1, E_2, R and $\|S_2\|$ can be upper-bounded by a constant. Note that the term $M(Q_{\mathcal{F}}) ((\mathcal{L}_{\mathcal{F}} + B)^{-1} \otimes I_m) ((\Lambda_1 + \Lambda_2) E_2 - \Lambda_1^2 E_1)$ can be upper-bounded by a function of the error signals using a Mean Value Theorem-based approach after adding and subtracting the term

$$M\left(\left(\left(\left(\mathcal{L}_{\mathcal{F}} + B\right)^{-1} \mathcal{L}_L\right) \otimes I_m\right) Q_L\right) \left(\left(\mathcal{L}_{\mathcal{F}} + B\right)^{-1} \otimes I_m\right) ((\Lambda_1 + \Lambda_2) E_2 - \Lambda_1^2 E_1)$$

within S_1 .

The developed robust decentralized controller for follower agent $i \in \mathcal{V}_{\mathcal{F}}$ is designed as

$$u_i = \sum_{j \in \mathcal{N}_{\mathcal{F}i}} a_{ij} \left((k_{s,j} + I_m) e_{2,j} - (k_{s,i} + I_m) e_{2,i} \right) - b_{ii} (k_{s,i} + I_m) e_{2,i} + \nu_i, \quad (3-8)$$

where the function $\nu_i : \prod_{j=1}^{|\mathcal{N}_{\mathcal{F}i}|+1} \mathbb{R}^m \rightarrow \mathbb{R}^m$ is the generalized solution to the differential equation

$$\begin{aligned} \dot{\nu}_i \triangleq & \sum_{j \in \mathcal{N}_{\mathcal{F}i}} a_{ij} ((k_{s,j} + I_m) \alpha_{2,j} e_{2,j} - (k_{s,i} + I_m) \alpha_{2,i} e_{2,i}) \\ & + \sum_{j \in \mathcal{N}_{\mathcal{F}i}} a_{ij} (\chi_j \operatorname{sgn}(e_{2,j}) - \chi_i \operatorname{sgn}(e_{2,i})) - (k_{s,i} + I_m) b_{ii} \alpha_{2,i} e_{2,i} - b_{ii} \chi_i \operatorname{sgn}(e_{2,i}) \end{aligned} \quad (3-9)$$

with $\nu_i(0) = \nu_{i0} \in \mathbb{R}^m$ as a user-specified initial condition, where $k_{s,i} \in \mathbb{R}^{m \times m}$ is a constant positive definite gain matrix, $\chi_i \in \mathbb{R}^{m \times m}$ is a constant diagonal positive definite gain matrix, and the function $\operatorname{sgn}(\cdot)$ is defined for all $\xi = \begin{bmatrix} \xi_1, & \dots, & \xi_v \end{bmatrix}^T \in \mathbb{R}^v$ as $\operatorname{sgn}(\xi) \triangleq \begin{bmatrix} \operatorname{sgn}(\xi_1), & \dots, & \operatorname{sgn}(\xi_v) \end{bmatrix}^T$. Note that the controller in (3-8) is continuous, only relies on the configuration coordinate and its first derivative, and is decentralized in communication: agent i requires its own error signal and the error signals of neighbors $j \in \mathcal{N}_{\mathcal{F}i}$. The use of neighbors' error signals in the control law provides cooperation among the follower agents. Assuming that a neighbor's state can be sensed, then only one-hop communication is necessary to compute the control authority in (3-8). In (3-8) and (3-9), the terms multiplied by the gain $k_{s,i}$ provide proportional and derivative feedback and the terms multiplied by the gain χ_i provide robust feedback which is used to reject the unknown time-varying disturbances, as shown in the following convergence analysis. Note that a strategy involving additive gradient-based control terms, such as that in [65], can be used if collision avoidance is necessary for the control objective.

After taking the time-derivative of (3-7), the closed-loop error system can be represented as

$$\begin{aligned} M\dot{R} = & -((\mathcal{L}_{\mathcal{F}} + B) \otimes I_m) (K_s + I_{\mathcal{F}m}) (\dot{E}_2 + \Lambda_2 E_2) - ((\mathcal{L}_{\mathcal{F}} + B) \otimes I_m) \beta \operatorname{sgn}(E_2) \\ & + \tilde{N} + ((\mathcal{L}_{\mathcal{F}} + B) \otimes I_m) N_d - ((\mathcal{L}_{\mathcal{F}} + B) \otimes I_m) E_2 - \frac{1}{2} \dot{M}R, \end{aligned} \quad (3-10)$$

where the first two terms are contributions from the derivative of the stack of follower agents' control inputs

$$\dot{u} = ((\mathcal{L}_{\mathcal{F}} + B) \otimes I_m) (K_s + I_{\mathcal{F}m}) \left(\dot{E}_2 + \Lambda_2 E_2 \right) - ((\mathcal{L}_{\mathcal{F}} + B) \otimes I_m) \beta \operatorname{sgn}(E_2),$$

$K_s \triangleq \operatorname{diag}(k_{s,L+1}, \dots, k_{s,L+\mathcal{F}}) \in \mathbb{R}^{\mathcal{F}m \times \mathcal{F}m}$ is a block diagonal gain matrix, $\beta \triangleq \operatorname{diag}(\chi_{L+1}, \dots, \chi_{L+\mathcal{F}}) \in \mathbb{R}^{\mathcal{F}m \times \mathcal{F}m}$ is a diagonal gain matrix, and the unknown auxiliary functions \tilde{N} and N_d are defined as

$$\tilde{N} \triangleq \dot{S}_1 + ((\mathcal{L}_{\mathcal{F}} + B) \otimes I_m) E_2 - \frac{1}{2} \dot{M}R, \quad (3-11)$$

$$N_d \triangleq ((\mathcal{L}_{\mathcal{F}} + B)^{-1} \otimes I_m) \left(\dot{d} + \dot{S}_2 \right). \quad (3-12)$$

Terms in \tilde{N} are segregated such that after taking advantage of the expressions $Q_{\mathcal{F}} = ((\mathcal{L}_{\mathcal{F}} + B)^{-1} \otimes I_m) E_1 - ((\mathcal{L}_{\mathcal{F}} + B)^{-1} \otimes I_m) (\mathcal{L}_L \otimes I_m) Q_L$, $\dot{E}_1 = E_2 - \Lambda_1 E_1$, and $\dot{E}_2 = ((\mathcal{L}_{\mathcal{F}} + B) \otimes I_m) R - \Lambda_2 E_2$, Assumptions 3.2 and 3.4, and a Mean Value Theorem-based approach (cf. [58, Lemma 5]), (3-11) can be upper-bounded by

$$\|\tilde{N}\| \leq \rho(\|Z\|) \|Z\|, \quad (3-13)$$

where $Z \in \mathbb{R}^{3\mathcal{F}m}$ is the composite error vector defined as $Z \triangleq \begin{bmatrix} E_1^T & E_2^T & R^T \end{bmatrix}^T$, and $\rho : \mathbb{R}_{\geq 0} \rightarrow \mathbb{R}_{\geq 0}$ is a strictly increasing, radially unbounded function. Moreover, other terms in (3-10) are segregated in the function N_d such that it and its first derivative can be upper-bounded such that, for all $k \in \{1, \dots, \mathcal{F}m\}$,

$$\sup_{t \in [0, \infty)} |N_d|_k \leq \delta_{a,k},$$

$$\sup_{t \in [0, \infty)} |\dot{N}_d|_k \leq \delta_{b,k},$$

after using Assumptions 3.3 and 3.4, where $|\cdot|_k$ denotes the absolute value of the k^{th} component of the vector argument, and $\delta_{a,k}, \delta_{b,k} \in \mathbb{R}_{>0}$ are constant bounds. In the subsequent convergence analysis, the terms in N_d and \dot{N}_d are compensated by

using the signum feedback terms in (3–9). For clarity in the following section, let the vectors $\Delta_{a,i}, \Delta_{b,i} \in \mathbb{R}^m$ be defined such that $\Delta_{a,i} \triangleq \left[\delta_{a,m(i-1)+1} \ \dots \ \delta_{a,m(i-1)+m} \right]^T$ and $\Delta_{b,i} \triangleq \left[\delta_{b,m(i-1)+1} \ \dots \ \delta_{b,m(i-1)+m} \right]^T$, which represent the contribution of the disturbance terms for each agent.

3.3 Convergence Analysis

An auxiliary function $P : \mathbb{R}^{\mathcal{F}m} \times \mathbb{R}^{\mathcal{F}m} \times \mathbb{R}_{\geq 0} \rightarrow \mathbb{R}$ is included in the subsequently defined candidate Lyapunov function so that sufficient gain conditions may be obtained for the compensation of the bounded disturbance terms in N_d . Let P be defined as the generalized solution to the differential equation

$$\begin{aligned} \dot{P} &= - \left(\dot{E}_2 + \Lambda_2 E_2 \right)^T (N_d - \beta \operatorname{sgn}(E_2)), \\ P(0) &= \sum_{k=1}^{\mathcal{F}m} \beta_{k,k} |E_2(0)|_k - E_2^T(0) N_d(0), \end{aligned} \quad (3-14)$$

where $\beta_{k,k}$ denotes the k^{th} diagonal entry of the diagonal gain matrix β . Provided the sufficient gain condition in (3–18) is satisfied, then $P \geq 0$ for all $t \in [0, \infty)$ (see Appendix A).

Remark 3.1. Because the closed-loop error system in (3–10) and the derivative of the signal P in (3–14) are discontinuous, the existence of Filippov solutions in the given differential equations is addressed before the Lyapunov-based convergence analysis is presented. Consider the composite vector $\eta \triangleq \left[Z^T, \nu_{L+1}^T, \dots, \nu_{L+\mathcal{F}}^T, \sqrt{P} \right]^T \in \mathbb{R}^{4\mathcal{F}m+1}$, composed of the stacked error signals, the signal contributing discontinuities to the derivative of the developed controller, and the aforementioned auxiliary signal P . Existence of Filippov solutions for the closed-loop dynamical system $\dot{\eta} = \mathcal{K}[h_1](\eta, t)$ can be established, where $h_1 : \mathbb{R}^{4\mathcal{F}m+1} \times \mathbb{R}_{\geq 0} \rightarrow \mathbb{R}^{4\mathcal{F}m+1}$ is a function defined as the RHS of $\dot{\eta}$ and $\mathcal{K}[h_1](\varrho, t) \triangleq \cap_{\delta>0} \cap_{\mu(S_m)=0} \overline{\text{co}} h_1(B_\delta(\varrho) \setminus S_m, t)$, where $\delta \in \mathbb{R}$, $\cap_{\mu(S_m)=0}$ denotes the intersection over the sets S_m of Lebesgue measure zero, $\overline{\text{co}}$ denotes convex closure,

and $B_\delta(\varrho) \triangleq \{\sigma \in \mathbb{R}^{4\mathcal{F}m+1} \mid \|\varrho - \sigma\| < \delta\}$, where $\sigma, \varrho \in \mathbb{R}^{4\mathcal{F}m+1}$ are used as dummy variables [59–61].

Let the auxiliary gain constant $\Phi \in \mathbb{R}$ be defined as

$$\Phi \triangleq \min \left\{ \min_{i \in \mathcal{V}_{\mathcal{F}}} \alpha_{1,i} - \frac{1}{2}, \min_{i \in \mathcal{V}_{\mathcal{F}}} \alpha_{2,i} - \frac{1}{2}, \lambda((\mathcal{L}_{\mathcal{F}} + B)^2) \right\}.$$

A continuously differentiable, positive definite candidate Lyapunov function $V_L : \mathcal{D} \rightarrow \mathbb{R}$ is defined as

$$V_L(y, t) \triangleq \frac{1}{2} E_1^T E_1 + \frac{1}{2} E_2^T E_2 + \frac{1}{2} R^T M(t) R + P, \quad (3-15)$$

where the composite vector $y \in \mathbb{R}^{3\mathcal{F}m+1}$ is defined as $y \triangleq \begin{bmatrix} Z^T & \sqrt{P} \end{bmatrix}^T$, \mathcal{D} is defined as the open and connected set

$$\mathcal{D} \triangleq \left\{ \sigma \in \mathbb{R}^{3\mathcal{F}m+1} \mid \|\sigma\| < \inf \left(\rho^{-1} \left(\left[2\sqrt{\Phi \lambda} \left(((\mathcal{L}_{\mathcal{F}} + B) \otimes I_m) K_s ((\mathcal{L}_{\mathcal{F}} + B) \otimes I_m) \right) \right], \infty \right) \right) \right\},$$

and $\rho^{-1}(\cdot)$ denotes the inverse mapping of a set argument. To facilitate the description of the semi-global property of the following Lyapunov-based convergence analysis, the set of stabilizing initial conditions $\mathcal{S}_{\mathcal{D}} \subset \mathcal{D}$ is defined as

$$\mathcal{S}_{\mathcal{D}} \triangleq \left\{ \sigma \in \mathcal{D} \mid \|\sigma\| < \sqrt{\frac{\lambda_1}{\lambda_2}} \inf \left(\rho^{-1} \left(\left[2\sqrt{\Phi \lambda} \left(((\mathcal{L}_{\mathcal{F}} + B) \otimes I_m) K_s ((\mathcal{L}_{\mathcal{F}} + B) \otimes I_m) \right) \right], \infty \right) \right) \right\}.$$

Due to the construction of V_L in (3–15), V_L satisfies the inequalities

$$\lambda_1 \|y\|^2 \leq V_L(y, t) \leq \lambda_2 \|y\|^2 \quad \forall t \in [0, \infty) \quad (3-16)$$

via Assumption 3.1, where $\lambda_1, \lambda_2 \in \mathbb{R}_{>0}$ are constants defined as $\lambda_1 \triangleq \frac{1}{2} \min \{1, \min_{j \in \mathcal{V}_{\mathcal{F}}} \underline{m}_j\}$ and $\lambda_2 \triangleq \max \{1, \frac{1}{2} \max_{j \in \mathcal{V}_{\mathcal{F}}} \bar{m}_j\}$. The following theorem describes the performance of the networked dynamical systems through the use of the Lyapunov function candidate in (3–15).

Theorem 3.1. For every follower agent $i \in \mathcal{V}_{\mathcal{F}}$, the decentralized controller in (3–8) guarantees that all signals are bounded under closed-loop control and that containment control is semi-globally achieved in the sense that $d(q_i, \text{Conv}\{q_l \mid l \in \mathcal{V}_L\}) \rightarrow 0$ as $t \rightarrow \infty$, provided that the gains $k_{s,i}$ are selected sufficiently large such that the initial condition $y(0)$ lies within the set of stabilizing initial conditions $S_{\mathcal{D}}$, Assumptions 3.1–3.5 are satisfied, and the gains $\alpha_{1,i}$, $\alpha_{2,i}$, χ_i are selected according to the sufficient conditions

$$\alpha_{1,i} > \frac{1}{2}, \quad \alpha_{2,i} > \frac{1}{2}, \quad (3-17)$$

$$\underline{\lambda}(\chi_i) > \|\Delta_{a,i}\|_{\infty} + \frac{1}{\alpha_{2,i}} \|\Delta_{b,i}\|_{\infty} \quad (3-18)$$

for all $i \in \mathcal{V}_{\mathcal{F}}$.

Proof. Using Filippov’s framework, a Filippov solution can be established for the closed-loop system $\dot{y} = h_2(y, t)$, where $h_2 : \mathbb{R}^{3\mathcal{F}m+1} \times \mathbb{R}_{\geq 0} \rightarrow \mathbb{R}^{3\mathcal{F}m+1}$ denotes the RHS of the derivative of the closed-loop error signals and \dot{P} . Accordingly, the time derivative of (3–15) exists a.e. on the time domain $[0, \infty)$ and $\dot{V}_L \stackrel{a.e.}{\in} \dot{\check{V}}_L$, where

$$\dot{\check{V}}_L = \cap_{\xi \in \partial V_L(y,t)} \xi^T \mathcal{K} \left[\begin{array}{ccccc} \dot{E}_1^T & \dot{E}_2^T & \dot{R}^T & \frac{1}{2}P^{-\frac{1}{2}}\dot{P} & 1 \end{array} \right]^T, \quad (3-19)$$

where ∂V_L is the generalized gradient of V_L and the entry 1 in (3–19) accommodates for the expression of M as time-dependent in (3–15). Because $V_L(y, t)$ is continuously differentiable,

$$\dot{\check{V}}_L \subseteq \nabla V_L \mathcal{K} \left[\begin{array}{ccccc} \dot{E}_1^T & \dot{E}_2^T & \dot{R}^T & \frac{1}{2}P^{-\frac{1}{2}}\dot{P} & 1 \end{array} \right]^T, \quad (3-20)$$

where $\nabla V_L \triangleq \left[\begin{array}{ccccc} E_1^T & E_2^T & R^T M & 2P^{\frac{1}{2}} & \frac{1}{2}R^T \dot{M}(t) R \end{array} \right]$. After using the calculus for $\mathcal{K}[\cdot]$ from [60] and substituting expressions from (3–5), (3–6), (3–10) and (3–14), (3–20) may

be written as

$$\begin{aligned}
\dot{V}_L \subseteq & E_1^T (E_2 - \Lambda_1 E_1) + E_2^T (((\mathcal{L}_{\mathcal{F}} + B) \otimes I_m) R - \Lambda_2 E_2) \\
& + R^T \left(-((\mathcal{L}_{\mathcal{F}} + B) \otimes I_m) (K_s + I_{\mathcal{F}m}) (\dot{E}_2 + \Lambda_2 E_2) \right. \\
& - ((\mathcal{L}_{\mathcal{F}} + B) \otimes I_m) \beta \mathcal{K} [\text{sgn}(E_2)] + \tilde{N} + (\mathcal{L}_{\mathcal{F}} + B) N_d \\
& \left. - ((\mathcal{L}_{\mathcal{F}} + B) \otimes I_m) E_2 - \frac{1}{2} \dot{M} R \right) + \frac{1}{2} R^T \dot{M} R - (\dot{E}_2 + \Lambda_2 E_2)^T (N_d - \beta \mathcal{K} [\text{sgn}(E_2)]),
\end{aligned} \tag{3-21}$$

where $\mathcal{K} [\text{sgn}(E_2)]_k = 1$ if $E_{2k} > 0$, $\mathcal{K} [\text{sgn}(E_2)]_k = -1$ if $E_{2k} < 0$, $\mathcal{K} [\text{sgn}(E_2)]_k \in [-1, 1]$ if $E_{2k} = 0$, and here the subscript k denotes the k^{th} vector entry [60]. The set in (3-21) reduces to a scalar since the RHS is continuous a.e. due to the structure of the error signals; i.e., the RHS is continuous except for the Lebesgue negligible set of time instances in which²

$$R^T ((\mathcal{L}_{\mathcal{F}} + B) \otimes I_m) \beta \mathcal{K} [\text{sgn}(E_2)] - R^T ((\mathcal{L}_{\mathcal{F}} + B) \otimes I_m) \beta \mathcal{K} [\text{sgn}(E_2)] \neq \{0\}.$$

After canceling common terms, using the Raleigh-Ritz theorem and triangle inequality, recalling that $\mathcal{L}_{\mathcal{F}} + B$ is positive definite and symmetric, and using the bounding strategy in (3-13), the scalar value \dot{V}_L can be upper-bounded a.e. as

$$\begin{aligned}
\dot{V}_L \stackrel{\text{a.e.}}{\leq} & \frac{1}{2} \|E_1\|^2 + \frac{1}{2} \|E_2\|^2 - \underline{\lambda}(\Lambda_1) \|E_1\|^2 - \underline{\lambda}(\Lambda_2) \|E_2\|^2 + \|R\| \rho(\|Z\|) \|Z\| \\
& - R^T ((\mathcal{L}_{\mathcal{F}} + B) \otimes I_m) K_s ((\mathcal{L}_{\mathcal{F}} + B) \otimes I_m) R - R^T ((\mathcal{L}_{\mathcal{F}} + B) \otimes I_m)^2 R.
\end{aligned} \tag{3-22}$$

² Due to the construction of R in (3-6), the set of time instances $\Theta \triangleq \{t \in \mathbb{R}_{\geq 0} \mid R^T ((\mathcal{L}_{\mathcal{F}} + B) \otimes I_m) \beta \mathcal{K} [\text{sgn}(E_2)] - R^T ((\mathcal{L}_{\mathcal{F}} + B) \otimes I_m) \beta \mathcal{K} [\text{sgn}(E_2)] \neq \{0\}\}$ can be represented by the union $\Theta = \cup_{k=1, \dots, \mathcal{F}m} \Theta_k$, where $\Theta_k \triangleq \{t \in \mathbb{R}_{\geq 0} \mid E_{2k} = 0 \wedge R_k \neq 0\}$. Because the signal $E_2 : \mathbb{R}_{\geq 0} \rightarrow \mathbb{R}^{\mathcal{F}m}$ is continuously differentiable, it can be shown that Θ_k is Lebesgue measure zero [58]. Because a finite union of Lebesgue measure zero sets is Lebesgue measure zero, Θ is Lebesgue measure zero. Hence, Θ is Lebesgue negligible.

Using the definition of the auxiliary gain constant Φ , which is positive given the sufficient gain conditions in (3–17) and the positive definite property of $\mathcal{L}_{\mathcal{F}} + B$ (note that the product $((\mathcal{L}_{\mathcal{F}} + B) \otimes I_m)^2$ is positive definite since $\mathcal{L}_{\mathcal{F}} + B$ is positive definite and symmetric), (3–22) is rewritten as

$$\dot{V}_L \stackrel{a.e.}{\leq} -\Phi \|Z\|^2 - \lambda(((\mathcal{L}_{\mathcal{F}} + B) \otimes I_m) K_s ((\mathcal{L}_{\mathcal{F}} + B) \otimes I_m)) \|R\|^2 + \|R\| \rho(\|Z\|) \|Z\|,$$

where the product $((\mathcal{L}_{\mathcal{F}} + B) \otimes I_m) K_s ((\mathcal{L}_{\mathcal{F}} + B) \otimes I_m)$ is positive definite since K_s is positive definite and $\mathcal{L}_{\mathcal{F}} + B$ is positive definite and symmetric. After completing the squares, \dot{V}_L is again upper-bounded a.e. by

$$\dot{V}_L \stackrel{a.e.}{\leq} - \left(\Phi - \frac{\rho^2(\|Z\|)}{4\lambda(((\mathcal{L}_{\mathcal{F}} + B) \otimes I_m) K_s ((\mathcal{L}_{\mathcal{F}} + B) \otimes I_m))} \right) \|Z\|^2.$$

Provided the gains $k_{s,i}$ are selected such that the respective minimum eigenvalues are sufficiently large such that $y(0) \in \mathcal{S}_{\mathcal{D}}$, there exists a constant $c \in \mathbb{R}_{>0}$ such that

$$\dot{V}_L \stackrel{a.e.}{\leq} -c \|Z\|^2 \tag{3–23}$$

for all $y \in \mathcal{D}$. Thus, the inequalities in (3–16) and (3–23) show that $V_L \in \mathcal{L}_{\infty}$ and therefore $E_1, E_2, R \in \mathcal{L}_{\infty}$. A simple analysis of the closed-loop error system shows that the remaining signals are also bounded. Furthermore, from (3–23), [61, Corollary 1] can be used to show $c \|Z\|^2 \rightarrow 0$ as $t \rightarrow \infty$ for all $y(0) \in \mathcal{S}_{\mathcal{D}}$. Because the vector Z contains the vector E_1 , $\|E_1\| \rightarrow 0$ as $t \rightarrow \infty$. By Lemma 3.1, $d(q_i, \text{Conv}\{q_l \mid l \in \mathcal{V}_L\}) \rightarrow 0 \forall i \in \mathcal{V}_{\mathcal{F}}$, i.e., each follower agent's state converges to the convex hull spanned by the leaders' states.

Note that the controller in (3–8) is decentralized in communication; however, because the stabilizing set of initial conditions $\mathcal{S}_{\mathcal{D}}$ depends on the graph dependent matrix $\mathcal{L}_{\mathcal{F}} + B$, the gains $k_{s,i}$ must be selected in a centralized manner before execution of the control. However, the set $\mathcal{S}_{\mathcal{D}}$ can be made arbitrarily large to include any initial

condition $y(0)$ by increasing the minimum eigenvalues of the gains $k_{s,i}$ to increase the minimum eigenvalue of the matrix $((\mathcal{L}_{\mathcal{F}} + B) \otimes I_m) K_s ((\mathcal{L}_{\mathcal{F}} + B) \otimes I_m)$. \square

3.4 Simulation

To demonstrate the robustness of the developed approach in performing containment control of follower agents with respect to a set of leader agents, numerical simulations are performed for a group of AUVs conducting surveillance. Each follower agent is modeled as a conventional, slender-bodied, fully actuated AUV with nonlinear dynamics as described in [66] (see [67] for more information on AUV dynamics). The state of each AUV is composed of surge (x), sway (y), heave (z), roll (ϕ), pitch (θ), and yaw (ψ). Actuation of the AUV is modeled by three independent forces acting at the center of mass of the vehicle and three independent moments which can be produced with a given thruster configuration and an appropriate thruster mapping algorithm, such as that described in [68].

Four leader agents are used to direct five follower agents such that the follower agents' states converge to the convex hull formed by the leaders' time-varying states, which have initial positions shown in Table 3-1, identical initial velocities of $[0.2 \text{ m/s}, 0 \text{ m/s}, 0.05 \text{ m/s}, 0 \text{ rad/s}, 0 \text{ rad/s}, -0.1 \text{ rad/s}]^T$, and identical accelerations of $[-0.02 \sin(0.1t), -0.02 \cos(0.1t), 0]^T \text{ m/s}^2$ in surge, sway and heave, respectively, such that the leaders form an inclined rectangle which translates in a helical trajectory. The follower AUVs have initial positions shown in Table 3-2 and identical initial velocities of $[2 \text{ m/s}, 0 \text{ m/s}, 0 \text{ m/s}, 0 \text{ rad/s}, 0 \text{ rad/s}, 0 \text{ rad/s}]^T$. All leader and follower agents have initial roll, pitch and yaw of 0 rad. The network topology is shown in Fig. 3-1. As in [69], the external disturbances for the follower AUVs are modeled as $[u_i \sin(0.5t), 0.5v_i \sin(2.5t), 0.2w_i \text{rand}]^T \text{ N}$ in surge, sway and heave, respectively, and 0 Nm in roll, pitch and yaw, where $u_i, v_i, w_i \in \mathbb{R}$ represent the linear velocities in surge, sway and heave, respectively, of the i^{th} follower agent, and $\text{rand} \in [-1, 1]$ is a uniformly

sampled random number generator. Identical gains for each follower agent i are selected as $k_{s,i} = \text{diag}(150, 150, 150, 1, 1, 1)$, $\chi_i = \text{diag}(50, 50, 50, 0.05, 0.2, 0.05)$, $\alpha_{1,i} = 0.2$, and $\alpha_{2,i} = 0.1$.

The agents' trajectories are shown in Fig. 3-2 and 3-3. At the labeled time instances, the black outline represents the projection of the leaders' convex hull onto the labeled dimensions, the black squares represent the follower agent positions, and the circles within the leader outline represent the equilibrium trajectories of the follower agents (which is a function of the network topology and leader trajectories, i.e., when $\|E_1\| \equiv 0$). In agreement with the analysis of the developed controller, the follower agents cooperatively become contained within the leader convex hull and converge to the containment equilibrium trajectories, despite the effects of model uncertainty and unknown time-varying exogenous disturbances. The Euclidean norms of the overall AUV force and moment actuation, shown in Fig. 3-4, demonstrate that reasonable actuation levels are used.

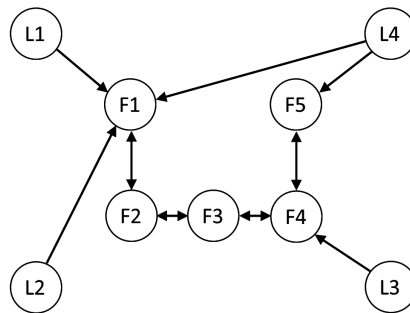


Figure 3-1. Network communication topology of leader (“L”) and follower (“F”) AUVs.

Table 3-1. Leader initial positions in surge (x), sway (y), and heave (z).

Leader	x (m)	y (m)	z (m)
1	-0.5	0.5	0
2	-0.5	-0.5	0
3	0.5	-0.5	0
4	0.5	0.5	0

Table 3-2. Follower initial positions in surge (x), sway (y), and heave (z).

Follower	x (m)	y (m)	z (m)
1	0	0.6	0.1
2	0.1	0.2	0.05
3	0.8	-0.2	0
4	-0.8	0.1	0.1
5	0.2	0.7	0.05

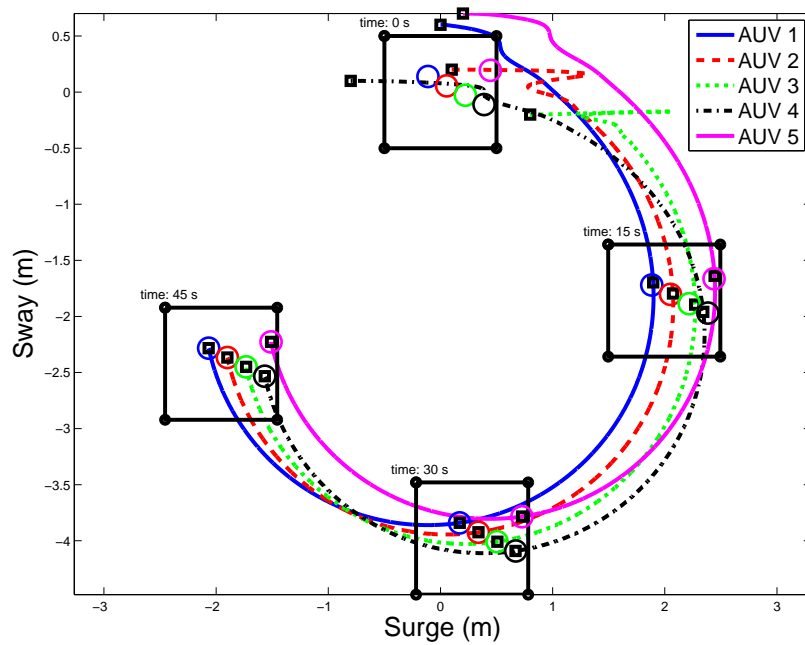


Figure 3-2. [Top view] Follower AUV trajectories in the surge (x) and sway (y) dimensions.

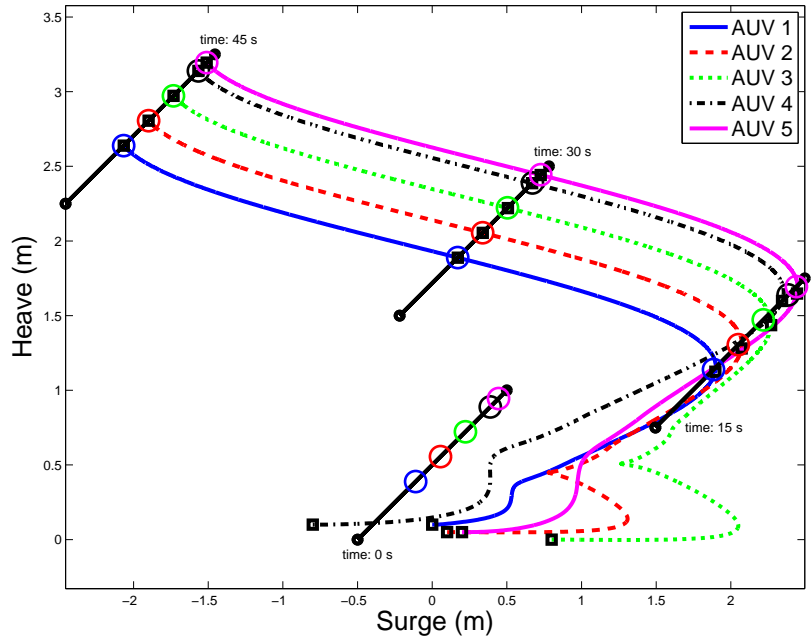


Figure 3-3. [Front view] Follower AUV trajectories in the surge (x) and heave (z) dimensions.

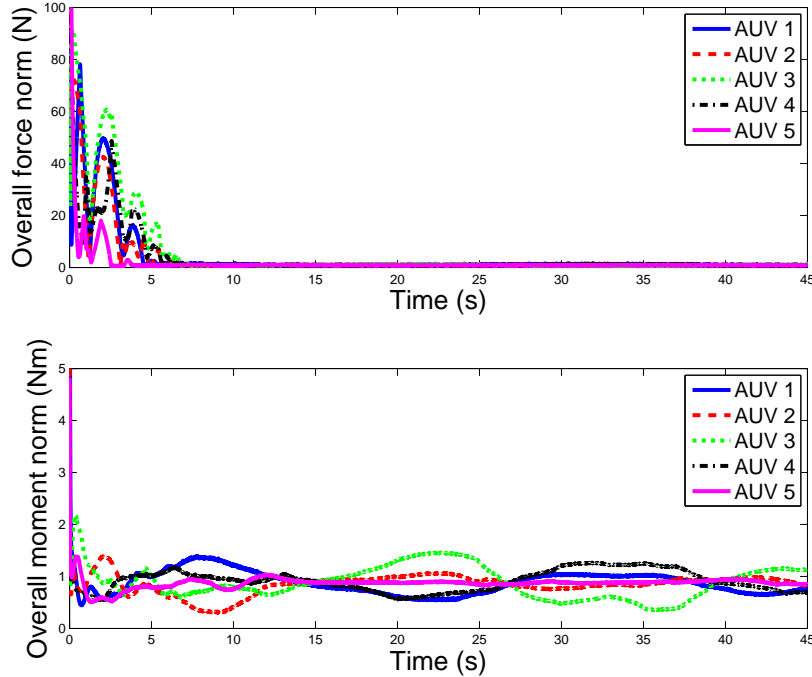


Figure 3-4. Euclidean norms of the follower AUV control efforts.

3.5 Concluding Remarks

A decentralized controller was developed for cooperative containment control of autonomous networked follower agents with a set of network leaders, which is a generalization of the popular single leader-follower network. The developed continuous controller provides robustness to input disturbances and uncertain, nonlinear Euler-Lagrange dynamics such that the state of each follower agent asymptotically converges to the convex hull spanned by the leaders' time-varying states for an arbitrary number of leaders. Some notable assumptions are that the agents' dynamics and disturbances are smooth, the graph containing the follower agents is connected and at least one follower agent is connected to at least one leader. Simulation results are provided to demonstrate the disturbance rejection capability of the developed controller.

CHAPTER 4

SYNCHRONIZATION OF UNCERTAIN EULER-LAGRANGE SYSTEMS WITH UNCERTAIN TIME-VARYING COMMUNICATION DELAYS

The work in the previous chapters is developed using a model which assumes that network neighbors communicate instantaneously. Efforts in this chapter investigate the effects of communication delay within a network of autonomous agents in addition to a method for mitigating the effects of communication delay. Dissimilar from effects such as state delay or input delay (cf. [70, 71]), communication delay makes the design of a reliable controller more difficult by imposing a lack of knowledge of recent information: a neighbor's current state is unknown until a period of delay has elapsed. This phenomenon can be present in a communication network due to lengthy information processing or a specific communication protocol, and can cause devastating effects, such as instability, on the performance of the network. Effects of communication delay on a general leader-follower network are exacerbated by the fact that, depending on the structure of the leader-follower network, a change in the leader's state may not affect a follower agent until multiple periods of delay have passed.

In this chapter, a novel decentralized controller is presented along with sufficient conditions for approximate convergence in leader-based synchronization of communication-delayed networked agents. The agents have heterogeneous dynamics modeled by uncertain, nonlinear Euler-Lagrange equations of motion affected by heterogeneous, unknown, exogenous disturbances. The developed controller requires only one-hop (delayed) communication from network neighbors and the communication delays are assumed to be heterogeneous, uncertain and time-varying. Each agent uses an estimate of the communication delay to provide feedback of estimated recent tracking error. The presented approach uses a Lyapunov-based convergence analysis in conjunction with Lyapunov-Krasovskii (LK) functionals to provide sufficient conditions which depend on the upper bound of the heterogeneous delays, feedback gains, and

network connectivity, among other factors. The novelty of the developed controller originates from the notion that the delayed version of a typical neighborhood error signal can be combined with an error signal which compares a neighbor's state with an agent's own state manually delayed by an estimate of the delay duration to achieve improved tracking performance and less sensitive stability criteria.

4.1 Problem Formulation

4.1.1 Dynamic Models and Properties

Let the dynamics of follower agent $i \in \mathcal{V}_{\mathcal{F}}$ be represented by Euler-Lagrange equations of motion of the form

$$M_i(q_i) \ddot{q}_i + C_i(q_i, \dot{q}_i) \dot{q}_i + F_i(\dot{q}_i) + G_i(q_i) = u_i + d_i(t), \quad (4-1)$$

where $q_i \in \mathbb{R}^m$ is the generalized configuration coordinate, $M_i : \mathbb{R}^m \rightarrow \mathbb{R}^{m \times m}$ is the inertia matrix, $C_i : \mathbb{R}^m \times \mathbb{R}^m \rightarrow \mathbb{R}^{m \times m}$ is the Coriolis/centrifugal matrix, $F_i : \mathbb{R}^m \rightarrow \mathbb{R}^m$ represents the effects of friction, $G_i : \mathbb{R}^m \rightarrow \mathbb{R}^m$ represents gravitational torques, $u_i \in \mathbb{R}^m$ is the vector of control inputs, and $d_i : \mathbb{R} \rightarrow \mathbb{R}^m$ is the time-varying, unknown, exogenous input disturbance. The time-varying state of the leader is denoted by $q_L : \mathbb{R} \rightarrow \mathbb{R}^m$. To facilitate subsequent analysis, the following assumptions are used concerning the Euler-Lagrange dynamics, external disturbance, leader trajectory, and network connectivity.

Assumption 4.1. For each follower agent $i \in \mathcal{V}_{\mathcal{F}}$, the inertia matrix is positive definite and symmetric, and there exist positive constants $\underline{m}, \bar{m} \in \mathbb{R}$ such that the inertia matrix satisfies the inequalities $\underline{m} \|\xi\|^2 \leq \xi^T M_i(\psi) \xi \leq \bar{m} \|\xi\|^2$ for all $\xi, \psi \in \mathbb{R}^m$ and $i \in \mathcal{V}_{\mathcal{F}}$.

Assumption 4.2. For each follower agent $i \in \mathcal{V}_{\mathcal{F}}$, the dynamics are sufficiently smooth such that the functions M_i, C_i, F_i, G_i are first-order differentiable, i.e., the first-order derivative is bounded if $q_i, \dot{q}_i, \ddot{q}_i \in \mathcal{L}_{\infty}$.

Assumption 4.3. For each follower agent $i \in \mathcal{V}_{\mathcal{F}}$, the vector of time-varying input disturbances is continuous and bounded such that $\sup_{t \in \mathbb{R}} \|d_i(t)\| \leq \bar{d}$ for some known positive constant $\bar{d} \in \mathbb{R}$.

Assumption 4.4. The leader state is bounded and sufficiently smooth such that

$$q_L, \dot{q}_L, \ddot{q}_L \in \mathcal{L}_\infty.$$

Assumption 4.5. The follower graph $\mathcal{G}_\mathcal{F}$ is undirected and connected and at least one follower agent is connected to the leader.

The communication delay between agents is modeled such that, at time t , agent $i \in \mathcal{V}_\mathcal{F}$ is unaware of the set of recent states $\{q_j(\sigma) \mid t - \tau_{ji}(t) < \sigma \leq t\}$ of a neighbor $j \in \bar{\mathcal{N}}_{\mathcal{F}i}$ ($i \neq j$), where $\tau_{ji} : \mathbb{R} \rightarrow \mathbb{R}_{\geq 0}$ is the positive, time-varying, uncertain communication delay. The communication delays in the network need not be homogenous, i.e., the communication delays may be different for each interaction link. The communication delay may even differ between an interacting pair of agents, i.e., it may be that $\tau_{ij}(t) \neq \tau_{ji}(t)$ for $i, j \in \mathcal{V}_\mathcal{F}$. The following assumption specifies the class of delays considered in this chapter.

Assumption 4.6. The uncertain, time-varying delay τ_{ji} is bounded above by a known constant $\bar{\tau} \in \mathbb{R}_{>0}$ such that $\sup_{t \in \mathbb{R}} \tau_{ji}(t) < \bar{\tau}$, τ_{ji} is differentiable, and τ_{ji} changes sufficiently slowly such that $\sup_{t \in \mathbb{R}} |\dot{\tau}_{ji}(t)| < 1$, for each $(j, i) \in \mathcal{E}_\mathcal{F} \cup \mathcal{E}_L$. There is no delay in agent $i \in \mathcal{V}_\mathcal{F}$ knowing its own state, q_i .

Each agent maintains an estimate of the duration of the communication delay for all incoming communication, i.e., agent $i \in \mathcal{V}_\mathcal{F}$ estimates τ_{ji} with $\hat{\tau}_{ji} : \mathbb{R} \rightarrow \mathbb{R}_{>0}$ for every neighbor $j \in \bar{\mathcal{N}}_{\mathcal{F}i}$, where $\hat{\tau}_{ji}$ is upper-bounded by the known constant $\bar{\hat{\tau}} \in \mathbb{R}_{>0}$ for each communication channel $(j, i) \in \mathcal{E}_\mathcal{F} \cup \mathcal{E}_L$.

Assumption 4.7. The difference between the communication delay τ_{ji} and delay estimate $\hat{\tau}_{ji}$ is upper-bounded by a known constant $\bar{\tilde{\tau}} \in \mathbb{R}_{>0}$ such that $\sup_{t \in \mathbb{R}} |\tau_{ji}(t) - \hat{\tau}_{ji}(t)| < \bar{\tilde{\tau}}$, $\hat{\tau}_{ji}$ is differentiable, and $\hat{\tau}_{ji}$ changes sufficiently slowly such that $\sup_{t \in \mathbb{R}} |\dot{\hat{\tau}}_{ji}(t)| < 1$, for each $(j, i) \in \mathcal{E}_\mathcal{F} \cup \mathcal{E}_L$.

There are multiple ways to obtain an estimate of communication delay, and the specific application may dictate the methodology used (cf. [35, 41, 72–75]). In this work, a specific method of estimating communication delay is not considered.

For implementation purposes, it is also assumed that for every agent $i \in \mathcal{V}_{\mathcal{F}}$, the delayed state $q_j(t - \tau_{ji}(t))$ has been communicated to agent i from every neighbor $j \in \bar{\mathcal{N}}_{\mathcal{F}i}$ for at least $\bar{\tau} + \bar{\tau}$ seconds before control implementation. Note that this approach does not omit the case in which some communication channels may have no delay.

4.1.2 Control Objective

The network-wide objective is to cooperatively drive the states of the networked agents towards the state of the network leader such that $\|q_i(t) - q_L(t)\| \rightarrow 0$ as $t \rightarrow \infty$ for all $i \in \mathcal{V}_{\mathcal{F}}$ using one-hop communication, despite the effects of modeling uncertainties; exogenous disturbances; uncertain, heterogeneous, time-varying communication delays between neighbors; and only a subset of the follower agents interacting with the leader.

4.2 Controller Development

Throughout the rest of the chapter, functional dependency is omitted where the meaning is clear.

4.2.1 Communication-Delayed Control

Error signals used for feedback controllers in network synchronization typically take the form $e_i \triangleq \sum_{j \in \mathcal{N}_{\mathcal{F}i}} a_{ij} (q_j(t) - q_i(t)) + b_i (q_L(t) - q_i(t))$ (cf. [3, 7, 8, 17]). However, because communication is delayed in the network, the error signal e_i is not implementable in this scenario. Alternatively, a new feedback signal $e_{\tau i} \in \mathbb{R}^m$ is developed to implement the delay estimates $\hat{\tau}_{ji}$ as

$$e_{\tau i} \triangleq \frac{\kappa_1}{|\mathcal{N}_{\mathcal{F}i}|} \sum_{j \in \mathcal{N}_{\mathcal{F}i}} a_{ij} (q_j(t - \tau_{ji}(t)) - q_i(t)) + \kappa_1 b_i (q_L(t - \tau_{Li}(t)) - q_i(t)) \\ + \frac{\kappa_2}{|\mathcal{N}_{\mathcal{F}i}|} \sum_{j \in \mathcal{N}_{\mathcal{F}i}} a_{ij} (q_j(t - \tau_{ji}(t)) - q_i(t - \hat{\tau}_{ji}(t))) + \kappa_2 b_i (q_L(t - \tau_{Li}(t)) - q_i(t - \hat{\tau}_{Li}(t))), \quad (4-2)$$

and an auxiliary delayed error signal $r_{\tau_i} \in \mathbb{R}^m$ is analogously defined as

$$\begin{aligned}
r_{\tau_i} \triangleq & \frac{\kappa_1}{|\mathcal{N}_{\mathcal{F}i}|} \sum_{j \in \mathcal{N}_{\mathcal{F}i}} a_{ij} (\dot{q}_j(t - \tau_{ji}(t)) - \dot{q}_i(t)) + \kappa_1 b_i (\dot{q}_L(t - \tau_{Li}(t)) - \dot{q}_i(t)) \\
& + \frac{\kappa_2}{|\mathcal{N}_{\mathcal{F}i}|} \sum_{j \in \mathcal{N}_{\mathcal{F}i}} a_{ij} (\dot{q}_j(t - \tau_{ji}(t)) - \dot{q}_i(t - \hat{\tau}_{ji}(t))) + \kappa_2 b_i (\dot{q}_L(t - \tau_{Li}(t)) - \dot{q}_i(t - \hat{\tau}_{Li}(t))) \\
& + \lambda e_{\tau_i},
\end{aligned} \tag{4-3}$$

where $\lambda \in \mathbb{R}_{>0}$ is a constant control gain and $\kappa_1 \in \mathbb{R}_{\geq 0}$, $\kappa_2 \in \mathbb{R}_{\geq 0}$ are constant weighting parameters selected such that $\kappa_1 + \kappa_2 = 1$. Thus, neighbors' delayed state and state derivative are to be used for control purposes with the implementable error signals e_{τ_i} and r_{τ_i} .¹ There are two unique types of feedback in e_{τ_i} . The first line of (4-2) provides the difference between a neighbor's delayed state and an agent's own current state and is normalized by the number of neighbors. This term helps provide overall stability of the networked systems and will be referred to as *feedback without self-delay*, as in [33]. The second line of (4-2) provides the normalized difference between a neighbor's delayed state and an agent's own state manually delayed by an estimate of the delay corresponding to that communication channel. As motivated in the following example, this term can improve performance in synchronization by correcting for estimated tracking errors in the recent history of the agents' trajectories. This type of feedback will be referred to as *feedback with inexact self-delay* if $\tau_{ji} \neq \hat{\tau}_{ji}$ for some $t \in \mathbb{R}$ and *feedback with exact self-delay* if $\tau_{ji} \equiv \hat{\tau}_{ji}$. The tuning parameters a_{ij} and b_i may be adjusted to emphasize either leader tracking or (follower) neighbor tracking in closed-loop performance.

¹ It is assumed that a neighbor's delayed state derivative is communicated, not computed; i.e., agent j obtains and then communicates $q_j(t)$ and $\dot{q}_j(t)$ to a neighbor i with a communication delay $\tau_{ji}(t)$. In other words, this approach does not solve the communication-delayed output feedback problem: numerical computation of the delayed state derivative may be skewed by effects of the time-varying delay.

A communication-delayed proportional-derivative (PD) controller, based on one-hop neighbor feedback, is designed for agent $i \in \mathcal{V}_{\mathcal{F}}$ as

$$u_i = kr_{\tau_i}, \quad (4-4)$$

where $k \in \mathbb{R}_{>0}$ is a constant control gain. Note that, as opposed to the controller in [43], it is not assumed that the communication delay duration is exactly known.

4.2.2 Motivating Example

Consider a simple network with the topology depicted in Fig. 4-1 and double integrator agent dynamics modeled as

$$m_1 \ddot{q}_1 = u_1,$$

$$m_2 \ddot{q}_2 = u_2,$$

with initial conditions $q_1(0) = 1$, $\dot{q}_1(0) = 0$, $q_2(0) = 2$, $\dot{q}_2(0) = -3$. Let the control gains be selected as $k = 10$, $\lambda = 1$, the network weight parameters be selected as $a_{12} = a_{21} = b_1 = 1$, the leader trajectory be designed as $q_L = t$, and the network be affected by communication delay such that $\tau_{L1} = 0$ and $\tau_{21} = \tau_{12} = 0.2$.

Fig. 4-2 depicts the network performance under the control policy in (4-4) using (a) only feedback without self-delay ($\kappa_1 = 1$, $\kappa_2 = 0$), (b) only feedback with exact self-delay ($\kappa_1 = 0$, $\kappa_2 = 1$, $\hat{\tau}_{21} = \hat{\tau}_{12} = \tau_{21} = \tau_{12}$), and (c) only feedback with inexact self-delay ($\kappa_1 = 0$, $\kappa_2 = 1$, $\hat{\tau}_{21} = \hat{\tau}_{12} = 0.25$). As shown in Fig. 4-2a, bounded convergence is obtained toward the leader state using only feedback without self-delay. Considerably better, asymptotic performance is obtained when only feedback with exact self-delay is used, as depicted in Fig. 4-2b. Even though the policy in (c) uses a communication delay estimate that is 25% away from the actual delay for feedback with inexact self-delay only, considerably better network performance is obtained compared to (a), as depicted in Fig. 4-2c. The policies in (b) and (c) obtain superior performance by regulating an error signal that better compares neighbors' state trajectories in

time; however, the policies in (b) and (c) are less robust to larger communication delays. For policies (b) and (c), the system is unstable for communication delays of $\tau_{12} = \tau_{21} = \hat{\tau}_{21} = \hat{\tau}_{12} = 0.5$. This issue can also be seen with faster follower agent dynamics and more volatile leader trajectories. In comparison, even though the performance is worsened for policy (a) with a delay of $\tau_{12} = \tau_{21} = 0.5$, the system is still stable. Thus, the approach in this chapter is to use a mixture of policies (a) and (c), as in the developed controller in (4-4), to promote overall stability and better tracking when faced with uncertain communication delays.

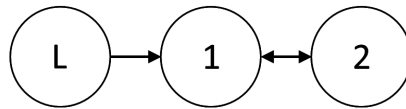


Figure 4-1. Network communication topology.

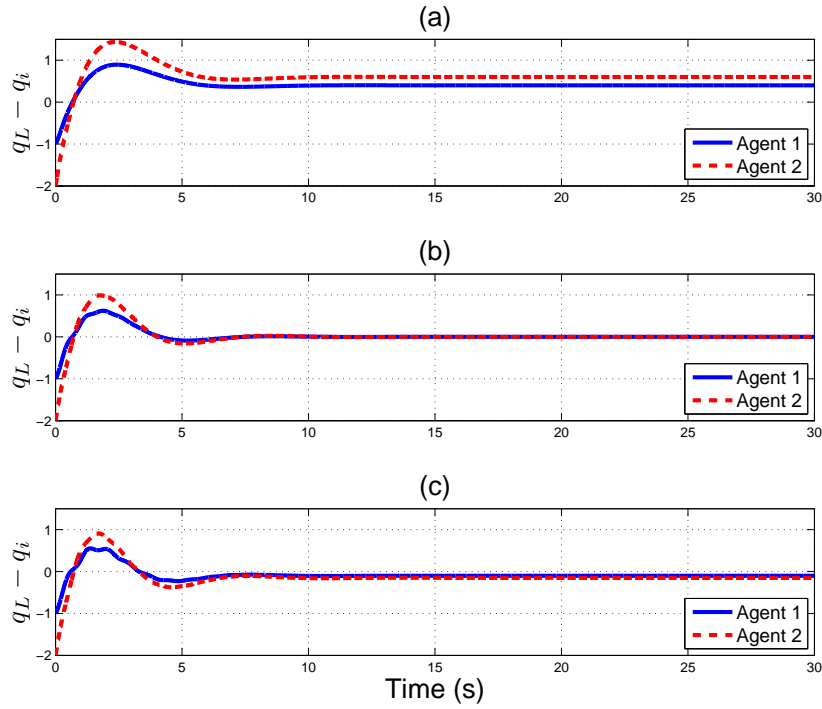


Figure 4-2. Leader-tracking error under communication-delayed control using (a) only feedback without self-delay, (b) only feedback with exact self-delay, and (c) only feedback with inexact self-delay.

4.3 Closed-loop Error System

For notational brevity, the networked systems' dynamics are grouped into block matrices and composite vectors as

$$M \triangleq \text{diag}(M_1, \dots, M_{\mathcal{F}}) \in \mathbb{R}^{\mathcal{F}m \times \mathcal{F}m},$$

$$C \triangleq \text{diag}(C_1, \dots, C_{\mathcal{F}}) \in \mathbb{R}^{\mathcal{F}m \times \mathcal{F}m},$$

$$F \triangleq [F_1^T, \dots, F_{\mathcal{F}}^T]^T \in \mathbb{R}^{\mathcal{F}m},$$

$$G \triangleq [G_1^T, \dots, G_{\mathcal{F}}^T]^T \in \mathbb{R}^{\mathcal{F}m},$$

$$U \triangleq [u_1^T, \dots, u_{\mathcal{F}}^T]^T \in \mathbb{R}^{\mathcal{F}m},$$

$$d \triangleq [d_1^T, \dots, d_{\mathcal{F}}^T]^T \in \mathbb{R}^{\mathcal{F}m},$$

$$Q_{\mathcal{F}} \triangleq [q_1^T, \dots, q_{\mathcal{F}}^T]^T \in \mathbb{R}^{\mathcal{F}m},$$

such that

$$M(Q_{\mathcal{F}}) \ddot{Q}_{\mathcal{F}} + C(Q_{\mathcal{F}}, \dot{Q}_{\mathcal{F}}) \dot{Q}_{\mathcal{F}} + F(\dot{Q}_{\mathcal{F}}) + G(Q_{\mathcal{F}}) = U + d(t). \quad (4-5)$$

Non-implemented error signals $E \triangleq Q_L - Q_{\mathcal{F}} \in \mathbb{R}^{\mathcal{F}m}$ and $R \triangleq \dot{E} + \lambda E \in \mathbb{R}^{\mathcal{F}m}$ are introduced to develop a network-wide closed-loop error system, where $Q_L \triangleq \mathbf{1}_{\mathcal{F}} \otimes q_L$. Clearly, if $\|E\| \rightarrow 0$, then the control objective is achieved.

To facilitate the description of the normalized neighbor feedback, let the matrix $\mathcal{A} \in \mathbb{R}^{\mathcal{F} \times \mathcal{F}}$ be defined as $\mathcal{A} \triangleq [\alpha_{ij}]$, where $\alpha_{ij} \triangleq \frac{a_{ij}}{|\mathcal{N}_{\mathcal{F}i}|}$. Additionally, let the matrix $\mathcal{D} \in \mathbb{R}^{\mathcal{F} \times \mathcal{F}}$ be defined as $\mathcal{D} \triangleq \text{diag}\{\mathfrak{d}_1, \dots, \mathfrak{d}_{\mathcal{F}}\}$, where $\mathfrak{d}_i \triangleq \sum_{j \in \mathcal{N}_{\mathcal{F}i}} \alpha_{ij}$. For convenience in describing the effects of the heterogeneous communication delays individually in the closed-loop system, let the constant matrix $\mathcal{A}_{ij} \in \mathbb{R}^{\mathcal{F}m \times \mathcal{F}m}$ be defined as $\mathcal{A}_{ij} \triangleq (\mathcal{A} \circ \mathbf{1}_{ij}) \otimes I_m$, where \circ denotes the Hadamard product and $\mathbf{1}_{ij} \in \mathbb{R}^{\mathcal{F} \times \mathcal{F}}$ denotes an indicator matrix, which has all zero entries except for the i^{th} row and j^{th} column, which has a value of 1. Similarly, let the constant matrix $\mathcal{D}_{ij} \in \mathbb{R}^{\mathcal{F}m \times \mathcal{F}m}$ be defined as $\mathcal{D}_{ij} \triangleq \alpha_{ij} \mathbf{1}_{ii} \otimes I_m$. Note that $\sum_{(j,i) \in \mathcal{E}_{\mathcal{F}}} \mathcal{A}_{ij} = \mathcal{A} \otimes I_m$ and $\sum_{(j,i) \in \mathcal{E}_{\mathcal{F}}} \mathcal{D}_{ij} = \mathcal{D} \otimes I_m$. Also, let $\mathcal{B}_i \in \mathbb{R}^{\mathcal{F} \times \mathcal{F}}$ be defined as $\mathcal{B}_i \triangleq B \circ \mathbf{1}_{ii}$; note that $\sum_{(L,i) \in \mathcal{E}_L} \mathcal{B}_i = B$. Finally, let the vectors $Q_{\tau_{ji}}, Q_{\hat{\tau}_{ji}}, Q_{L\tau_{Li}} : \mathbb{R} \rightarrow \mathbb{R}^{\mathcal{F}m}$ be defined as $Q_{\tau_{ji}}(t) \triangleq Q_{\mathcal{F}}(t - \tau_{ji}(t))$, $Q_{\hat{\tau}_{ji}}(t) \triangleq Q_{\mathcal{F}}(t - \hat{\tau}_{ji}(t))$, $Q_{L\tau_{Li}}(t) \triangleq Q_L(t - \tau_{Li}(t))$.

By taking the time-derivative of R and premultiplying by the block inertia matrix M , the closed-loop error system is represented using (4-4) and (4-5) as

$$M\dot{R} = C\dot{Q}_{\mathcal{F}} + F + G - d + M\dot{Q}_L + \lambda M\dot{E} - kR_{\mathcal{T}}, \quad (4-6)$$

where

$$\begin{aligned}
R_\tau &\triangleq [r_{\tau_1}^T, \dots, r_{\tau_m}^T]^T \\
&= (\kappa_1 + \kappa_2) \sum_{(j,i) \in \mathcal{E}_\mathcal{F}} \mathcal{A}_{ij} \left(\dot{Q}_{\tau_{ji}} + \lambda Q_{\tau_{ji}} \right) - \kappa_1 (\mathcal{D} \otimes I_m) \left(\dot{Q}_\mathcal{F} + \lambda Q_\mathcal{F} \right) \\
&\quad - \kappa_2 \sum_{(j,i) \in \mathcal{E}_\mathcal{F}} \mathcal{D}_{ij} \left(\dot{Q}_{\hat{\tau}_{ji}} + \lambda Q_{\hat{\tau}_{ji}} \right) \\
&\quad + (\kappa_1 + \kappa_2) \sum_{(L,i) \in \mathcal{E}_L} (\mathcal{B}_i \otimes I_m) \left(\dot{Q}_{L\tau_{Li}} + \lambda Q_{L\tau_{Li}} \right) - \kappa_1 (B \otimes I_m) \left(\dot{Q}_\mathcal{F} + \lambda Q_\mathcal{F} \right) \\
&\quad - \kappa_2 \sum_{(L,i) \in \mathcal{E}_L} (\mathcal{B}_i \otimes I_m) \left(\dot{Q}_{\hat{\tau}_{Li}} + \lambda Q_{\hat{\tau}_{Li}} \right).
\end{aligned}$$

After using the Fundamental Theorem of Calculus, the fact that $\left(\dot{Q}_L + \lambda Q_L \right) \in \text{Null}(\mathcal{L}_\mathcal{F} \otimes I_m)$ due to the structure of the Laplacian matrix, and adding and subtracting the terms

$$\begin{aligned}
&k \sum_{(j,i) \in \mathcal{E}_\mathcal{F}} (\kappa_1 \mathcal{A}_{ij} - \kappa_2 \mathcal{L}_{ij}) \int_{t-\tau_{ji}}^t \left(\ddot{Q}_L(s) + \lambda \dot{Q}_L(s) \right) ds, \\
&\quad k \kappa_2 \sum_{(j,i) \in \mathcal{E}_\mathcal{F}} \mathcal{D}_{ij} \int_{t-\hat{\tau}_{ji}}^{t-\tau_{ji}} \left(\ddot{Q}_L(s) + \lambda \dot{Q}_L(s) \right) ds, \\
&\quad k \kappa_2 \sum_{(L,i) \in \mathcal{E}_L} (\mathcal{B}_i \otimes I_m) \int_{t-\hat{\tau}_{Li}}^{t-\tau_{Li}} \left(\ddot{Q}_L(s) + \lambda \dot{Q}_L(s) \right) ds,
\end{aligned}$$

(4–6) may be re-expressed as

$$\begin{aligned}
M\dot{R} = & C\dot{Q}_{\mathcal{F}} + F + G - d + M\ddot{Q}_L + \lambda M\dot{E} - kL_B R \\
& + k \sum_{(j,i) \in \mathcal{E}_{\mathcal{F}}} \left[(\kappa_1 \mathcal{A}_{ij} - \kappa_2 \mathcal{L}_{ij}) \int_{t-\tau_{ji}}^t \dot{R}(\sigma) d\sigma - \kappa_2 \mathcal{D}_{ij} \int_{t-\hat{\tau}_{ji}}^{t-\tau_{ji}} \dot{R}(\sigma) d\sigma \right] \\
& - k \sum_{(j,i) \in \mathcal{E}_{\mathcal{F}}} (\kappa_1 \mathcal{A}_{ij} - \kappa_2 \mathcal{L}_{ij}) \int_{t-\tau_{ji}}^t \left(\ddot{Q}_L(\sigma) + \lambda \dot{Q}_L(\sigma) \right) d\sigma \\
& + k\kappa_2 \sum_{(j,i) \in \mathcal{E}_{\mathcal{F}}} \mathcal{D}_{ij} \int_{t-\hat{\tau}_{ji}}^{t-\tau_{ji}} \left(\ddot{Q}_L(\sigma) + \lambda \dot{Q}_L(\sigma) \right) d\sigma \\
& - k\kappa_2 \sum_{(L,i) \in \mathcal{E}_L} (\mathcal{B}_i \otimes I_m) \int_{t-\hat{\tau}_{Li}}^t \dot{R}(\sigma) d\sigma \\
& - k\kappa_1 \sum_{(L,i) \in \mathcal{E}_L} (\mathcal{B}_i \otimes I_m) \int_{t-\tau_{Li}}^t \left(\ddot{Q}_L(\sigma) + \lambda \dot{Q}_L(\sigma) \right) d\sigma \\
& + k\kappa_2 \sum_{(L,i) \in \mathcal{E}_L} (\mathcal{B}_i \otimes I_m) \int_{t-\hat{\tau}_{Li}}^{t-\tau_{Li}} \left(\ddot{Q}_L(\sigma) + \lambda \dot{Q}_L(\sigma) \right) d\sigma, \tag{4-7}
\end{aligned}$$

where $\mathcal{L}_{ij} \triangleq \mathcal{D}_{ij} - \mathcal{A}_{ij} \in \mathbb{R}^{\mathcal{F}m \times \mathcal{F}m}$, and $L_B \triangleq (B + \mathcal{D} - \mathcal{A}) \otimes I_m \in \mathbb{R}^{\mathcal{F}m \times \mathcal{F}m}$, which is symmetric and positive definite by Assumption 4.5 and [55]. The terms $C\dot{Q}_{\mathcal{F}}, F, G, d, M\ddot{Q}_L, \lambda M\dot{E}$ in (4-7) can be compensated using traditional robust control methods; however, compensating for the terms which contain $\int_{t-\tau_{ji}}^t \dot{R}(\sigma) d\sigma$, $\int_{t-\hat{\tau}_{ji}}^{t-\tau_{ji}} \dot{R}(\sigma) d\sigma$, and $\int_{t-\hat{\tau}_{Li}}^t \dot{R}(\sigma) d\sigma$ is difficult due to the delayed state feedback and amplification by the gain k . The following sections demonstrate that the decentralized controller in (4-4) yields convergence to a neighborhood around the leader state for each follower agent despite these delay-contributing terms for small enough time-varying heterogeneous network delays and accurate enough delay estimates.

4.4 Convergence Analysis

Some constants, functions, and sets are introduced to facilitate the convergence analysis. Let $c, \phi \in \mathbb{R}_{>0}$ denote tunable constant parameters and let the constant $\underline{c} \in \mathbb{R}$ be defined as $\underline{c} \triangleq c \left(\lambda - \frac{1}{2} \right)$. Let the auxiliary constants $\underline{k}, \eta, \theta \in \mathbb{R}$ be defined as $\underline{k} \triangleq k \left(\underline{\lambda}(L_B) - \frac{(\bar{\tau} + \hat{\tau})k^3}{2\phi} - \iota_1 k \right) - \frac{c}{2}$, $\eta \triangleq \min \left\{ \frac{c}{2}, \frac{k}{6} \right\}$, and $\theta \triangleq \frac{1}{2} \min \left\{ 2\eta, \frac{1}{\bar{\tau} + \hat{\tau}}, \omega, \frac{\omega}{\bar{\tau}}, \hat{\omega}, \frac{\hat{\omega}}{\bar{\tau}} \right\}$,

where the unknown constants $\omega, \hat{\omega} \in \mathbb{R}$ are defined as $\omega \triangleq 1 - \sup_{t \in \mathbb{R}, (j,i) \in \mathcal{E}_{\mathcal{F}}} \hat{\tau}_{ji}$ and $\hat{\omega} \triangleq 1 - \sup_{t \in \mathbb{R}, (j,i) \in \mathcal{E}_{\mathcal{F}} \cup \mathcal{E}_L} \hat{\tau}_{ji}$, which are positive by Assumptions 4.6 and 4.7, and the auxiliary constant $\iota_1 \in \mathbb{R}_{\geq 0}$ is defined as

$$\iota_1 \triangleq \left(\bar{Q}_L + \lambda \bar{\bar{Q}}_L \right) \left(\bar{\tau} \sum_{(j,i) \in \mathcal{E}_{\mathcal{F}}} \|\kappa_1 \mathcal{A}_{ij} - \kappa_2 \mathcal{L}_{ij}\| + \kappa_2 \bar{\tau} \sum_{(j,i) \in \mathcal{E}_{\mathcal{F}}} \|\mathcal{D}_{ij}\| + (\kappa_1 \bar{\tau} + \kappa_2 \bar{\tau}) \sum_{(L,i) \in \mathcal{E}_L} \|\mathcal{B}_i\| \right),$$

where the constant upper bounds $\bar{Q}_L, \bar{\bar{Q}}_L \in \mathbb{R}_{\geq 0}$ are defined such that $\sup_{t \in \mathbb{R}} \|\dot{Q}_L(t)\| \leq \bar{Q}_L$ and $\sup_{t \in \mathbb{R}} \|\ddot{Q}_L(t)\| \leq \bar{\bar{Q}}_L$.

The convergence analysis is constructed with the state $y \in \mathbb{R}^{2\mathcal{F}m+6}$ defined as the composite vector² $y \triangleq \left[Z^T, \Psi_{1a}^{\frac{1}{2}}, \Psi_{1b}^{\frac{1}{2}}, \Psi_{2a}^{\frac{1}{2}}, \Psi_{2b}^{\frac{1}{2}}, \Psi_{3a}^{\frac{1}{2}}, \Psi_{3b}^{\frac{1}{2}} \right]^T$, where $Z \in \mathbb{R}^{2\mathcal{F}m}$ is the composite error vector $Z \triangleq \begin{bmatrix} E^T & R^T \end{bmatrix}^T$, and $\Psi_{1a}, \Psi_{1b}, \Psi_{2a}, \Psi_{2b}, \Psi_{3a}, \Psi_{3b}$ denote LK functionals defined as

$$\Psi_{1a} \triangleq \frac{\phi \iota_2 |\mathcal{E}_{\mathcal{F}}|}{k^2} \int_{t-\bar{\tau}}^t \int_s^t \|\dot{R}(\sigma)\|^2 d\sigma ds, \quad (4-8)$$

$$\Psi_{1b} \triangleq \frac{\phi (\iota_3 |\mathcal{E}_{\mathcal{F}}| + \iota_4 |\mathcal{E}_L|)}{k^2} \int_{t-\bar{\tau}-\bar{\tau}}^t \int_s^t \|\dot{R}(\sigma)\|^2 d\sigma ds, \quad (4-9)$$

$$\begin{aligned} \Psi_{2a} &\triangleq \frac{2\phi |\mathcal{E}_{\mathcal{F}}| (\bar{\tau} \iota_2 |\mathcal{E}_{\mathcal{F}}| + (\bar{\tau} + \bar{\tau}) (\iota_3 |\mathcal{E}_{\mathcal{F}}| + \iota_4 |\mathcal{E}_L|))}{\omega \underline{m}^2} \\ &\cdot \sum_{(j,i) \in \mathcal{E}_{\mathcal{F}}} \int_{t-\tau_{ji}}^t \left(\|(\kappa_1 \mathcal{A}_{ij} - \kappa_2 \mathcal{L}_{ij}) R(\sigma)\|^2 + \kappa_2^2 \|\mathcal{D}_{ij} R(\sigma)\|^2 \right) d\sigma, \end{aligned} \quad (4-10)$$

$$\begin{aligned} \Psi_{2b} &\triangleq \frac{2\phi \kappa_2^2 |\mathcal{E}_{\mathcal{F}}| (\bar{\tau} \iota_2 |\mathcal{E}_{\mathcal{F}}| + (\bar{\tau} + \bar{\tau}) (\iota_3 |\mathcal{E}_{\mathcal{F}}| + \iota_4 |\mathcal{E}_L|))}{\hat{\omega} \underline{m}^2} \\ &\cdot \int_{t-\hat{\tau}_{ji}}^t \left(|\mathcal{E}_{\mathcal{F}}| \sum_{(j,i) \in \mathcal{E}_{\mathcal{F}}} \|\mathcal{D}_{ij} R(\sigma)\|^2 + |\mathcal{E}_L| \sum_{(L,i) \in \mathcal{E}_L} \|(\mathcal{B}_i \otimes I_m) R(\sigma)\|^2 \right) d\sigma, \end{aligned} \quad (4-11)$$

² The LK functionals are interpreted as time-varying signals and are incorporated into the overall system state to facilitate the convergence analysis.

$$\begin{aligned} \Psi_{3a} \triangleq & \frac{2\phi |\mathcal{E}_{\mathcal{F}}| (\bar{\tau} \iota_2 |\mathcal{E}_{\mathcal{F}}| + (\bar{\tau} + \bar{\tau}) (\iota_3 |\mathcal{E}_{\mathcal{F}}| + \iota_4 |\mathcal{E}_L|))}{\omega \underline{m}^2} \sum_{(j,i) \in \mathcal{E}_{\mathcal{F}}} \int_{t-\tau_{ji}}^t \int_s^t \left(\|(\kappa_1 \mathcal{A}_{ij} - \kappa_2 \mathcal{L}_{ij}) R(\sigma)\|^2 \right. \\ & \left. + \kappa_2^2 \|\mathcal{D}_{ij} R(\sigma)\|^2 \right) d\sigma ds, \end{aligned} \quad (4-12)$$

$$\begin{aligned} \Psi_{3b} \triangleq & \frac{2\phi \kappa_2^2 |\mathcal{E}_{\mathcal{F}}| (\bar{\tau} \iota_2 |\mathcal{E}_{\mathcal{F}}| + (\bar{\tau} + \bar{\tau}) (\iota_3 |\mathcal{E}_{\mathcal{F}}| + \iota_4 |\mathcal{E}_L|))}{\hat{\omega} \underline{m}^2} \\ & \cdot \int_{t-\hat{\tau}_{ji}}^t \int_s^t \left(|\mathcal{E}_{\mathcal{F}}| \sum_{(j,i) \in \mathcal{E}_{\mathcal{F}}} \|\mathcal{D}_{ij} R(\sigma)\|^2 + |\mathcal{E}_L| \sum_{(L,i) \in \mathcal{E}_L} \|(\mathcal{B}_i \otimes I_m) R(\sigma)\|^2 \right) d\sigma ds, \end{aligned} \quad (4-13)$$

where the constants $\iota_2, \iota_3, \iota_4 \in \mathbb{R}_{>0}$ are defined as

$$\begin{aligned} \iota_2 \triangleq & \bar{\lambda} \left(\sum_{(j,i) \in \mathcal{E}_{\mathcal{F}}} (\kappa_1 \mathcal{A}_{ij} - \kappa_2 \mathcal{L}_{ij}) (\kappa_1 \mathcal{A}_{ij} - \kappa_2 \mathcal{L}_{ij})^T \right), \\ \iota_3 \triangleq & \kappa_2^2 \bar{\lambda} \left(\sum_{(j,i) \in \mathcal{E}_{\mathcal{F}}} \mathcal{D}_{ij}^2 \right), \quad \iota_4 \triangleq \kappa_2^2 \bar{\lambda} \left(\sum_{(L,i) \in \mathcal{E}_L} \mathcal{B}_i^2 \right). \end{aligned}$$

To facilitate the description of the stability result in the following convergence analysis, the constant parameters $N_{d0}, N_{d1}, N_{d2} \in \mathbb{R}_{\geq 0}$ are defined as

$$N_{d0} \triangleq \bar{d} + \bar{m} \bar{Q}_L + \sup_{t \in \mathbb{R}} S_0(Q_L, \dot{Q}_L), \quad (4-14)$$

$$N_{d1} \triangleq \frac{2}{\underline{m}} \|L_B\| \left(\frac{\bar{d}}{k \underline{m}} + \frac{\bar{Q}_L}{k} + \frac{\iota_1}{\underline{m}} \right) + \sup_{t \in \mathbb{R}} S_1(Q_L, \dot{Q}_L), \quad (4-15)$$

$$N_{d2} \triangleq \frac{4\bar{d}^2}{k^2 \underline{m}^2} + \frac{2\bar{d}}{\underline{m}} \left(\frac{\bar{Q}_L}{k^2} + \frac{\iota_1}{k \underline{m}} \right) + 4 \left(\frac{\bar{Q}_L}{k} + \frac{\iota_1}{\underline{m}} \right)^2 + \sup_{t \in \mathbb{R}} S_2(Q_L, \dot{Q}_L), \quad (4-16)$$

and the functions $\tilde{N}_0, \tilde{N}_1, \tilde{N}_2 : \Pi_{p=1}^6 \mathbb{R}^{\mathcal{F}^m} \rightarrow \mathbb{R}$ are defined as

$$\tilde{N}_0 \triangleq S_0(Q_{\mathcal{F}}, \dot{Q}_{\mathcal{F}}) - S_0(Q_L, \dot{Q}_L) + f_0(E, R, Q_{\mathcal{F}}, \dot{Q}_{\mathcal{F}}), \quad (4-17)$$

$$\tilde{N}_1 \triangleq S_1(Q_{\mathcal{F}}, \dot{Q}_{\mathcal{F}}) - S_1(Q_L, \dot{Q}_L) + f_1(E, R), \quad (4-18)$$

$$\tilde{N}_2 \triangleq S_2(Q_{\mathcal{F}}, \dot{Q}_{\mathcal{F}}) - S_2(Q_L, \dot{Q}_L) + f_2(E, R, Q_{\mathcal{F}}, \dot{Q}_{\mathcal{F}}), \quad (4-19)$$

where the auxiliary functions $S_0, S_1, S_2 : \mathbb{R}^{\mathcal{F}m} \times \mathbb{R}^{\mathcal{F}m} \rightarrow \mathbb{R}$, $f_0 : \Pi_{p=1}^4 \mathbb{R}^{\mathcal{F}m} \rightarrow \mathbb{R}$, $f_1 : \mathbb{R}^{\mathcal{F}m} \times \mathbb{R}^{\mathcal{F}m} \rightarrow \mathbb{R}$, $f_2 : \Pi_{p=1}^4 \mathbb{R}^{\mathcal{F}m} \rightarrow \mathbb{R}$, are defined as

$$\begin{aligned}
S_0 &\triangleq \left\| C\dot{Q}_{\mathcal{F}} + F + G \right\|, & S_1 &\triangleq \frac{2}{k\underline{m}^2} \|L_B\| S_0, \\
S_2 &\triangleq \frac{4}{k^2\underline{m}^2} S_0^2 + \frac{2}{\underline{m}} \left(\frac{\bar{d}}{k^2\underline{m}} + \frac{\bar{Q}_L}{k^2} + \frac{\iota_1}{k\underline{m}} \right) S_0, \\
f_0 &\triangleq \lambda\bar{m} \|R - \lambda E\| + \frac{1}{2} \left\| \dot{M}R \right\|, \\
f_1 &\triangleq \frac{4}{\underline{m}^2} \|L_B\|^2 \|R\| + \frac{2\lambda}{k\underline{m}} \|L_B\| \|R - \lambda E\| + \frac{2}{\underline{m}^2} \left\| \sum_{(j,i) \in \mathcal{E}_{\mathcal{F}}} (\kappa_1 \mathcal{A}_{ij} - \kappa_2 \mathcal{L}_{ij}) \right\|^2 \|R\| \\
&\quad + \frac{2\kappa_2^2 |\mathcal{E}_L|}{\underline{m}^2} \sum_{(L,i) \in \mathcal{E}_L} \|\mathcal{B}_i\|^2 \|R\| \\
&\quad + \frac{2|\mathcal{E}_{\mathcal{F}}| (1 + \bar{\tau})}{\omega \underline{m}^2} \sum_{(j,i) \in \mathcal{E}_{\mathcal{F}}} (\|\kappa_1 \mathcal{A}_{ij} - \kappa_2 \mathcal{L}_{ij}\|^2 + \kappa_2^2 \|\mathcal{D}_{ij}\|^2) \|R\| \\
&\quad + \frac{2\kappa_2^2 |\mathcal{E}_{\mathcal{F}}|^2 (1 + \bar{\tau})}{\hat{\omega} \underline{m}^2} \sum_{(j,i) \in \mathcal{E}_{\mathcal{F}}} \|\mathcal{D}_{ij}\|^2 \|R\| + \frac{2\kappa_2^2 |\mathcal{E}_{\mathcal{F}}| |\mathcal{E}_L| (1 + \bar{\tau})}{\hat{\omega} \underline{m}^2} \sum_{(L,i) \in \mathcal{E}_L} \|\mathcal{B}_i\|^2 \|R\|, \\
f_2 &\triangleq \frac{2\lambda}{k^2 \underline{m}} S_0 \|R - \lambda E\| + 2\lambda \left(\frac{\bar{d}}{k^2 \underline{m}} + \frac{\bar{Q}_L}{k^2} + \frac{\iota_1}{k \underline{m}} \right) \|R - \lambda E\| + \frac{4\lambda^2}{k^2} \|R - \lambda E\|^2.
\end{aligned}$$

The functions $\tilde{N}_0, \tilde{N}_1, \tilde{N}_2$ contain terms which can be upper-bounded by a function of the error signals E and R . By [58, Lemma 5], there exist strictly increasing, radially unbounded functions $\rho_0, \rho_1, \rho_2 : \mathbb{R}_{\geq 0} \rightarrow \mathbb{R}_{\geq 0}$ which upper-bound $\tilde{N}_0, \tilde{N}_1, \tilde{N}_2$ as³

$$\left| \tilde{N}_0 \right| \leq \rho_0 (\|Z\|) \|Z\|, \quad \left| \tilde{N}_1 \right| \leq \rho_1 (\|Z\|) \|Z\|, \quad \left| \tilde{N}_2 \right| \leq \rho_2 (\|Z\|) \|Z\|, \quad (4-20)$$

³ While the *smallest* upper-bounding functions of the dynamics in $\tilde{N}_0, \tilde{N}_1, \tilde{N}_2$ may not be known, the bounding functions ρ_0, ρ_1, ρ_2 may feasibly be constructed; for example, a friction coefficient may be unknown, but a sufficient upper bound can easily be determined.

where the bounds for $|\tilde{N}_0|$ and $|\tilde{N}_2|$ are facilitated by adding and subtracting the expression $f_0(E, R, Q_L, \dot{Q}_L)$ in \tilde{N}_0 and the expression $f_2(E, R, Q_L, \dot{Q}_L)$ in \tilde{N}_2 .

The set $\mathcal{D} \subset \mathbb{R}^{2\mathcal{F}m+6}$ is defined as

$$\mathcal{D} \triangleq \left\{ \xi \in \mathbb{R}^{2\mathcal{F}m+6} \mid \|\xi\| < \inf \left\{ \rho^{-1} \left(\left[\sqrt{\eta}, \infty \right) \right) \right\} \right\},$$

where $\rho : \mathbb{R}_{\geq 0} \rightarrow \mathbb{R}_{\geq 0}$ is a strictly increasing, radially unbounded function defined as

$$\begin{aligned} \rho(\|Z\|) \triangleq & \left(\frac{3\rho_0^2(\|Z\|)}{2\underline{k}} + \frac{3\phi^2\rho_1^2(\|Z\|)}{2\underline{k}} (\bar{\tau}\iota_2|\mathcal{E}_{\mathcal{F}}| + (\bar{\tau} + \bar{\bar{\tau}})(\iota_3|\mathcal{E}_{\mathcal{F}}| + \iota_4|\mathcal{E}_L|)) \right)^2 \\ & + \phi(\bar{\tau}\iota_2|\mathcal{E}_{\mathcal{F}}| + (\bar{\tau} + \bar{\bar{\tau}})(\iota_3|\mathcal{E}_{\mathcal{F}}| + \iota_4|\mathcal{E}_L|)) \rho_2^2(\|Z\|) \Big)^{\frac{1}{2}}, \end{aligned} \quad (4-21)$$

where the inverse image $\rho^{-1}(\Theta) \subset \mathbb{R}$ for a set $\Theta \subset \mathbb{R}$ is defined as $\rho^{-1}(\Theta) \triangleq \{\xi \in \mathbb{R} \mid \rho(\xi) \in \Theta\}$. The stabilizing set of initial conditions, $\mathcal{S}_{\mathcal{D}}$, is defined as

$$\mathcal{S}_{\mathcal{D}} \triangleq \left\{ \xi \in \mathcal{D} \mid \|\xi\| < \sqrt{\frac{\min\{\frac{c}{2}, \frac{\bar{m}}{2}, 1\}}{\max\{\frac{c}{2}, \frac{\bar{m}}{2}, 1\}}} \inf \left\{ \rho^{-1} \left(\left[\sqrt{\eta}, \infty \right) \right) \right\} \right\}. \quad (4-22)$$

The following assumption provides a sufficient condition for the subsequent convergence analysis by describing how small the network communication delays and delay estimate errors should be to ensure convergence for a given network configuration.

Assumption 4.8. For a given network graph \mathcal{G} and leader trajectory q_L , the communication delay upper bound $\bar{\tau} > 0$ and delay estimate error upper bound $\bar{\bar{\tau}} > 0$ are sufficiently small such that there exists a selection for the gain k and tuning parameter ϕ such that

$$\lambda(L_B) - \frac{(\bar{\tau} + \bar{\bar{\tau}})k^3}{2\phi} - \iota_1 k > 0, \quad (4-23)$$

$$\inf \left\{ \rho^{-1} \left(\left[\sqrt{\eta}, \infty \right) \right) \right\} > \sqrt{\frac{2 \max \left\{ \frac{c}{2}, \frac{m}{2}, 1 \right\}}{\theta \min \left\{ \frac{c}{2}, \frac{m}{2}, 1 \right\}}} \cdot \left(\frac{3 \left(N_{d0}^2 + \phi^2 N_{d1}^2 \left(\bar{\tau} \iota_2 |\mathcal{E}_{\mathcal{F}}| + (\bar{\tau} + \bar{\tilde{\tau}}) (\iota_3 |\mathcal{E}_{\mathcal{F}}| + \iota_4 |\mathcal{E}_L|) \right)^2 \right)}{2\underline{k}} \right. \\ \left. + \phi \left(\bar{\tau} \iota_2 |\mathcal{E}_{\mathcal{F}}| + (\bar{\tau} + \bar{\tilde{\tau}}) (\iota_3 |\mathcal{E}_{\mathcal{F}}| + \iota_4 |\mathcal{E}_L|) \right) \left(\frac{1}{4} + N_{d2} \right) + \frac{\iota_1}{4} \right)^{\frac{1}{2}}. \quad (4-24)$$

Remark 4.1. Assumption 4.8 ensures that there exists a selection for c such that $\underline{k} > 0$.

Accordingly, let the value for c be assigned such that

$$0 < c < 2k \left(\underline{\lambda}(L_B) - \frac{(\bar{\tau} + \bar{\tilde{\tau}})}{2\phi} k^3 - \iota_1 k \right).$$

Assumption 4.8 also ensures that there exist stabilizing initial conditions and that the ultimate bound on the convergence of each agent toward the leader state is within the considered domain \mathcal{D} .

Remark 4.2. Due to the presence of \underline{k} , $\bar{\tau}$, and $\bar{\tilde{\tau}}$ in (4-21), there exist sufficiently small values for $\bar{\tau}$ and $\bar{\tilde{\tau}}$ such that there exists a value for the gain k such that (4-23) is satisfied and $\inf \left\{ \rho^{-1} \left(\left[\sqrt{\eta}, \infty \right) \right) \right\} > \delta$ for any $\delta \in \mathbb{R}_{>0}$, i.e., the set $\mathcal{S}_{\mathcal{D}}$ can contain any initial condition for a small enough $\bar{\tau}$ and $\bar{\tilde{\tau}}$. The tuning parameter ϕ is included to more easily see the effect of communication delay on system convergence: the inequality in (4-23) may be satisfied for large delay and delay estimate error upper bounds by increasing ϕ , but doing so may result in a smaller set of stabilizing initial conditions $\mathcal{S}_{\mathcal{D}}$ and cause the sufficient condition in (4-24) to be unsatisfied. Thus, if the leader has a trajectory with low acceleration and the follower agents have less volatile dynamics and small disturbances, the conditions in Assumption 4.8 can be more easily satisfied for larger delay and delay estimate error upper bounds by increasing ϕ , as seen in the effects of (4-15), (4-16), (4-18), and (4-19) on (4-22) and (4-24).

The following theorem describes the convergence provided by the controller in (4-4) for the synchronization of a network of agents with uncertain nonlinear dynamics

given by (4–1) which are affected by heterogeneous uncertain time-varying delays and input disturbances.

Theorem 4.1. *The communication-delayed controller in (4–4) provides UUB synchronization for a network of agents with dynamics given by (4–1) in the sense that $\limsup_{t \rightarrow \infty} \|q_i(t) - q_L(t)\| < \varepsilon$ for some $\varepsilon \in \mathbb{R}_{>0}$ and every follower agent $i \in \mathcal{V}_{\mathcal{F}}$ for all initial conditions $y(0) \in \mathcal{S}_{\mathfrak{D}}$, provided that Assumptions 4.1–4.8 are satisfied and the gain λ satisfies*

$$\lambda > \frac{1}{2}. \quad (4-25)$$

Proof. Consider the candidate Lyapunov function $V_L : \mathfrak{D} \times \mathbb{R} \rightarrow \mathbb{R}_{\geq 0}$ defined as

$$V_L \triangleq \frac{c}{2} E^T E + \frac{1}{2} R^T M R + \Psi_{1a} + \Psi_{1b} + \Psi_{2a} + \Psi_{2b} + \Psi_{3a} + \Psi_{3b}, \quad (4-26)$$

which satisfies the inequalities

$$\min \left\{ \frac{c}{2}, \frac{\bar{m}}{2}, 1 \right\} \|y\|^2 \leq V_L(y, t) \leq \max \left\{ \frac{c}{2}, \frac{\bar{m}}{2}, 1 \right\} \|y\|^2$$

for all $y \in \mathbb{R}^{2\mathcal{F}m+6}$ and $t \in \mathbb{R}$, where the block inertia matrix M is interpreted as a function of time, and the LK functionals $\Psi_{1a}, \Psi_{1b}, \Psi_{2a}, \Psi_{2b}, \Psi_{3a}, \Psi_{3b}$ are defined in (4–8)–(4–13).

By using the Leibniz rule and the definitions of $\bar{\tau}, \tilde{\tau}, \omega, \hat{\omega}$, the time derivatives of LK functionals Ψ_{1a}, Ψ_{1b} and upper bounds of the time derivatives of LK functionals $\Psi_{2a}, \Psi_{2b}, \Psi_{3a}, \Psi_{3b}$ are determined as

$$\dot{\Psi}_{1a} = \frac{\phi \iota_2 |\mathcal{E}_{\mathcal{F}}|}{k^2} \left(\bar{\tau} \|\dot{R}\|^2 - \int_{t-\bar{\tau}}^t \|\dot{R}(\sigma)\|^2 d\sigma \right), \quad (4-27)$$

$$\dot{\Psi}_{1b} = \frac{\phi (\iota_3 |\mathcal{E}_{\mathcal{F}}| + \iota_4 |\mathcal{E}_L|)}{k^2} \left((\bar{\tau} + \tilde{\tau}) \|\dot{R}\|^2 - \int_{t-\bar{\tau}-\tilde{\tau}}^t \|\dot{R}(\sigma)\|^2 d\sigma \right), \quad (4-28)$$

$$\begin{aligned}
\dot{\Psi}_{2a} \leq & \frac{2\phi |\mathcal{E}_{\mathcal{F}}| (\bar{\tau}\iota_2 |\mathcal{E}_{\mathcal{F}}| + (\bar{\tau} + \bar{\tilde{\tau}}) (\iota_3 |\mathcal{E}_{\mathcal{F}}| + \iota_4 |\mathcal{E}_L|))}{\underline{m}^2} \\
& \cdot \sum_{(j,i) \in \mathcal{E}_{\mathcal{F}}} \left(\frac{1}{\hat{\omega}} (\|(\kappa_1 \mathcal{A}_{ij} - \kappa_2 \mathcal{L}_{ij}) R\|^2 + \kappa_2^2 \|\mathcal{D}_{ij} R\|^2) \right. \\
& \left. - \left(\|(\kappa_1 \mathcal{A}_{ij} - \kappa_2 \mathcal{L}_{ij}) R(t - \tau_{ji})\|^2 + \kappa_2^2 \|\mathcal{D}_{ij} R(t - \tau_{ji})\|^2 \right) \right), \tag{4-29}
\end{aligned}$$

$$\begin{aligned}
\dot{\Psi}_{2b} \leq & \frac{2\phi \kappa_2^2 |\mathcal{E}_{\mathcal{F}}| (\bar{\tau}\iota_2 |\mathcal{E}_{\mathcal{F}}| + (\bar{\tau} + \bar{\tilde{\tau}}) (\iota_3 |\mathcal{E}_{\mathcal{F}}| + \iota_4 |\mathcal{E}_L|))}{\underline{m}^2} \\
& \cdot \left(\frac{|\mathcal{E}_{\mathcal{F}}|}{\hat{\omega}} \sum_{(j,i) \in \mathcal{E}_{\mathcal{F}}} \|\mathcal{D}_{ij} R\|^2 + \frac{|\mathcal{E}_L|}{\hat{\omega}} \sum_{(L,i) \in \mathcal{E}_L} \|(\mathcal{B}_i \otimes I_m) R\|^2 \right. \\
& \left. - |\mathcal{E}_{\mathcal{F}}| \sum_{(j,i) \in \mathcal{E}_{\mathcal{F}}} \|\mathcal{D}_{ij} R(t - \hat{\tau}_{ji})\|^2 - |\mathcal{E}_L| \sum_{(L,i) \in \mathcal{E}_L} \|(\mathcal{B}_i \otimes I_m) R(t - \hat{\tau}_{ji})\|^2 \right), \tag{4-30}
\end{aligned}$$

$$\begin{aligned}
\dot{\Psi}_{3a} \leq & \frac{2\phi |\mathcal{E}_{\mathcal{F}}| (\bar{\tau}\iota_2 |\mathcal{E}_{\mathcal{F}}| + (\bar{\tau} + \bar{\tilde{\tau}}) (\iota_3 |\mathcal{E}_{\mathcal{F}}| + \iota_4 |\mathcal{E}_L|))}{\underline{m}^2} \\
& \cdot \sum_{(j,i) \in \mathcal{E}_{\mathcal{F}}} \left(- \int_{t-\tau_{ji}}^t (\|(\kappa_1 \mathcal{A}_{ij} - \kappa_2 \mathcal{L}_{ij}) R(\sigma)\|^2 + \kappa_2^2 \|\mathcal{D}_{ij} R(\sigma)\|^2) d\sigma \right. \\
& \left. + \frac{\bar{\tau}}{\omega} (\|(\kappa_1 \mathcal{A}_{ij} - \kappa_2 \mathcal{L}_{ij}) R\|^2 + \kappa_2^2 \|\mathcal{D}_{ij} R\|^2) \right), \tag{4-31}
\end{aligned}$$

$$\begin{aligned}
\dot{\Psi}_{3b} \leq & \frac{2\phi \kappa_2^2 |\mathcal{E}_{\mathcal{F}}| (\bar{\tau}\iota_2 |\mathcal{E}_{\mathcal{F}}| + (\bar{\tau} + \bar{\tilde{\tau}}) (\iota_3 |\mathcal{E}_{\mathcal{F}}| + \iota_4 |\mathcal{E}_L|))}{\underline{m}^2} \\
& \cdot \left(- \int_{t-\hat{\tau}_{ji}}^t \left(|\mathcal{E}_{\mathcal{F}}| \sum_{(j,i) \in \mathcal{E}_{\mathcal{F}}} \|\mathcal{D}_{ij} R(\sigma)\|^2 + |\mathcal{E}_L| \sum_{(L,i) \in \mathcal{E}_L} \|(\mathcal{B}_i \otimes I_m) R(\sigma)\|^2 \right) d\sigma \right. \\
& \left. + \frac{\bar{\tilde{\tau}} |\mathcal{E}_{\mathcal{F}}|}{\hat{\omega}} \sum_{(j,i) \in \mathcal{E}_{\mathcal{F}}} \|\mathcal{D}_{ij} R\|^2 + \frac{\bar{\tilde{\tau}} |\mathcal{E}_L|}{\hat{\omega}} \sum_{(L,i) \in \mathcal{E}_L} \|(\mathcal{B}_i \otimes I_m) R\|^2 \right) \tag{4-32}
\end{aligned}$$

Based on (4-8)-(4-13), feedback of the LK functionals in the state y of the Lyapunov function V_L is facilitated by developing the inequalities

$$\frac{\Psi_{1a}}{\bar{\tau}} \leq \frac{\phi \iota_2 |\mathcal{E}_{\mathcal{F}}|}{k^2} \int_{t-\bar{\tau}}^t \|\dot{R}(\sigma)\|^2 d\sigma, \tag{4-33}$$

$$\frac{\Psi_{1b}}{(\bar{\tau} + \bar{\tilde{\tau}})} \leq \frac{\phi (\iota_3 |\mathcal{E}_{\mathcal{F}}| + \iota_4 |\mathcal{E}_L|)}{k^2} \int_{t-\bar{\tau}-\bar{\tilde{\tau}}}^t \|\dot{R}(\sigma)\|^2 d\sigma, \tag{4-34}$$

$$\begin{aligned} \frac{\omega}{2}\Psi_{2a} + \frac{\omega}{2\bar{\tau}}\Psi_{3a} &\leq \frac{2\phi|\mathcal{E}_{\mathcal{F}}|(\bar{\tau}\iota_2|\mathcal{E}_{\mathcal{F}}| + (\bar{\tau} + \bar{\bar{\tau}})(\iota_3|\mathcal{E}_{\mathcal{F}}| + \iota_4|\mathcal{E}_L|))}{m^2} \\ &\cdot \sum_{(j,i) \in \mathcal{E}_{\mathcal{F}}} \int_{t-\tau_{ji}}^t \left(\|(\kappa_1\mathcal{A}_{ij} - \kappa_2\mathcal{L}_{ij})R(\sigma)\|^2 + \kappa_2^2 \|\mathcal{D}_{ij}R(\sigma)\|^2 \right) d\sigma, \end{aligned} \quad (4-35)$$

$$\begin{aligned} \frac{\hat{\omega}}{2}\Psi_{2b} + \frac{\hat{\omega}}{2\hat{\tau}}\Psi_{3b} &\leq \frac{2\phi\kappa_2^2|\mathcal{E}_{\mathcal{F}}|(\bar{\tau}\iota_2|\mathcal{E}_{\mathcal{F}}| + (\bar{\tau} + \bar{\bar{\tau}})(\iota_3|\mathcal{E}_{\mathcal{F}}| + \iota_4|\mathcal{E}_L|))}{m^2} \\ &\cdot \int_{t-\hat{\tau}_{ji}}^t \left(|\mathcal{E}_{\mathcal{F}}| \sum_{(j,i) \in \mathcal{E}_{\mathcal{F}}} \|\mathcal{D}_{ij}R(\sigma)\|^2 + |\mathcal{E}_L| \sum_{(L,i) \in \mathcal{E}_L} \|(\mathcal{B}_i \otimes I_m)R(\sigma)\|^2 \right) d\sigma. \end{aligned} \quad (4-36)$$

The inequality in (4-33) can be demonstrated using the bounds

$$\begin{aligned} \Psi_{1a} &\leq \frac{\phi\iota_2|\mathcal{E}_{\mathcal{F}}|}{k^2} \int_{t-\bar{\tau}}^t \sup_{s \in [t-\bar{\tau}, t]} \int_{\mathcal{S}} \|\dot{R}(\sigma)\|^2 d\sigma ds \\ &\leq \frac{\phi\bar{\tau}\iota_2|\mathcal{E}_{\mathcal{F}}|}{k^2} \sup_{s \in [t-\bar{\tau}, t]} \int_{\mathcal{S}} \|\dot{R}(\sigma)\|^2 d\sigma \\ &\leq \frac{\phi\bar{\tau}\iota_2|\mathcal{E}_{\mathcal{F}}|}{k^2} \int_{t-\bar{\tau}}^t \|\dot{R}(\sigma)\|^2 d\sigma, \end{aligned}$$

and a similar procedure is used to obtain the inequalities in (4-34)-(4-36). Two final inequalities are developed to facilitate the convergence analysis as

$$\begin{aligned} kR^T \sum_{(j,i) \in \mathcal{E}_{\mathcal{F}}} \left[(\kappa_1\mathcal{A}_{ij} - \kappa_2\mathcal{L}_{ij}) \int_{t-\tau_{ji}}^t \dot{R}(\sigma) d\sigma - \kappa_2\mathcal{D}_{ij} \int_{t-\hat{\tau}_{ji}}^{t-\tau_{ji}} \dot{R}(\sigma) d\sigma \right] &\leq \\ \frac{(\bar{\tau} + \bar{\bar{\tau}})k^4}{2\phi} R^T R + \frac{\phi\iota_2|\mathcal{E}_{\mathcal{F}}|}{2k^2} \int_{t-\bar{\tau}}^t \|\dot{R}(\sigma)\|^2 d\sigma + \frac{\phi\iota_3|\mathcal{E}_{\mathcal{F}}|}{2k^2} \int_{t-\bar{\tau}-\bar{\bar{\tau}}}^t \|\dot{R}(\sigma)\|^2 d\sigma, \end{aligned} \quad (4-37)$$

$$k\kappa_2 R^T \sum_{(L,i) \in \mathcal{E}_L} (\mathcal{B}_i \otimes I_m) \int_{t-\hat{\tau}_{Li}}^t \dot{R}(\sigma) d\sigma \leq \frac{(\bar{\tau} + \bar{\bar{\tau}})k^4}{2\phi} R^T R + \frac{\phi\iota_4|\mathcal{E}_L|}{2k^2} \int_{t-\bar{\tau}-\bar{\bar{\tau}}}^t \|\dot{R}(\sigma)\|^2 d\sigma, \quad (4-38)$$

which serve to separate the error signal R from a delay contributing expression that can be compensated using the aforementioned LK functionals. The process to obtain the inequalities in (4-37)-(4-38) is described in Appendix C.

By using the closed-loop error system in (4-7), the time derivative of (4-26) can be expressed as

$$\begin{aligned}
\dot{V}_L = & cE^T (R - \lambda E) + R^T \left(C\dot{Q}_F + F + G - d + M\ddot{Q}_L + \lambda M\dot{E} - kL_B R \right) + \frac{1}{2} R^T \dot{M} R \\
& + kR^T \sum_{(j,i) \in \mathcal{E}_F} \left[(\kappa_1 \mathcal{A}_{ij} - \kappa_2 \mathcal{L}_{ij}) \int_{t-\tau_{ji}}^t \dot{R}(\sigma) d\sigma - \kappa_2 \mathcal{D}_{ij} \int_{t-\hat{\tau}_{ji}}^{t-\tau_{ji}} \dot{R}(\sigma) d\sigma \right] \\
& - kR^T \sum_{(j,i) \in \mathcal{E}_F} (\kappa_1 \mathcal{A}_{ij} - \kappa_2 \mathcal{L}_{ij}) \int_{t-\tau_{ji}}^t \left(\ddot{Q}_L(\sigma) + \lambda \dot{Q}_L(\sigma) \right) d\sigma \\
& + k\kappa_2 R^T \sum_{(j,i) \in \mathcal{E}_F} \mathcal{D}_{ij} \int_{t-\hat{\tau}_{ji}}^{t-\tau_{ji}} \left(\ddot{Q}_L(\sigma) + \lambda \dot{Q}_L(\sigma) \right) d\sigma \\
& - k\kappa_2 R^T \sum_{(L,i) \in \mathcal{E}_L} (\mathcal{B}_i \otimes I_m) \int_{t-\hat{\tau}_{Li}}^t \dot{R}(\sigma) d\sigma \\
& + kR^T \left(-\kappa_1 \sum_{(L,i) \in \mathcal{E}_L} (\mathcal{B}_i \otimes I_m) \int_{t-\tau_{Li}}^t \left(\ddot{Q}_L(\sigma) + \lambda \dot{Q}_L(\sigma) \right) d\sigma \right. \\
& \left. + \kappa_2 \sum_{(L,i) \in \mathcal{E}_L} (\mathcal{B}_i \otimes I_m) \int_{t-\hat{\tau}_{Li}}^{t-\tau_{Li}} \left(\ddot{Q}_L(\sigma) + \lambda \dot{Q}_L(\sigma) \right) d\sigma \right) \\
& + \dot{\Psi}_{1a} + \dot{\Psi}_{1b} + \dot{\Psi}_{2a} + \dot{\Psi}_{2b} + \dot{\Psi}_{3a} + \dot{\Psi}_{3b}. \tag{4-39}
\end{aligned}$$

After using the expressions in (4-27)-(4-32), the inequalities in (4-33)-(4-38), and canceling terms, (4-39) can be upper-bounded as

$$\begin{aligned}
\dot{V}_L = & cE^T (R - \lambda E) + \frac{1}{2}R^T \dot{M}R + \frac{(\bar{\tau} + \bar{\tilde{\tau}})k^4}{\phi}R^T R \\
& - \frac{\Psi_{1a}}{2\bar{\tau}} - \frac{\Psi_{1b}}{2(\bar{\tau} + \bar{\tilde{\tau}})} - \frac{\omega}{2}\Psi_{2a} - \frac{\hat{\omega}}{2}\Psi_{2b} - \frac{\omega}{2\bar{\tau}}\Psi_{3a} - \frac{\hat{\omega}}{2\bar{\tilde{\tau}}}\Psi_{3b} \\
& + R^T \left(C\dot{Q}_{\mathcal{F}} + F + G - d + M\ddot{Q}_L + \lambda M\dot{E} - kL_B R \right) + k\iota_1 \|R\| \\
& + \frac{\phi\bar{\tau}\iota_2 |\mathcal{E}_{\mathcal{F}}| + \phi(\bar{\tau} + \bar{\tilde{\tau}})(\iota_3 |\mathcal{E}_{\mathcal{F}}| + \iota_4 |\mathcal{E}_L|)}{k^2} \|\dot{R}\|^2 \\
& + \frac{2\phi |\mathcal{E}_{\mathcal{F}}| (\bar{\tau}\iota_2 |\mathcal{E}_{\mathcal{F}}| + (\bar{\tau} + \bar{\tilde{\tau}})(\iota_3 |\mathcal{E}_{\mathcal{F}}| + \iota_4 |\mathcal{E}_L|))}{m^2} \left(\right. \\
& \frac{(1 + \bar{\tau})}{\omega} \sum_{(j,i) \in \mathcal{E}_{\mathcal{F}}} (\|(\kappa_1 \mathcal{A}_{ij} - \kappa_2 \mathcal{L}_{ij}) R\|^2 + \kappa_2^2 \|\mathcal{D}_{ij} R\|^2) \\
& + \frac{\kappa_2^2 |\mathcal{E}_{\mathcal{F}}| (1 + \bar{\tau})}{\hat{\omega}} \sum_{(j,i) \in \mathcal{E}_{\mathcal{F}}} \|\mathcal{D}_{ij} R\|^2 + \frac{\kappa_2^2 |\mathcal{E}_L| (1 + \bar{\tau})}{\hat{\omega}} \sum_{(L,i) \in \mathcal{E}_L} \|(\mathcal{B}_i \otimes I_m) R\|^2 \\
& - \sum_{(j,i) \in \mathcal{E}_{\mathcal{F}}} \left(\|(\kappa_1 \mathcal{A}_{ij} - \kappa_2 \mathcal{L}_{ij}) R(t - \tau_{ji})\|^2 + \kappa_2^2 \|\mathcal{D}_{ij} R(t - \tau_{ji})\|^2 \right) \\
& \left. - \kappa_2^2 |\mathcal{E}_{\mathcal{F}}| \sum_{(j,i) \in \mathcal{E}_{\mathcal{F}}} \|\mathcal{D}_{ij} R(t - \hat{\tau}_{ji})\|^2 - \kappa_2^2 |\mathcal{E}_L| \sum_{(L,i) \in \mathcal{E}_L} \|(\mathcal{B}_i \otimes I_m) R(t - \hat{\tau}_{ji})\|^2 \right).
\end{aligned}$$

After expanding the term $\|\dot{R}\|^2$ using the closed-loop error system in (4–7), evaluating the resulting integrals, using Young’s inequality and the inequality $\|\sum_{i=1}^n \xi\|^2 \leq n \sum_{i=1}^n \|\xi\|^2$ for $\xi \in \mathbb{R}^{\mathcal{F}m}$, canceling terms, and using the bounding expressions in (4–14)-(4–19), \dot{V}_L can be further upper-bounded as

$$\begin{aligned}
\dot{V}_L \leq & -c \left(\lambda - \frac{1}{2} \right) \|E\|^2 - k \left(\lambda(L_B) - \frac{(\bar{\tau} + \bar{\tilde{\tau}})k^3}{\phi} - \frac{c}{2k} \right) \|R\|^2 \\
& - \frac{\Psi_{1a}}{2\bar{\tau}} - \frac{\Psi_{1b}}{2(\bar{\tau} + \bar{\tilde{\tau}})} - \frac{\omega}{2}\Psi_{2a} - \frac{\hat{\omega}}{2}\Psi_{2b} - \frac{\omega}{2\bar{\tau}}\Psi_{3a} - \frac{\hat{\omega}}{2\bar{\tilde{\tau}}}\Psi_{3b} \\
& + \left(N_{d0} + \tilde{N}_0 \right) \|R\| + \phi(\bar{\tau}\iota_2 |\mathcal{E}_{\mathcal{F}}| + (\bar{\tau} + \bar{\tilde{\tau}})(\iota_3 |\mathcal{E}_{\mathcal{F}}| + \iota_4 |\mathcal{E}_L|)) \\
& \cdot \left(\left(N_{d1} + \tilde{N}_1 \right) \|R\| + N_{d2} + \tilde{N}_2 \right) + k\iota_1 \|R\|, \tag{4–40}
\end{aligned}$$

where $\lambda - \frac{1}{2}$ is positive by (4–25). After using the inequality $k\iota_1 \|R\| \leq k^2\iota_1 \|R\|^2 + \frac{\iota_1}{4}$, the definitions for \underline{c} and \underline{k} , and the expressions in (4–20), (4–40) can be upper-bounded as

$$\begin{aligned} \dot{V}_L &\leq -\underline{c}\|E\|^2 - \underline{k}\|R\|^2 - \frac{\Psi_{1a}}{2\bar{\tau}} - \frac{\Psi_{1b}}{2(\bar{\tau} + \bar{\tau})} - \frac{\omega}{2}\Psi_{2a} - \frac{\hat{\omega}}{2}\Psi_{2b} - \frac{\omega}{2\bar{\tau}}\Psi_{3a} - \frac{\hat{\omega}}{2\bar{\tau}}\Psi_{3b} \\ &\quad + (N_{d0} + \rho_0(\|Z\|)\|Z\| + \phi(\bar{\tau}\iota_2|\mathcal{E}_{\mathcal{F}}| + (\bar{\tau} + \bar{\tau})(\iota_3|\mathcal{E}_{\mathcal{F}}| + \iota_4|\mathcal{E}_L|))) \\ &\quad \cdot (N_{d1} + \rho_1(\|Z\|)\|Z\|)\|R\| \\ &\quad + \phi(\bar{\tau}\iota_2|\mathcal{E}_{\mathcal{F}}| + (\bar{\tau} + \bar{\tau})(\iota_3|\mathcal{E}_{\mathcal{F}}| + \iota_4|\mathcal{E}_L|))(N_{d2} + \rho_2(\|Z\|)\|Z\|) + \frac{\iota_1}{4}. \end{aligned} \quad (4-41)$$

By using a fraction of the feedback $-\underline{k}\|R\|^2$ to perform nonlinear damping on the other terms multiplied by $\|R\|$, and using the inequality $\rho_2(\|Z\|)\|Z\| \leq \rho_2^2(\|Z\|)\|Z\|^2 + \frac{1}{4}$, (4–41) can be upper-bounded as

$$\begin{aligned} \dot{V}_L &\leq -\eta\|Z\|^2 - \frac{\Psi_{1a}}{2\bar{\tau}} - \frac{\Psi_{1b}}{2(\bar{\tau} + \bar{\tau})} - \frac{\omega}{2}\Psi_{2a} - \frac{\hat{\omega}}{2}\Psi_{2b} - \frac{\omega}{2\bar{\tau}}\Psi_{3a} - \frac{\hat{\omega}}{2\bar{\tau}}\Psi_{3b} \\ &\quad - \left(\eta - \frac{3\rho_0^2(\|Z\|)}{2\underline{k}} - \frac{3\phi^2\rho_1^2(\|Z\|)}{2\underline{k}} (\bar{\tau}\iota_2|\mathcal{E}_{\mathcal{F}}| + (\bar{\tau} + \bar{\tau})(\iota_3|\mathcal{E}_{\mathcal{F}}| + \iota_4|\mathcal{E}_L|))^2 \right. \\ &\quad \left. - \phi(\bar{\tau}\iota_2|\mathcal{E}_{\mathcal{F}}| + (\bar{\tau} + \bar{\tau})(\iota_3|\mathcal{E}_{\mathcal{F}}| + \iota_4|\mathcal{E}_L|))\rho_2^2(\|Z\|) \right) \|Z\|^2 \\ &\quad + \frac{3N_{d0}^2}{2\underline{k}} + \frac{3\phi^2N_{d1}^2}{2\underline{k}} (\bar{\tau}\iota_2|\mathcal{E}_{\mathcal{F}}| + (\bar{\tau} + \bar{\tau})(\iota_3|\mathcal{E}_{\mathcal{F}}| + \iota_4|\mathcal{E}_L|))^2 \\ &\quad + \phi(\bar{\tau}\iota_2|\mathcal{E}_{\mathcal{F}}| + (\bar{\tau} + \bar{\tau})(\iota_3|\mathcal{E}_{\mathcal{F}}| + \iota_4|\mathcal{E}_L|)) \left(\frac{1}{4} + N_{d2} \right) + \frac{\iota_1}{4}. \end{aligned} \quad (4-42)$$

Provided Assumption 4.8 is satisfied, (4–42) can be upper-bounded as

$$\begin{aligned} \dot{V}_L &\leq -\theta\|y\|^2 + \frac{3N_{d0}^2}{2\underline{k}} + \frac{3\phi^2N_{d1}^2}{2\underline{k}} (\bar{\tau}\iota_2|\mathcal{E}_{\mathcal{F}}| + (\bar{\tau} + \bar{\tau})(\iota_3|\mathcal{E}_{\mathcal{F}}| + \iota_4|\mathcal{E}_L|))^2 \\ &\quad + \phi(\bar{\tau}\iota_2|\mathcal{E}_{\mathcal{F}}| + (\bar{\tau} + \bar{\tau})(\iota_3|\mathcal{E}_{\mathcal{F}}| + \iota_4|\mathcal{E}_L|)) \left(\frac{1}{4} + N_{d2} \right) + \frac{\iota_1}{4} \end{aligned}$$

for all $y \in \mathfrak{D}$, and thus,

$$\begin{aligned} \dot{V}_L &\leq -\frac{\theta}{2}\|y\|^2 \quad \forall \|y\| \geq \sqrt{\frac{2}{\theta}} \left(\frac{3N_{d0}^2}{2\underline{k}} + \frac{3\phi^2N_{d1}^2}{2\underline{k}} (\bar{\tau}\iota_2|\mathcal{E}_{\mathcal{F}}| + (\bar{\tau} + \bar{\tau})(\iota_3|\mathcal{E}_{\mathcal{F}}| + \iota_4|\mathcal{E}_L|))^2 \right. \\ &\quad \left. + \phi(\bar{\tau}\iota_2|\mathcal{E}_{\mathcal{F}}| + (\bar{\tau} + \bar{\tau})(\iota_3|\mathcal{E}_{\mathcal{F}}| + \iota_4|\mathcal{E}_L|)) \left(\frac{1}{4} + N_{d2} \right) + \frac{\iota_1}{4} \right)^{\frac{1}{2}}. \end{aligned} \quad (4-43)$$

By (4–43), [76, Theorem 4.18] and Assumption 4.8,

$$\begin{aligned} \limsup_{t \rightarrow \infty} \|q_i(t) - q_L(t)\| &\leq \limsup_{t \rightarrow \infty} \|y(t)\| \leq \sqrt{\frac{2 \max\{\frac{c}{2}, \frac{\bar{m}}{2}, 1\}}{\theta \min\{\frac{c}{2}, \frac{\bar{m}}{2}, 1\}}} \\ &\cdot \left(\frac{3 \left(N_{d0}^2 + \phi^2 N_{d1}^2 (\bar{\tau} \iota_2 |\mathcal{E}_{\mathcal{F}}| + (\bar{\tau} + \bar{\bar{\tau}}) (\iota_3 |\mathcal{E}_{\mathcal{F}}| + \iota_4 |\mathcal{E}_L|)) \right)^2}{2\underline{k}} \right. \\ &\quad \left. + \phi (\bar{\tau} \iota_2 |\mathcal{E}_{\mathcal{F}}| + (\bar{\tau} + \bar{\bar{\tau}}) (\iota_3 |\mathcal{E}_{\mathcal{F}}| + \iota_4 |\mathcal{E}_L|)) \left(\frac{1}{4} + N_{d2} \right) + \frac{\iota_1}{4} \right)^{\frac{1}{2}} \quad (4-44) \end{aligned}$$

uniformly in time for all $i \in \mathcal{V}_{\mathcal{F}}$ and $y(0) \in \mathcal{S}_{\mathfrak{D}}$, since $\|q_i - q_L\| \leq \|Q_{\mathcal{F}} - Q_L\| = \|E\| \leq \|y\|$ for all $i \in \mathcal{V}_{\mathcal{F}}$. Hence, since $y, q_L, \dot{q}_L \in \mathcal{L}_{\infty}$, it is clear that $q_i, \dot{q}_i \in \mathcal{L}_{\infty}$ for all $i \in \mathcal{V}_{\mathcal{F}}$, and each agent's control effort is bounded during the entire state trajectory. \square

Although this convergence analysis only provides sufficient conditions, the restriction in Assumption 4.8 and the UUB nature of the result in Theorem 4.1 correspond with several intuitive notions about communication-delayed networked systems:

1. Communication-delayed systems may not be stable for arbitrarily large gains in proportional and derivative feedback control (as seen in (4–23)).
2. A larger communication delay may reduce the set of stabilizing initial conditions and increase the ultimate upper bound of the norm of the tracking error trajectory (as seen in (4–22) and (4–44)).
3. Quickly varying communication delays may reduce the set of stabilizing initial conditions and increase the ultimate upper bound of the norm of the tracking error trajectory (as seen in the effect of ω on f_1).
4. The effects of volatile dynamics (i.e., larger values for ρ_0, ρ_1, ρ_2 in \mathfrak{D}) and a higher leader trajectory acceleration are exacerbated by the presence of communication delay and may reduce the set of stabilizing initial conditions (as seen in the effect of ρ on (4–22)).
5. The topology of the network may affect the overall leader-tracking performance (as seen in the definition of \underline{k}). The selection of which follower agents are connected

to the leader, the topology of the follower agent network, and the inter-agent edge weights affect $\lambda(L_B)$, for which a larger value facilitates satisfaction of the inequality in (4-23).

Furthermore, as the communication delay and delay estimate tend toward zero (ignoring the singularity of $\bar{\tau} \equiv 0$, which obviates the need for the LK functional-based approach taken in this chapter), the effects of the delay vanish and the convergence analysis resembles that of a high-gain robust control analysis, similar to that in Chapter 2.

4.5 Simulation

Simulation results are provided to demonstrate the capability of the proposed controller in (4-4) to obtain approximate convergence in leader-follower synchronization, despite the effects of uncertain, time-varying, heterogeneous communication delays and uncertain, nonlinear, heterogeneous dynamics affected by uncertain input disturbances. The leader-follower network is modeled with four follower agents, where only one agent interacts with the leader, as depicted in Fig. 4-3. Each follower agent has nonlinear dynamics modeled as

$$u_i = \begin{bmatrix} p_{1,i} + 2p_{3,i}c_{2,i} & p_{2,i} + p_{3,i}c_{2,i} \\ p_{2,i} + p_{3,i}c_{2,i} & p_{2,i} \end{bmatrix} \ddot{q}_i + \begin{bmatrix} -p_{3,i}s_{2,i}\dot{q}_{i,2} & -p_{3,i}s_{2,i}(\dot{q}_{i,1} + \dot{q}_{i,2}) \\ p_{3,i}s_{2,i}\dot{q}_{i,1} & 0 \end{bmatrix} \dot{q}_i + \begin{bmatrix} f_{d1,i} & 0 \\ 0 & f_{d2,i} \end{bmatrix} \dot{q}_i + d_i,$$

where $p_{1,i}, p_{2,i}, p_{3,i}, f_{d1,i}, f_{d2,i} \in \mathbb{R}_{>0}$ are constant parameters described in Table 2-1, $q_i \in \mathbb{R}^2$ describes the generalized position coordinate in radians, $q_{i,1}, q_{i,2}$ respectively denote the first and second entries of the vector q_i , $c_{2,i} \triangleq \cos(q_{i,2})$, $s_{2,i} \triangleq \sin(q_{i,2})$, and the disturbance $d_i \in \mathbb{R}^2$ is modeled as $d_i = \begin{bmatrix} \Delta_{1,i} \sin(\Theta_{1,i}t) \\ \Delta_{2,i} \sin(\Theta_{2,i}t) \end{bmatrix} \text{ N} \cdot \text{m}$, where the constant parameters $\Delta_i, \Theta_i \in \mathbb{R}_{>0}$ are described in Table 4-1. The generalized coordinates

are initialized as $q_1(0) = \begin{bmatrix} -0.5 \\ 5.0 \end{bmatrix}$ rad, $q_2(0) = \begin{bmatrix} 0.0 \\ 1.0 \end{bmatrix}$ rad, $q_3(0) = \begin{bmatrix} 0.5 \\ 0.0 \end{bmatrix}$ rad, $q_4(0) = \begin{bmatrix} -1.0 \\ 0.75 \end{bmatrix}$ rad, and $\dot{q}_i(0) = \begin{bmatrix} 0.0 \\ 0.0 \end{bmatrix}$ rad/s for $i = 1, \dots, 4$. The nonzero adjacency gains are selected as $a_{ij} = 1 \forall (j, i) \in \mathcal{E}_{\mathcal{F}}$ and the nonzero pinning gains are selected as $b_i = 1 \forall i : (L, i) \in \mathcal{E}_L$. The leader state is assigned the trajectory $q_L = \begin{bmatrix} \sin(t) \\ 0.5 \cos(t) \end{bmatrix}$ rad. The uncertain communication delay for each inter-agent interaction lies between 5 and 50 milliseconds and is modeled as $\tau_{ji} = \alpha_{ji} + \beta_{ji} \text{rand}(-1, 1)$, where the constant parameters $\alpha_{ji}, \beta_{ji} \in \mathbb{R}_{>0}$ are given in Table 4-2 and $\text{rand}(-1, 1)$ samples randomly in $(-1, 1)$ with a uniform distribution. To maintain consistency between simulation trials, the random number generator is started with the same seed for each simulation.

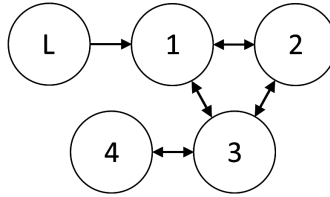


Figure 4-3. Network communication topology.

Table 4-1. Disturbance parameters.

	Robot 1	Robot 2	Robot 3	Robot 4
$\Lambda_{1,i}$ (N · m)	1.0	2.0	1.5	0.5
$\Theta_{1,i}$ (rad/s)	1.0	2.0	3.0	5.0
$\Lambda_{2,i}$ (N · m)	0.5	0.2	0.7	0.9
$\Theta_{2,i}$ (rad/s)	4.0	3.0	1.0	2.0

Table 4-2. Communication delay and delay estimate parameters for each communication link.

Channel	α_{ji} (s)	β_{ji} (s)	$\hat{\tau}_{ji}$ (s)
(L, 1)	0.01	0.002	0.011
(1, 2)	0.04	0.01	0.041
(1, 3)	0.025	0.009	0.028
(2, 1)	0.02	0.005	0.018
(2, 3)	0.035	0.006	0.032
(3, 1)	0.03	0.002	0.032
(3, 2)	0.01	0.005	0.012
(3, 4)	0.045	0.003	0.048
(4, 3)	0.03	0.008	0.034

The contributions of self-delayed feedback and feedback without self-delay, both alone and mixed, are compared by simulating the closed-loop system with various values for κ_1 and κ_2 . Specifically, gain tuning was performed for three different implementations of the control policy in (4-4): (a) feedback without self-delay ($\kappa_1 = 1, \kappa_2 = 0$), (b) only feedback with self-delay ($\kappa_1 = 0, \kappa_2 = 1$), and (c) a mixture of feedback with self-delay and without self-delay ($\kappa_1 > 0, \kappa_2 > 0, \kappa_1 + \kappa_2 = 1$). The gains k and λ were tuned by selecting values such that every combination of $k \in \{0.1, 0.2, \dots, 30\}$ and $\lambda \in \{0.1, 0.2, \dots, 15\}$ is used in simulation. For implementation (c), every combination of the aforementioned values for k and λ was used in conjunction with each value of κ_1 and κ_2 such that $\kappa_1 \in \{0.01, 0.02, \dots, 0.99\}, \kappa_2 = 1 - \kappa_1$. To better simulate a real-world scenario, inexact estimates for the communication delays are used for feedback with self-delay. The estimates of the communication delays are constant and are shown in Table 4-2. The simulation results using these different gain combinations were vetted

using the leader tracking-based cost function

$$J \triangleq \sum_{i=1}^4 \sum_{j=1}^2 \text{rms}(q_{L,j} - q_{i,j}),$$

where $\text{rms}(\cdot)$ denotes the RMS of the argument's sampled trajectory between 0 and 20 seconds, $q_{L,j}$ denotes the j^{th} entry of the vector q_L , and $q_{i,j}$ denotes the j^{th} entry of the vector q_i . The gain combinations which produced the lowest cost for the three different control implementations and the associated costs are shown in Table 4-3, and the according simulation results are shown in Fig. 4-4 - 4-6.

As seen in Table 4-3, for the given simulation setting, control implementation (c) (mixture of feedback without self-delay and feedback with self-delay) gives a 12.5% performance increase over implementation (a) (no self-delayed feedback) and a 58.8% performance increase over implementation (b) (only self-delayed feedback). Whereas implementation (a) remains stable for a selection of the gain k up to 30, implementation (b) produces an unstable closed-loop system if $k \geq 3.6$ and $\lambda = 15$, which demonstrates the sensitivity of only using feedback with self-delay. Implementation (c) produces the best leader-tracking performance by combining feedback without self-delay, which is helpful in stabilization, and feedback with self-delay, which can provide better tracking performance by comparing signals closer in time.

Table 4-3. Tuned gains and associated costs for (a) feedback without self-delay, (b) only feedback with self-delay, and (c) a mixture of feedback with self-delay and without self-delay.

	k	λ	κ_1	κ_2	J
(a)	30	15	1	0	52.2
(b)	3.5	15	0	1	111
(c)	30	15	0.71	0.29	45.7

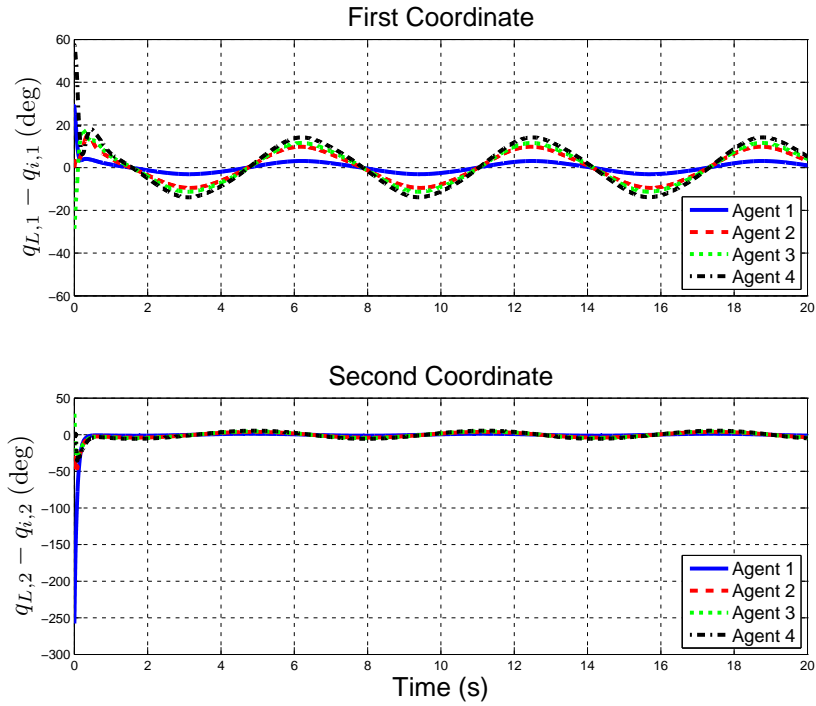


Figure 4-4. Leader-tracking error under communication-delayed closed-loop control using only feedback without self-delay ($\kappa_1 = 1, \kappa_2 = 0$).

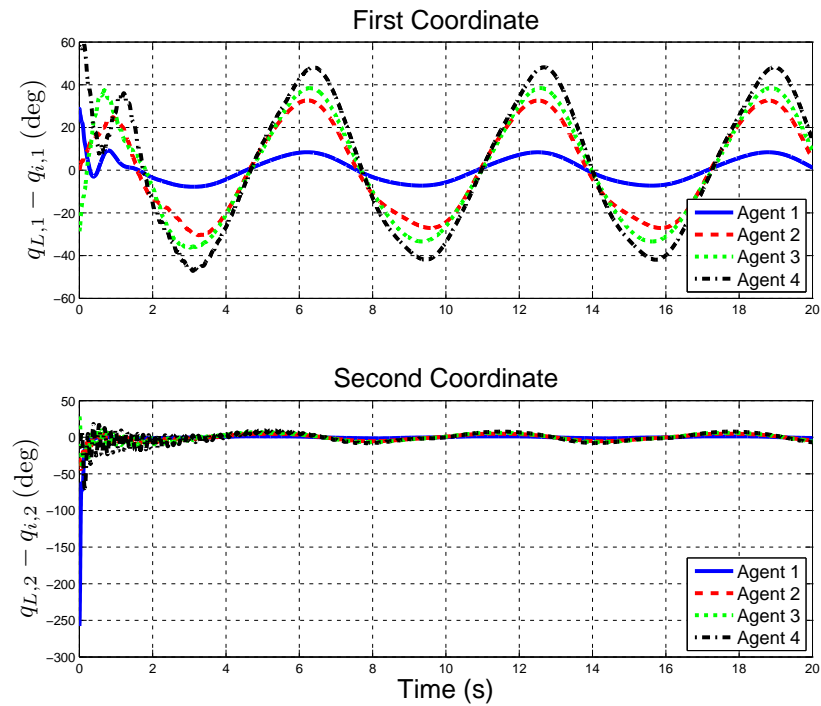


Figure 4-5. Leader-tracking error under communication-delayed closed-loop control using only feedback with self-delay ($\kappa_1 = 0, \kappa_2 = 1$).

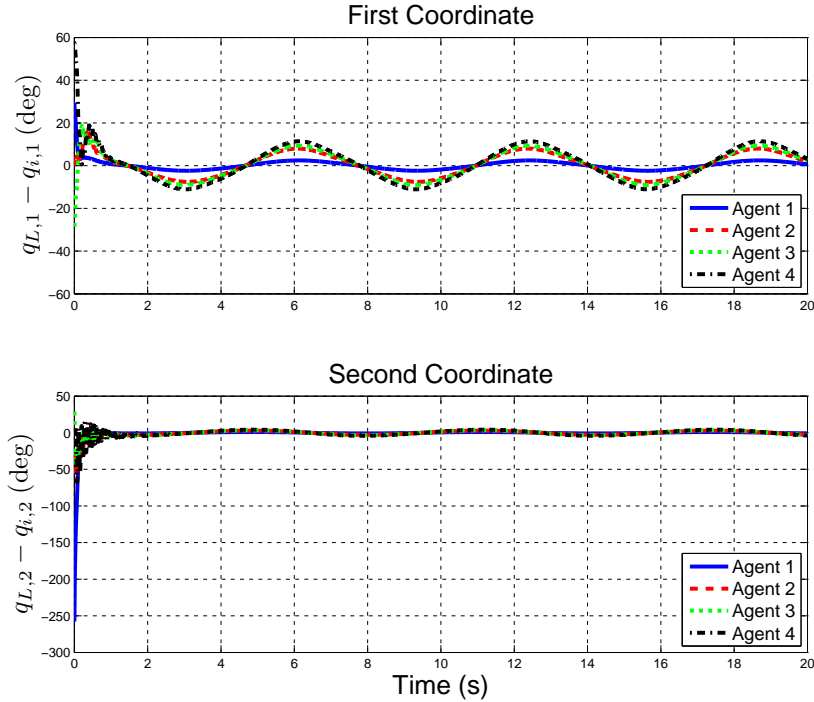


Figure 4-6. Leader-tracking error under communication-delayed closed-loop control using a mixture of feedback without self-delay and feedback with inexact self-delay ($\kappa_1 = 0.69$, $\kappa_2 = 0.31$).

4.6 Concluding Remarks

A convergence analysis is presented which provides sufficient conditions for UUB leader-synchronization of a network of communication-delayed agents using a novel, decentralized, neighborhood-based PD controller. The agents are modeled with dynamics described by heterogeneous, uncertain Euler-Lagrange equations of motion affected by time-varying, unknown exogenous disturbances. The communication delay is considered to be heterogeneous, time-varying, and uncertain. An estimate of the communication delay is used in the controller to estimate recent tracking errors. The benefit of using a mixture of feedback without self-delay and feedback with inexact self-delay is demonstrated in simulation. Salient dependencies for the sufficient conditions for approximate convergence in synchronization are the upper bounds of the heterogeneous communication delays and delay estimate errors, feedback gains, and network

connectivity. Some prominent assumptions are that the follower communication network is undirected and at least one follower agent receives information from the leader.

The approach in this chapter provides a framework for exploring other methods to improve the performance of decentralized control in networks affected by communication delay. For example, the controller in (4-4) may be improved by the development of a decentralized algorithm which changes edge weights or the neighbor set based on local network structure and estimates of neighbors' communication delays; customization of κ_1 and κ_2 for each neighbor based on the delay estimates; and decentralized communication-based algorithms which allow each agent to predict the leader trajectory, similar to that in [43], thereby reducing the impact of the propagation of communication delays through agents' dynamics.

CHAPTER 5 DECENTRALIZED SYNCHRONIZATION OF UNCERTAIN NONLINEAR SYSTEMS WITH A REPUTATION ALGORITHM

This chapter considers a decentralized network control scenario in which agents use both communication and sensing to interact. The communication is assumed to be continuously available, but have possible inaccuracies due to poor self localization. The neighbor sensor measurements are assumed to provide accurate relative position information, but only occur intermittently. Because the sensor measurements are modeled as intermittent, and therefore may not be frequent enough to be implemented in closed-loop control, they are used to vet communicated information so that an agent can rely more on information from more reliable neighbors. A reputation algorithm is developed in which each agent quantitatively evaluates the trust of each neighbor based on the discrepancy between communicated and sensed information. The trust values are then used in the reputation algorithm so that agents communicate about a mutually shared neighbor to collaboratively obtain a reputation. Each agent's contribution to the reputation algorithm is weighted by that neighbor's own reputation. The result of the reputation algorithm is used to update consensus weights which affect the relative weighting in the decentralized control policy's use of a neighbor's communicated information compared to other neighbors', if an agent has multiple neighbors. However, the consensus weight updates alter the feedback structure of and introduce discontinuities into the network-wide closed-loop system. Concepts from switching theory and the sensitivity of the solution to the Lyapunov Equation are used to address the effects of asymmetric consensus weight updates and develop a dwell-time that must elapse between successive updates in the network.

5.1 Problem Formulation

5.1.1 Network Properties

Similar to the previous chapters, the follower graph is modeled such that the network topology is static, i.e., $\mathcal{V}_{\mathcal{F}}$ and $\mathcal{E}_{\mathcal{F}}$ do not vary in time. However, dissimilar

to the previous chapters, the edge weights are modeled as time-varying such that $a_{ij} : \mathbb{R} \rightarrow \mathbb{R}_{>0}$ if $(j, i) \in \mathcal{E}_{\mathcal{F}}$ and $a_{ij} = 0$ otherwise for every follower-to-follower edge $(j, i) \in \mathcal{E}_{\mathcal{F}}$. Furthermore, this chapter considers the more general directed graph to describe the network topology, i.e., interaction links may not necessarily be bidirectional. The following assumption specifies the class of networks considered in the following analysis, where the term “strongly-connected” indicates that there exists a sequence of directed edges between any two nodes.

Assumption 5.1. The graph $\mathcal{G}_{\mathcal{F}}$ is strongly-connected and at least one agent is connected to the leader.

5.1.2 Dynamic Models and Properties

Let the dynamics of each follower agent $i \in \mathcal{V}_{\mathcal{F}}$ be modeled with uncertain second-order nonlinear dynamics as

$$\ddot{x}_i = f_i(x_i, \dot{x}_i) + u_i, \quad (5-1)$$

where $x_i \in \mathbb{R}^m$ is the state, $f_i : \mathbb{R}^m \times \mathbb{R}^m \rightarrow \mathbb{R}^m$ denotes the uncertain nonlinear drift dynamics, and $u_i \in \mathbb{R}^m$ is the control input to be designed. The time-varying trajectory of the leader state is denoted by $x_L : \mathbb{R} \rightarrow \mathbb{R}^m$, which is known by at least one of the follower agents. The following assumptions concerning the follower agents’ dynamics and the leader trajectory are made to simplify the analysis.

Assumption 5.2. The drift dynamics, f_i , are first-order differentiable, i.e., the first-order derivative exists and is bounded if $x_i, \dot{x}_i, \ddot{x}_i$ are bounded, for every follower agent $i \in \mathcal{V}_{\mathcal{F}}$.

Assumption 5.3. The leader state trajectory is sufficiently smooth such that $x_L, \dot{x}_L, \ddot{x}_L$ are bounded.

Note that the dynamics in (5-1) can be represented in Euler-Lagrange form if the inertia matrix is known and used in the controller. The inertia matrix is omitted from the dynamics to simplify the subsequent analysis.

5.1.3 Neighbor Communication and Sensing

Neighboring follower agents use both communication and sensing to interact with each other. Communication of continuous estimates of the state information (x_j, \dot{x}_j) of agent $j \in \mathcal{V}_{\mathcal{F}}$ is available to its neighbor $i \in \mathcal{N}_{\mathcal{F}j}$ at all times; however, the communicated information may be inaccurate due to imperfect knowledge of the agent's own state in the global coordinate system. For example, a UAV in a network may transmit an inaccurate estimate of its own position. However, intermittent neighbor sensing of an agent $j \in \mathcal{V}_{\mathcal{F}}$ by a neighbor $i \in \mathcal{N}_{\mathcal{F}j}$ provides accurate relative position information $(x_j - x_i)$ at isolated points in time. For example, an agent may be able to observe neighbors using a camera, but may only determine the relative position intermittently due to occlusions, low hardware refresh rates, etc. As a consequence, neighbor sensing may not be frequent enough for stability in a control algorithm which uses neighbor sensing alone. Thus, each agent must use both continuous, possibly inaccurate neighbor communication and accurate, intermittent neighbor sensing to accomplish a control objective. Because the intermittent neighbor sensing is accurate, it may be used to vet and intelligently use the communicated state information. Let $\hat{x}_i, \dot{\hat{x}}_i$ denote the estimates of x_i, \dot{x}_i computed by agent $i \in \mathcal{V}_{\mathcal{F}}$. The following assumptions concerning the communicated state information are made to facilitate the following analysis.

Assumption 5.4. The difference between the estimated state information $\hat{x}_i, \dot{\hat{x}}_i$ and the actual state information x_i, \dot{x}_i is bounded for each follower agent $i \in \mathcal{V}_{\mathcal{F}}$, i.e., there exist known positive constants $\bar{x}, \bar{\dot{x}} \in \mathbb{R}$ such that $\|\hat{x}_i - x_i\| \leq \bar{x}$ and $\|\dot{\hat{x}}_i - \dot{x}_i\| \leq \bar{\dot{x}}$ for each $i \in \mathcal{V}_{\mathcal{F}}$ and all time.

Assumption 5.5. Information communicated from the leader agent is accurate.

As seen in the following section, Assumption 5.5 is critical to achieving close synchronization with the leader. Whereas it may be difficult to guarantee perfect state communication for each agent, it is plausible to guarantee Assumption 5.5 by

outfitting only the leader agent with more robust localization equipment or monitoring by personnel.

5.1.4 Control Objective

Similar to traditional synchronization approaches (cf. [3, 7, 8, 77]), the objective is to drive the states of the networked agents towards the state of the network leader such that $\limsup_{t \rightarrow \infty} \|x_i(t) - x_L(t)\| \leq \varepsilon$ with a small ε through advantageous use of the communicated and sensed information.

5.2 Controller Development

5.2.1 Error System

The error signal in decentralized control traditionally has the form $\sum_{j \in \mathcal{N}_{\mathcal{F}i}} a_{ij} (x_j - x_i) + b_i (x_L - x_i)$. However, since accurate state information is not always available to each agent, a decentralized neighbor-based error signal is developed based on communicated information as

$$\hat{e}_i \triangleq \sum_{j \in \mathcal{N}_{\mathcal{F}i}} a_{ij} (\hat{x}_j - \hat{x}_i) + b_i (x_L - \hat{x}_i). \quad (5-2)$$

In (5-2), the first term provides communication-based feedback for comparison to neighboring follower agents and the second term provides communication-based feedback for comparison to the leader agent, if that connection exists. Hence, instead of imposing discontinuities on the error signal by using the accurate sensed relative state whenever a sensor measurement is available, the strategy is to use the communicated information for feedback and update the edge weights a_{ij} based on the discrepancy between the communicated and sensed information, as demonstrated in Section 5.2.3. These edge weights will be updated so that neighbors which seem to provide more accurate information have a greater impact on the synchronization performance.

An auxiliary error signal is analogously defined as

$$\hat{r}_i \triangleq \sum_{j \in \mathcal{N}_{\mathcal{F}i}} a_{ij} (\dot{\hat{x}}_j - \dot{\hat{x}}_i) + b_i (\dot{x}_L - \dot{\hat{x}}_i) + \lambda \hat{e}_i, \quad (5-3)$$

where $\lambda \in \mathbb{R}$ is a positive constant tuning parameter.

5.2.2 Decentralized Controller

The auxiliary error signal in (5–3) is used to design a decentralized controller as

$$u_i = k\hat{r}_i, \quad (5-4)$$

where $k \in \mathbb{R}$ is a constant positive control gain. The following section demonstrates how the discrepancies between communicated and sensed information are advantageously used in the control method in (5–4).

5.2.3 Reputation Algorithm

Each agent $i \in \mathcal{V}_{\mathcal{F}}$ assigns a trust value, $\sigma_{ij} \in [0, 1]$, to each neighbor $j \in \mathcal{N}_{\mathcal{F}i}$, where 0 corresponds to no trust and 1 corresponds to highest trust. The trust value is computed using communicated information \hat{x}_j , internal information \hat{x}_i , and sensed relative position information $x_j - x_i$ from time instances when sensor measurements are available. Let $t_{ij}^1, t_{ij}^2, \dots \in \mathbb{R}$ denote the time instances in which agent i obtains a sensor measurement of $x_j - x_i$, let $\bar{t} \in \mathbb{R}$ denote a positive number, and let $S_{ij}(t) \triangleq \{t_{ij}^l \mid (l \in \mathbb{Z}_{>0}) \wedge (t - \bar{t} \leq t_{ij}^l \leq t)\}$ denote the set of neighbor sensing time instances which have occurred after $t - \bar{t}$ up until the current time.¹ The use of \bar{t} is motivated by expiring relevancy of old neighbor sensing data and mitigation of computation burden in determining a trust value (cf. [78]). There are numerous options in selecting a trust metric (see the survey in [79]), and any trust metric which maps into $(0, 1]$ and has a positive lower bound for a bounded input is appropriate for the analysis developed in this chapter. In this work, a trust metric is designed as

$$\sigma_{ij} \triangleq \begin{cases} 1 & |S_{ij}| = 0 \\ \frac{1}{|S_{ij}|} \sum_{t_{ij}^l \in S_{ij}} e^{-s \|\tilde{x}_{ij}(t_{ij}^l) - \hat{x}_{ij}(t_{ij}^l)\|} & \text{otherwise,} \end{cases} \quad (5-5)$$

¹ Recall that sensor measurements occur at isolated points in time, i.e., $S_{ij}(t)$ is a finite set for all $t \in \mathbb{R}$.

where $s \in \mathbb{R}$ is a positive tuning parameter, $\tilde{x}_{ij} \triangleq x_j - x_i$ is the relative position obtained via neighbor sensing, and $\hat{x}_{ij} \triangleq \hat{x}_j - \hat{x}_i$ is the relative position obtained via communication of the state estimate \hat{x}_j and the internal position estimate \hat{x}_i maintained by agent i .² In (5-5), a trust value of 1 is computed if there are no recent sensor measurements (i.e., $S_{ij}(t)$ is an empty set). If there are recent sensor measurements, the term $e^{-s\|\tilde{x}_{ij}(t_{ij}^l) - \hat{x}_{ij}(t_{ij}^l)\|}$ maps the discrepancy between the estimated relative position and the actual relative position to $(0, 1]$. The result is then averaged with the corresponding values for the other sensor measurements to obtain the overall trust value. Note that \tilde{x}_{ij} and \hat{x}_{ij} may differ due to an inaccurate estimate of \hat{x}_i , i.e., an agent's trust of a neighbor may be affected by an inaccurate estimate of its own state. However, because \hat{x}_i is necessary to provide a continuous comparison to neighbors' states, there is no utility in determining a trust value for an agent's own state. Future work may investigate methods to better estimate an agent's own state based on neighbor feedback.

Each follower agent $i \in \mathcal{V}_{\mathcal{F}}$ maintains a reputation value $\zeta_{ij} : \prod_{l=1}^{2|\mathcal{N}_{\mathcal{F}_i} \cap \mathcal{N}_{\mathcal{F}_j}|+2} \mathbb{R} \rightarrow \mathbb{R}$ for every neighbor $j \in \mathcal{N}_{\mathcal{F}_i}$ based on recommendations from mutual neighbors, where the reputation is updated using trust values as

$$\dot{\zeta}_{ij} = \sum_{n \in \mathcal{N}_{\mathcal{F}_i} \cap \mathcal{N}_{\mathcal{F}_j}} \eta_{\zeta i} \zeta_{in} (\zeta_{nj} - \zeta_{ij}) + \eta_{\sigma i} (\sigma_{ij} - \zeta_{ij}) \quad (5-6)$$

with the initial condition $\zeta_{ij}(0) = 1$, where a higher reputation corresponds to higher reliability and $\eta_{\zeta i}, \eta_{\sigma i} \in \mathbb{R}_{>0}$ are tunable gains that weigh how much recommended information is relied upon compared to directly observed information. Similar to [49], the first term in (5-6) contributes towards the reputation update by agent i of agent j based on the reputation of j held by mutual neighbors $n \in \mathcal{N}_{\mathcal{F}_i} \cap \mathcal{N}_{\mathcal{F}_j}$ via communication.

² Similar to [78], the summation in (5-5) can be weighted by how much time has elapsed since the measurements took place, if relevant for the intended application.

Dissimilar to [49], the contribution of a mutual neighbor to the reputation update is weighted by the reputation of that agent, as seen in the multiplication by ζ_{in} . Thus, an agent which has a low reputation has less significant impact in recommendation of a reputation value. The second term in (5–6) directly uses the observation-based trust value to update reputation. As shown in Appendix D, for each connection $(j, i) \in \mathcal{E}_{\mathcal{F}}$, the reputation value ζ_{ij} is bounded such that $\zeta_{ij} \in [\underline{\sigma}^*, 1]$ for all $t \in \mathbb{R}$, where $\underline{\sigma}^* \in \mathbb{R}$ is a bounding constant such that $\sigma_{ij} \geq \underline{\sigma}^*$ for all $t \in \mathbb{R}$, and $\underline{\sigma}^* > 0$ by Assumption 5.4.

5.2.4 Edge Weight Updates

The reputation values, ζ_{ij} , are used to update the edge weight values, a_{ij} , which quantify how much influence a neighbor has in the decentralized control policy in (5–4). However, changes to the edge weight values affect the feedback in (5–4), which affects the response of the closed-loop system. To control the effects of the edge weight updates on the systems' feedback structure, and based on the subsequent convergence analysis, the edge weights are updated at discrete times in predefined time intervals. Thus, the adjacency matrix A and the Laplacian matrix $\mathcal{L}_{\mathcal{F}}$ are functions of time, i.e., $A : \mathbb{R} \rightarrow \mathbb{R}^{\mathcal{F} \times \mathcal{F}}$ and $\mathcal{L}_{\mathcal{F}} : \mathbb{R} \rightarrow \mathbb{R}^{\mathcal{F} \times \mathcal{F}}$, where the adjacency matrix is initialized such that $a_{ij}(0) = \frac{1}{|\mathcal{N}_{\mathcal{F}i}|}$ if $(j, i) \in \mathcal{E}_{\mathcal{F}}$, i.e., all follower-to-follower connections are equally weighted at $t = 0$. However, if the edge weights are updated too rapidly, then the resulting frequent discontinuities in the switched closed-loop system may cause instability (cf. [80, Chapter 2]). Thus, a dwell-time (cf. [80, Chapter 3]), $\tau_d \in \mathbb{R}_{>0}$, is developed to describe the minimum amount of time that must elapse before an agent $i \in \mathcal{V}_{\mathcal{F}}$ can update its edge weight values, $\{a_{ij} \mid j \in \mathcal{N}_{\mathcal{F}i}\}$, since its last update (or the initial time), and is computed before the control implementation. Implementation of the dwell-time is decentralized in the sense that an agent may update its edge weights at different times from other neighbors as long as the elapsed time between successive updates is not shorter than the dwell-time. The network topology-dependent minimum dwell-time is given in Section 5.5 and is based on the subsequent convergence analysis.

Let $t_{di}^1, t_{di}^2, \dots \in \mathbb{R}$ denote the times at which agent $i \in \mathcal{V}_{\mathcal{F}}$ updates its edge weight values $\{a_{ij} \mid j \in \mathcal{N}_{\mathcal{F}i}\}$, where $t_{di}^{l+1} - t_{di}^l \geq \tau_d$ for all $l \in \mathbb{Z}_{>0}$. The edge weights stay constant between updates and the reputation values are mapped to the edge weight values at each update time as

$$a_{ij}(t_{di}^l) = \frac{\zeta_{ij}(t_{di}^l)}{\sum_{n \in \mathcal{N}_{\mathcal{F}i}} \zeta_{in}(t_{di}^l)}, \quad l \in \mathbb{Z}_{>0}, \quad (5-7)$$

which results in a piecewise continuous control policy in (5-4), where the reputation values are normalized in (5-7) so that $\sum_{j \in \mathcal{N}_{\mathcal{F}i}} a_{ij} = 1$. Note that since $\zeta_{ij} \geq \underline{\sigma}^*$ for all $(j, i) \in \mathcal{E}_{\mathcal{F}}$ and $t \in \mathbb{R}$, there exists a constant $\underline{a}^* \in \mathbb{R}$ such that $0 < \underline{a}^* < 1$ and $a_{ij} \in [\underline{a}^*, 1]$ for all $(j, i) \in \mathcal{E}_{\mathcal{F}}$ and $t \in \mathbb{R}$.

5.3 Closed-loop Error System

To facilitate analysis of the closed-loop system, the operator $\mathcal{P} : \mathbb{R}^{\mathcal{F} \times \mathcal{F}} \rightarrow \mathbb{R}^{\mathcal{F} \times \mathcal{F}}$ is defined as the (positive definite and symmetric) solution to the continuous algebraic Lyapunov Equation (CALE) such that $M^T \mathcal{P}(M) + \mathcal{P}(M)M = -I_{\mathcal{F}}$ for a Hurwitz matrix $M \in \mathbb{R}^{\mathcal{F} \times \mathcal{F}}$.

Lemma 5.1. *If Assumption 5.1 is satisfied, then the matrix $-\mathcal{L}_{\mathcal{F}} - B$ is Hurwitz.*

Proof. See Appendix E. □

For convenience, the vectors x_i , \hat{x}_i , and x_L are stacked such that $X \triangleq [x_1^T, \dots, x_{\mathcal{F}}^T]^T \in \mathbb{R}^{\mathcal{F}m}$, $\hat{X} \triangleq [\hat{x}_1^T, \dots, \hat{x}_{\mathcal{F}}^T]^T \in \mathbb{R}^{\mathcal{F}m}$, $X_L \triangleq [x_L^T, \dots, x_L^T]^T \in \mathbb{R}^{\mathcal{F}m}$. To facilitate the description of the agents' progress towards synchronization, the error signals $E \triangleq X_L - X \in \mathbb{R}^{\mathcal{F}m}$ and $R \triangleq \dot{E} + \lambda E \in \mathbb{R}^{\mathcal{F}m}$ are introduced. Using the dynamics in (5-1), the controller in (5-4), and the definitions of E and R , the closed-loop dynamics can be represented as

$$\begin{aligned} \dot{R} = & \ddot{X}_L - F(X, \dot{X}) + \lambda \dot{E} - k((\mathcal{L}_{\mathcal{F}} + B) \otimes I_m) R \\ & + k((\mathcal{L}_{\mathcal{F}} + B) \otimes I_m) \left(\dot{\hat{X}} - \dot{X} + \lambda (\hat{X} - X) \right), \end{aligned} \quad (5-8)$$

where $F \triangleq [f_1^T, \dots, f_{\mathcal{F}}^T]^T \in \mathbb{R}^{\mathcal{F}m}$ and the second line in (5–8) isolates the effects of inaccurate state estimation on the closed-loop system. After some algebraic manipulation, (5–8) can be expressed as

$$\begin{aligned} \dot{R} = & N_d + \tilde{N} - k((\mathcal{L}_{\mathcal{F}} + B) \otimes I_m) R - (\mathcal{P}(-\mathcal{L}_{\mathcal{F}} - B) \otimes I_m)^{-1} E \\ & + k((\mathcal{L}_{\mathcal{F}} + B) \otimes I_m) \left(\dot{X} - \dot{X} + \lambda (\hat{X} - X) \right), \end{aligned} \quad (5-9)$$

where the functions $N_d : \Pi_{l=1}^3 \mathbb{R}^{\mathcal{F}m} \rightarrow \mathbb{R}^{\mathcal{F}m}$ and $\tilde{N} : \Pi_{l=1}^6 \mathbb{R}^{\mathcal{F}m} \rightarrow \mathbb{R}^{\mathcal{F}m}$ are defined as

$$\begin{aligned} N_d & \triangleq \ddot{X}_L - F(X_L, \dot{X}_L), \\ \tilde{N} & \triangleq F(X_L, \dot{X}_L) - F(X, \dot{X}) + \lambda \dot{E} + (\mathcal{P}(-\mathcal{L}_{\mathcal{F}} - B) \otimes I_m)^{-1} E. \end{aligned}$$

Terms are segregated into N_d and \tilde{N} such that $\|N_d\|$ can be upper-bounded through Assumption 5.3 by a constant and $\|\tilde{N}\|$ can be upper-bounded by a function of the error signals E and R through a Mean Value Theorem-based approach, where the matrix $(\mathcal{P}(-\mathcal{L}_{\mathcal{F}} - B))^{-1}$ is upper bounded by a constant, as shown in the following section. Accordingly, let the known constant $\bar{N}_d \in \mathbb{R}$ be defined such that

$$\sup_{t \in \mathbb{R}} \|N_d\| \leq \bar{N}_d. \quad (5-10)$$

Additionally, by Assumption 5.2 and [58, Lemma 5], there exists a strictly increasing, radially unbounded function $\rho : \mathbb{R} \rightarrow \mathbb{R}$ which facilitates an upper-bound for $\|\tilde{N}\|$ as

$$\|\tilde{N}\| \leq \rho(\|Z\|) \|Z\|, \quad (5-11)$$

where the composite vector $Z \in \mathbb{R}^{2\mathcal{F}m}$ is defined as $Z \triangleq [E^T, R^T]^T$.

5.4 Convergence Analysis

Some additional expressions are introduced to facilitate the convergence analysis.

Let the set \mathcal{P} be defined as

$$\mathcal{P} \triangleq \left\{ \mathcal{P}(-\mathcal{L}_{\mathcal{F}} - B) \mid a_{ij} \in [a^*, 1], \sum_{j \in \mathcal{N}_{\mathcal{F}i}} a_{ij} = 1, \forall (j, i) \in \mathcal{E}_{\mathcal{F}} \right\},$$

which is the set of solutions for the CALE for every possible value of the matrix $-\mathcal{L}_{\mathcal{F}} - B$ under the edge weight update law in (5–7). Because \mathcal{P} is a bounded set, there exist positive constants $\underline{p}^*, \bar{p}^* \in \mathbb{R}$ defined as $\underline{p}^* \triangleq \inf_{P \in \mathcal{P}} \lambda(P)$ and $\bar{p}^* \triangleq \sup_{P \in \mathcal{P}} \bar{\lambda}(P)$. These constants are used to define a minimum sufficient dwell-time, $\tau_d^* \in \mathbb{R}$, which is designed for use in the convergence theorem as

$$\tau_d^* \triangleq \frac{\ln(\mu^*)}{\frac{\psi}{\max\{\bar{p}^*, 1\}} - \beta^*},$$

where the positive constants $\psi, \mu^* \in \mathbb{R}$ are defined as $\psi \triangleq \frac{1}{2} \min\{\lambda, \frac{k}{4}\}$ and $\mu^* \triangleq \frac{\max\{\bar{p}^*, 1\}}{\min\{\underline{p}^*, 1\}}$, and $\beta^* \in \mathbb{R}$ is a selectable positive constant which satisfies $0 < \beta^* < \frac{\psi}{\max\{\bar{p}^*, 1\}}$. As shown in the following convergence analysis, there is a trade-off in the selection of β^* between convergence rate and how rapidly the agents may update their edge weights.

To further facilitate the subsequent analysis, let the open and connected set \mathcal{D} be defined as

$$\mathcal{D} \triangleq \{Z \in \mathbb{R}^{2\mathcal{F}m} \mid \|Z\| < \chi^*\},$$

where $\chi^* \triangleq \inf\left(\rho^{-1}\left(\left[\frac{1}{\bar{p}^*} \sqrt{\frac{k\psi}{3}}, \infty\right)\right)\right) \in \mathbb{R}$ and the inverse image $\rho^{-1}(\Theta) \subset \mathbb{R}$ for a set $\Theta \subset \mathbb{R}$ is defined as $\rho^{-1}(\Theta) \triangleq \{\xi \in \mathbb{R} \mid \rho(\xi) \in \Theta\}$. The set of stabilizing initial conditions is a subset of \mathcal{D} and is defined as

$$\mathcal{S} \triangleq \left\{ Z \in \mathbb{R}^{2\mathcal{F}m} \mid \|Z\| < \frac{\chi^*}{\mu^*} \right\}. \quad (5-12)$$

Finally, the constant parameter $\bar{\mathcal{L}}_B \in \mathbb{R}$ is defined as $\bar{\mathcal{L}}_B \triangleq \sqrt{|\mathcal{E}_{\mathcal{F}}| + \mathcal{F} + \sum_{i \in \mathcal{V}_{\mathcal{F}}} b_i^2}$, which upper-bounds $\sup_{t \in \mathbb{R}} \|\mathcal{L}_{\mathcal{F}}(t) + B\|$ since $\|\mathcal{L}_{\mathcal{F}}(t) + B\| \leq \|\mathcal{L}_{\mathcal{F}}(t) + B\|_F \leq \bar{\mathcal{L}}_B$ for all $t \in \mathbb{R}$ by the triangle inequality and the fact that $0 < a_{ij} \leq 1$, $a_{ii} = 0$ for all $i, j \in \mathcal{V}_{\mathcal{F}}$.

The following theorem describes sufficient conditions for the approximate convergence of the follower agents' states towards the leader's state under the decentralized control policy in (5-4).

Theorem 5.1. *The decentralized controller in (5-4) along with the edge weight update policy in (5-7) provide UUB leader synchronization for a network of agents with nonlinear dynamics described in (5-1) and neighbor communication and sensing feedback described in Section 5.1.3 in the sense that $\limsup_{t \rightarrow \infty} \|x_i(t) - x_L(t)\| \leq \varepsilon$ for some $\varepsilon \in \mathbb{R}_{>0}$ and every follower agent $i \in \mathcal{V}_{\mathcal{F}}$ for all initial conditions $Z(0) \in \mathcal{S}$, provided that Assumptions 5.1-5.5 are satisfied, the dwell-time τ_d satisfies $\tau_d \geq \tau_d^*$, and the state estimate errors are sufficiently small such that there exists a selection for the gain k which satisfies the inequality*

$$\frac{3(\bar{p}^* \bar{N}_d)^2}{k} + 3k(\bar{p}^* \mathcal{F} \bar{\mathcal{L}}_B(\bar{x} + \lambda \bar{x}))^2 < \frac{\psi \chi^*}{\mu^* \max\{\bar{p}^*, 1\}}. \quad (5-13)$$

Remark 5.1. The inequality in (5-13) can be satisfied for sufficiently small estimate error upper bounds \bar{x}, \bar{x} ; however, as intuition would indicate, stability is not guaranteed for arbitrarily large estimate error upper bounds. Future research may overcome this restriction by developing an algorithm which severs neighbor connections if the apparent error in the communicated state estimates exceeds a threshold, i.e., $a_{ij} \neq 0$ if and only if $(j, i) \in \mathcal{E}_{\mathcal{F}}$ and $\sigma_{ij} > \sigma_T$, where $\sigma_T \in (0, 1)$ is a threshold parameter.

Proof. Let the set $\{t_d^0, t_d^1, \dots\}$ be defined as the union of the switching instances by each agent, including the initial time, such that $t_d^{l+1} > t_d^l$ for all $l \in \mathbb{Z}_{\geq 0}$. Additionally, let the mapping $\Lambda : [0, \infty) \rightarrow \mathbb{Z}_{\geq 0}$ be defined such that $\Lambda(t)$ is the number of switches that have occurred until time t , i.e., $\Lambda(t) \triangleq \arg \min_{l \in \mathbb{Z}_{\geq 0}} \{t - t_d^l \mid t - t_d^l \geq 0\}$. A candidate multiple

Lyapunov function, $V_L : \mathcal{D} \times \mathbb{R} \rightarrow \mathbb{R}$, is defined as

$$V_L(Z, t) \triangleq W_{\Lambda(t)}(Z),$$

where the function $W_l : \mathcal{D} \rightarrow \mathbb{R}$ belongs to a family of Lyapunov-like functions $\{W_l \mid l \in \mathbb{Z}_{\geq 0}\}$ defined as

$$W_l(Z) \triangleq \frac{1}{2}E^T E + \frac{1}{2}R^T (\mathcal{P}(-\mathcal{L}_{\mathcal{F}}(t_d^l) - B) \otimes I_m) R,$$

which satisfies the inequalities

$$\frac{1}{2} \min\{\underline{p}^*, 1\} \|Z\|^2 \leq W_l(Z) \leq \frac{1}{2} \max\{\bar{p}^*, 1\} \|Z\|^2 \quad (5-14)$$

for all $Z \in \mathbb{R}^{2\mathcal{F}m}$ and $l \in \mathbb{Z}_{\geq 0}$. Using the closed-loop error system in (5-9), the derivative of V_L can be expressed as

$$\begin{aligned} \dot{V}_L = & E^T (R - \lambda E) + R^T \left(\mathcal{P} \left(-\mathcal{L}_{\mathcal{F}} \left(t_d^{\Lambda(t)} \right) - B \right) \otimes I_m \right) \\ & \cdot \left(N_d + \tilde{N} - \left(\mathcal{P} \left(-\mathcal{L}_{\mathcal{F}} \left(t_d^{\Lambda(t)} \right) - B \right) \otimes I_m \right)^{-1} E + k \left(\left(-\mathcal{L}_{\mathcal{F}} \left(t_d^{\Lambda(t)} \right) - B \right) \otimes I_m \right) R \right. \\ & \left. + k \left(\left(\mathcal{L}_{\mathcal{F}} \left(t_d^{\Lambda(t)} \right) + B \right) \otimes I_m \right) \left(\dot{\hat{X}} - \dot{X} + \lambda (\hat{X} - X) \right) \right) \end{aligned}$$

for all $t \in [t_d^l, t_d^{l+1})$. After using the definitions of \underline{p}^* , \bar{p}^* , and $\bar{\mathcal{L}}_B$, the relation

$$\begin{aligned} kR^T \left(\left(\mathcal{P} \left(-\mathcal{L}_{\mathcal{F}} - B \right) \left(-\mathcal{L}_{\mathcal{F}} - B \right) \right) \otimes I_m \right) R = & \frac{k}{2} R^T \left[\left(\mathcal{P} \left(-\mathcal{L}_{\mathcal{F}} - B \right) \left(-\mathcal{L}_{\mathcal{F}} - B \right) \right) \otimes I_m \right. \\ & \left. + \left(\left(-\mathcal{L}_{\mathcal{F}} - B \right)^T \mathcal{P} \left(-\mathcal{L}_{\mathcal{F}} - B \right) \right) \otimes I_m \right] R = -\frac{k}{2} \|R\|^2, \end{aligned}$$

the bounding expressions in (5-10) and (5-11), and canceling terms, \dot{V}_L can be upper-bounded as

$$\begin{aligned} \dot{V}_L \leq & -\lambda \|E\|^2 - \frac{k}{2} \|R\|^2 + \bar{p}^* \bar{N}_d \|R\| + \bar{p}^* \rho(\|Z\|) \|Z\| \|R\| \\ & + k \bar{p}^* \bar{\mathcal{L}}_B \left\| \dot{\hat{X}} - \dot{X} + \lambda (\hat{X} - X) \right\| \|R\| \end{aligned}$$

for all $t \in [t_d^l, t_d^{l+1})$. After some algebraic manipulation, \dot{V}_L can be upper-bounded as

$$\begin{aligned} \dot{V}_L \leq & -\lambda \|E\|^2 - \frac{k}{4} \|R\|^2 + \frac{3(\bar{p}^* \bar{N}_d)^2}{k} + \frac{3(\bar{p}^* \rho(\|Z\|) \|Z\|)^2}{k} \\ & + 3k \left(\bar{p}^* \bar{\mathcal{L}}_B \left\| \dot{\hat{X}} - \dot{X} + \lambda (\hat{X} - X) \right\| \right)^2 \end{aligned}$$

for all $t \in [t_d^l, t_d^{l+1})$. By using the definition of the auxiliary constant ψ , Assumption 5.4, and the triangle inequality, \dot{V}_L is then upper-bounded as

$$\dot{V}_L \leq -\psi \|Z\|^2 - \left(\psi - \frac{3(\bar{p}^* \rho(\|Z\|))^2}{k} \right) \|Z\|^2 + \varepsilon_1$$

for all $t \in [t_d^l, t_d^{l+1})$, where the constant $\varepsilon_1 \in \mathbb{R}$ is defined as $\varepsilon_1 \triangleq \frac{3(\bar{p}^* \bar{N}_d)^2}{k} + 3k (\bar{p}^* \bar{\mathcal{L}}_B (\bar{x} + \lambda \bar{x}))^2$. Provided the initial condition satisfies $Z(0) \in \mathcal{S}$, then

$$\dot{V}_L \leq -\psi \|Z\|^2 + \varepsilon_1$$

for all $t \in [t_d^l, t_d^{l+1})$. By using the right-side inequality in (5-14), the upper bound of \dot{V}_L can be expressed as

$$\begin{aligned} \dot{V}_L & \leq -\frac{\psi}{\max\{\bar{p}^*, 1\}} V_L - \left(\frac{\psi}{\max\{\bar{p}^*, 1\}} V_L - \varepsilon_1 \right) \\ & \leq -\frac{\psi}{\max\{\bar{p}^*, 1\}} V_L \quad \forall V_L \geq \frac{\max\{\bar{p}^*, 1\}}{\psi} \varepsilon_1 \end{aligned} \quad (5-15)$$

for all $t \in [t_d^l, t_d^{l+1})$. Using the comparison lemma (cf. [76, Lemma 3.4]) with the inequality in (5-15), V_L can be shown to be upper-bounded as

$$V_L(Z, t) \leq \max \left\{ e^{-\frac{\psi}{\max\{\bar{p}^*, 1\}}(t-t_d^l)} V_L(Z(t_d^l), t_d^l), \frac{\max\{\bar{p}^*, 1\}}{\psi} \varepsilon_1 \right\} \quad (5-16)$$

for all $t \in [t_d^l, t_d^{l+1})$. By using (5-16), the ultimate bound of the trajectory of V_L can be determined by considering the following three cases, where the constant $\varepsilon_2 \in \mathbb{R}$ is defined as $\varepsilon_2 \triangleq \frac{\max\{\bar{p}^*, 1\}}{\psi} \varepsilon_1$ and $B_r \subset \mathbb{R}^{2\mathcal{F}m}$ denotes a closed ball of radius $r \in \mathbb{R}_{>0}$ centered about the origin.

Case 1: The trajectory of V_L has not entered B_{ε_2} .

Consider that at time $t' \in [t_d^l, t_d^{l+1})$, $\{V_L(Z, t) \mid t \leq t'\} \cap B_{\varepsilon_2} = \emptyset$. The inequality in (5–16) can be conservatively upper-bounded to account for the effects of switches as

$$\begin{aligned} V_L(Z(t'), t') &\leq e^{-\frac{\psi(t'-t_d^l)}{\max\{\bar{p}^*, 1\}}} \mu^* W_{l-1}(Z(t_d^l)) \\ &\leq e^{-\frac{\psi(t'-t_d^l)}{\max\{\bar{p}^*, 1\}}} \mu^* e^{-\frac{\psi(t_d^l-t_d^{l-1})}{\max\{\bar{p}^*, 1\}}} W_{l-1}(Z(t_d^{l-1})) \\ &\leq \dots \\ &\leq e^{-\frac{\psi t'}{\max\{\bar{p}^*, 1\}}} (\mu^*)^l W_0(Z(0)). \end{aligned} \quad (5-17)$$

By use of a minimum dwell-time, (5–17) may be upper-bounded as

$$V_L(Z(t'), t') \leq e^{-\beta^* t'} W_0(Z(0)) \quad (5-18)$$

if the dwell-time between switching events is greater than or equal to τ_d^* . Given (5–16) and (5–18), it is clear that use of a dwell-time $\tau_d \geq \tau_d^*$ guarantees that V_L is upper-bounded by an exponential decay from the initial condition $V_L(Z(0), 0)$ towards B_{ε_2} for any $t' \in [t_d^l, t_d^{l+1})$ such that $\{V_L(Z, t) \mid t \leq t'\} \cap B_{\varepsilon_2} = \emptyset$.

Case 2: The trajectory of V_L has reached, or started in, the ball B_{ε_2} , and no switch has occurred since entering B_{ε_2} .

Consider that $V_L(Z(t'), t') \in B_{\varepsilon_2}$ at a time $t' \in [t_d^l, t_d^{l+1})$. Then by (5–16), $V_L(Z, t) \in B_{\varepsilon_2}$ for all $t \in [t_d^l, t_d^{l+1})$.

Case 3: The trajectory of V_L was in the ball B_{ε_2} , and then a switch occurred.

Consider that the trajectory of V_L was inside the ball B_{ε_2} the instant before a switch occurred at time t_d^l . The Lyapunov function V_L can only increase so much such that $V_L(Z(t_d^l), t_d^l) \in B_{\mu^* \varepsilon_2}$ by the definition of μ^* , i.e., $\frac{W_l(Z(t_d^l), t_d^l)}{W_{l-1}(Z(t_d^l), t_d^l)} \leq \mu^*$. Using the definition of the dwell-time τ_d^* , it can be shown that $W_l(Z(t_d^l + \tau_d^*), t_d^l + \tau_d^*) \leq \varepsilon_2$, i.e., the trajectory of V_L re-enters the ball B_{ε_2} before the next switching instance.

Thus, Cases 1-3 together imply that $\limsup_{t \rightarrow \infty} V_L(Z, t) \leq \mu^* \varepsilon_2$, where the inequality in (5–13) guarantees that $B_{\mu^* \varepsilon_2}$ is contained within the set \mathcal{D} . Therefore,

$\limsup_{t \rightarrow \infty} \|Z(t)\| \leq \sqrt{\frac{2\mu^*\varepsilon_2}{\min\{\underline{p}^*, 1\}}}$ by the inequalities in (5–14). Since $\|x_i - x_L\| \leq \|E\| \leq \|Z\|$ for every $i \in \mathcal{V}_{\mathcal{F}}$, we have that $\limsup_{t \rightarrow \infty} \|x_i(t) - x_L(t)\| \leq \sqrt{\frac{2\mu^*\varepsilon_2}{\min\{\underline{p}^*, 1\}}}$. An analysis of the closed-loop system shows that the decentralized controller is bounded for all time. \square

Remark 5.2. The minimum dwell-time used to ensure stability refers to the time that must elapse between any agents' updates. To accomplish this without requiring centralized communication during control implementation, the agents can be pre-programmed with a set of times in which they are allowed to update their consensus weights using a previously computed minimum dwell-time. The following section demonstrates how to compute the minimum dwell-time.

5.5 Satisfaction of Sufficient Conditions

In this section, bounds are computed for \underline{p}^* and \bar{p}^* so that the size of \mathcal{S} can be lower-bounded with known information, (5–13) can be verified, and a value for τ_d can be computed which satisfies $\tau_d \geq \tau_d^*$ (a sufficient condition for convergence in Theorem 5.1) before the decentralized controller is implemented.

5.5.1 A Lower Bound on the Solution of the CALE

Using [81, Theorem 3], \underline{p}^* can be lower-bounded as $\underline{p}^* \geq \inf_{M \in \mathcal{L}_B} \frac{1}{2\sqrt{\lambda(M^T M)}}$, where the set \mathcal{L}_B is defined as the set of all possible values for the matrix $-\mathcal{L}_{\mathcal{F}} - B$ as

$$\mathcal{L}_B \triangleq \left\{ -\mathcal{L}_{\mathcal{F}} - B \mid a_{ij} \in [\underline{a}^*, 1], \sum_{j \in \mathcal{N}_{\mathcal{F}i}} a_{ij} = 1, \forall (j, i) \in \mathcal{E}_{\mathcal{F}} \right\}.$$

Because $\sqrt{\lambda(M^T M)} = \|M\| \leq \|M\|_F$ for all $M \in \mathbb{R}^{\mathcal{F} \times \mathcal{F}}$, we have that $\underline{p}^* \geq \inf_{M \in \mathcal{L}_B} \frac{1}{2\|M\|_F} \geq \frac{1}{2\mathcal{L}_B}$. Thus, a parameter $\underline{p} \in \mathbb{R}$ can be used to lower bound \underline{p}^* using known information as

$$\underline{p}^* \geq \underline{p} \triangleq \frac{1}{2\sqrt{|\mathcal{E}_{\mathcal{F}}| + \mathcal{F} + \sum_{i \in \mathcal{V}_{\mathcal{F}}} b_i^2}}.$$

5.5.2 An Upper Bound on the Solution of the CALE

Due to the sensitivity of the CALE (cf. [82, Theorem 8.3.3]), it is difficult to find an analytical upper bound for the norm of the solution of the CALE for an arbitrarily large space of Hurwitz matrices (cf. [83]). An upper bound can easily be computed if the Hurwitz matrix argument is also negative definite (cf. [84]), but the matrix $-\mathcal{L}_{\mathcal{F}} - B$ may not be negative definite. However, a bound on the perturbation of the solution to the CALE due to a perturbation of the matrix argument can be developed using [82, Theorem 8.3.3] as

$$\frac{\|\Delta\mathcal{P}(M)\|}{\|\mathcal{P}(M) + \Delta\mathcal{P}(M)\|} \leq 2 \|\Delta M\| \|\mathcal{P}(M)\|, \quad (5-19)$$

where $\Delta\mathcal{P}(M)$ denotes the perturbation of the solution of the CALE for a perturbation of the argument, ΔM , such that

$$(M + \Delta M)^T (\mathcal{P}(M) + \Delta\mathcal{P}(M)) + (\mathcal{P}(M) + \Delta\mathcal{P}(M)) (M + \Delta M) = -I_{\mathcal{F}},$$

where $M, M + \Delta M$ are Hurwitz matrices. Using (5-19) and the triangle inequality, a local bound for the perturbation of the solution of the CALE for a given Hurwitz matrix M can be developed as

$$\|\Delta\mathcal{P}(M)\| \leq \frac{2 \|\Delta M\| \|\mathcal{P}(M)\|^2}{1 - 2 \|\Delta M\| \|\mathcal{P}(M)\|} \quad (5-20)$$

for all ΔM such that $M + \Delta M$ is Hurwitz and $\|\Delta M\| < \frac{1}{2\|\mathcal{P}(M)\|}$. Thus, a natural approach to develop an upper bound for \bar{p}^* is to iteratively sample in the set \mathcal{P} , compute an upper bound for the variation of the solution of the CALE in a neighborhood about each sampled point in \mathcal{P} , continue until the union of the considered neighborhoods covers the space \mathcal{P} , and use the largest upper bound for the solution of the CALE to upper bound \bar{p}^* . To see that this is possible, consider the following lemma. Let $\underline{a} \in \mathbb{R}$ be a positive known lower bound of \underline{a}^* , which can be computed with (5-5), (5-7), and \bar{x} from Assumption 5.4. Let the set $\bar{\mathcal{L}}_B$ be defined as $\bar{\mathcal{L}}_B \triangleq \{-\mathcal{L}_{\mathcal{F}} - B \mid a_{ij} \in [\underline{a}, 1] \forall (j, i) \in \mathcal{E}_{\mathcal{F}}\}$, which is a superset of \mathcal{L}_B and contains only Hurwitz matrices by Lemma 5.1. Note that the set \mathcal{P} is contained within the set $\{\mathcal{P}(M) \mid M \in \bar{\mathcal{L}}_B\}$. Additionally, let the set operator Δ be

defined as $\Delta(M) \triangleq \left\{ M + \Delta M \mid (M \in \bar{\mathcal{L}}_B) \wedge \left(\Delta M \in \mathbb{R}^{\mathcal{F} \times \mathcal{F}} : \|\Delta M\| \leq \frac{\varphi}{2\|\mathcal{P}(M)\|} \right) \right\}$, where $\varphi \in \mathbb{R}$ satisfies $0 < \varphi < 1$.

Lemma 5.2. *For any finite selection of matrices $\{M_1, \dots, M_w\} \in \bar{\mathcal{L}}_B$, $w \in \mathbb{Z}_{>0}$, which satisfies $\cup_{n \in \{1, \dots, w\}} \Delta(M_n) \supseteq \bar{\mathcal{L}}_B$, \bar{p}^* is bounded above as $\bar{p} \leq \max_{n \in \{1, \dots, w\}} \frac{1}{1-\varphi} \|\mathcal{P}(M_n)\|$.*

Proof. See Appendix F. □

Thus, an algorithm to upper bound \bar{p}^* can be developed which populates the space $\bar{\mathcal{L}}_B$ with finitely many $\{M_1, \dots, M_w\}$ until $\cup_{n \in \{1, \dots, w\}} \Delta(M_n)$ covers $\bar{\mathcal{L}}_B$. The following simple, finite-duration algorithm accomplishes this by creating a uniform mesh of points in (and on the border of) the set $\bar{\mathcal{L}}_B$ which is refined until the smallest radius of the closed balls $\{\Delta(M_1), \dots, \Delta(M_w)\}$ is greater than or equal to the maximum distance between adjacent points in the uniform mesh, thereby covering the set $\bar{\mathcal{L}}_B$. Let the set C_v be defined as a uniform spacing of $v \in \mathbb{Z}_{>0}$ ($v \geq 2$) points between \underline{a} and 1 inclusively such that $C_v \triangleq \left\{ \alpha_1, \dots, \alpha_v \mid \alpha_i = \underline{a} + \frac{(i-1)(1-\underline{a})}{v-1} \right\}$, let \mathcal{L}_v be defined as the finite set $\mathcal{L}_v \triangleq \{-\mathcal{L}_{\mathcal{F}} - B \mid a_{ij} \in C_v \forall (j, i) \in \mathcal{E}_{\mathcal{F}}\}$, and let $\bar{p} \in \mathbb{R}$ denote an upper bound of \bar{p}^* .

Algorithm 5.1 Upper bound of \bar{p}^* .

$v \leftarrow 2$

$\bar{p} \leftarrow \max_{M \in \mathcal{L}_v} \frac{1}{1-\varphi} \|\mathcal{P}(M)\|$

while $\min_{M \in \mathcal{L}_v} \frac{\varphi}{2\|\mathcal{P}(M)\|} < \sqrt{2} \left(\frac{1-\underline{a}}{v-1} \right)$

$v \leftarrow v + 1$

$\bar{p} \leftarrow \max_{M \in \mathcal{L}_v} \frac{1}{1-\varphi} \|\mathcal{P}(M)\|$

end while

The while statement condition in Algorithm 5.1 is developed using an upper bound on the distance (in the sense of the Euclidean norm) between adjacent points in \mathcal{L}_v .

Adjacent points in the set \mathcal{L}_v differ by a matrix $\tilde{\mathcal{L}}_v \in \mathbb{R}^{\mathcal{F} \times \mathcal{F}}$ which has $\pm \frac{1-\underline{a}}{v-1}$ in an off-

diagonal entry and $\pm \frac{1-\underline{a}}{v-1}$ on the diagonal entry of the same row. The distance between

adjacent points in \mathcal{L}_v can then be upper-bounded as $\|\tilde{\mathcal{L}}_v\| \leq \|\tilde{\mathcal{L}}_v\|_F \leq \sqrt{2} \left(\frac{1-\underline{a}}{v-1} \right)^2$. Also,

note that a larger selection of the parameter φ can decrease the number of iterations in Algorithm 5.1, but this may result in a more conservative upper bound for \bar{p}^* . While this algorithm theoretically terminates in finite operations, it may require too many operations to be feasibly run for a large-sized network. Algorithm 5.1 is only shown for proof of concept; for actual implementation, a more sophisticated optimization routine may be developed from Algorithm 5.1, or a more traditional optimization technique can be used to approximate \bar{p}^* or $\max \{ \mathcal{P}(M) \mid M \in \bar{\mathcal{L}}_B \}$.

5.5.3 Computation of Sufficient Conditions

With the bounding constants \underline{p} and \bar{p} that satisfy $\underline{p} \leq \underline{p}^*$ and $\bar{p} \geq \bar{p}^*$, the size of the set of stabilizing initial conditions \mathcal{S} can be lower bounded and satisfaction of (5–13) and $\tau_d \geq \tau_d^*$ can be guaranteed. Specifically, a conservative estimate $\underline{\mathcal{S}} \subseteq \mathcal{S}$ can be computed as

$$\underline{\mathcal{S}} \triangleq \left\{ Z \in \mathbb{R}^{2\mathcal{F}m} \mid \|Z\| < \frac{\chi}{\mu} \right\},$$

where the constants $\chi, \mu \in \mathbb{R}$ are defined as $\chi \triangleq \inf \left(\rho^{-1} \left(\left[\frac{1}{\bar{p}} \sqrt{\frac{k\psi}{3}}, \infty \right) \right) \right) \in \mathbb{R}$ and $\mu \triangleq \frac{\max\{\bar{p}, 1\}}{\min\{\underline{p}, 1\}}$. Additionally, (5–13) is satisfied if the following computable condition is satisfied

$$\frac{3(\bar{p}\bar{N}_d)^2}{k} + 3k(\bar{p}\mathcal{F}\bar{\mathcal{L}}_B(\bar{x} + \lambda\bar{x}))^2 < \frac{\psi\chi}{\mu \max\{\bar{p}, 1\}}.$$

Finally, τ_d can be selected such that

$$\tau_d = \frac{\ln(\mu)}{\frac{\psi}{\max\{\bar{p}, 1\}} - \beta},$$

where the tuning parameter $\beta \in \mathbb{R}$ is selected such that $0 < \beta < \frac{\psi}{\max\{\bar{p}, 1\}}$. The inequality $\tau_d \geq \tau_d^*$ is clearly satisfied if β^* is assigned as $\beta^* = \beta$. As with β^* , the selection of β involves a trade-off between convergence rate and the frequency of an agent's edge weight updates.

Note that the methods used to compute the bounds \underline{p} and \bar{p} in Sections 5.5.1 and 5.5.2 produce conservative estimates. More sophisticated optimization approaches may yield less conservative bounds and take less computational resources.

5.6 Simulation

The performance of the consensus weight update law given in (5-5)-(5-7) with the controller in (5-4) is demonstrated using the four-agent network depicted in Fig. 5-1 and the heterogeneous nonlinear dynamics

$$\ddot{x}_i = \begin{bmatrix} \kappa_i \sin(x_{i,2}) \dot{x}_{i,2} & \kappa_i \sin(x_{i,2}) (\dot{x}_{i,1} + \dot{x}_{i,2}) \\ -\kappa_i \sin(x_{i,2}) \dot{x}_{i,1} & 0 \end{bmatrix} \dot{x}_i - \begin{bmatrix} v_{1,i} & 0 \\ 0 & v_{2,i} \end{bmatrix} \dot{x}_i + u_i,$$

where the constant parameters $\kappa_i, v_{1,i}, v_{2,i} \in \mathbb{R}$ are described in Table 5-1 and $x_{1,i}, x_{2,i}$ respectively denote the first and second entries of the vector x_i . The only nonzero pinning gain is selected as $b_1 = 3$ and the control gains are selected as $k = 60, \lambda = 20$. The tuning parameter s and constant \bar{t} , used in the trust metric in (5-5), are selected as $s = 1$ and $\bar{t} = 10$ s. The gains used in the reputation algorithm in (5-6) are selected as $\eta_{\zeta i} = 10, \eta_{\sigma i} = 0.1$ for all $i \in \mathcal{V}_{\mathcal{F}}$. The simulation is meant to model a real-world scenario in that it is anticipated that the trust values will be lower-bounded as $\sigma_{ij} \geq 0.2$ for all $i \in \mathcal{V}_{\mathcal{F}}, j \in \mathcal{N}_{\mathcal{F}i}$, which, as previously mentioned, implies that $\zeta_{ij} \geq 0.2$ for all $i \in \mathcal{V}_{\mathcal{F}}, j \in \mathcal{N}_{\mathcal{F}i}$. The MATLAB optimization routine `fmincon` is executed to obtain estimates of \underline{p}^* and \bar{p}^* using the gains k and λ , the network topology depicted in Fig. 5-1, the pinning gain b_1 , and the bounds $0.2 \leq \zeta_{ij} \leq 1$, resulting in the estimates $\underline{p} = 0.119$ and $\bar{p} = 8.28$. The dwell-time for the consensus weight updates is then computed as $\tau_d = 2.4$ s using the assignment $\beta = 0.001 \frac{2\psi}{\max\{\bar{p}, 1\}}$. The agents' onboard sensor equipment is modeled to have a frequency of 20 Hz, where at each sensor measurement an agent has a 50% chance of sensing a neighbor. Only one neighbor can be observed in a single sensor measurement, and the neighbor seen is a random selection, where each neighbor is equally likely to be seen. The onboard position estimates are modeled to be affected by

an offset such that $\hat{x}_i = x_i + \Delta x_i$, where $\Delta x_1 = \begin{bmatrix} 1 \\ 1 \end{bmatrix}$, $\Delta x_2 = \begin{bmatrix} -1 \\ -1 \end{bmatrix}$, $\Delta x_3 = \begin{bmatrix} 0.5 \\ \sin(t) \end{bmatrix}$,

and

$$\Delta x_4 = \begin{cases} \begin{bmatrix} -0.5 \\ -0.5 \end{bmatrix} & \text{if } t < 60 \\ (90 + 30 \sin(7t)) \begin{bmatrix} 1 \\ 1 \end{bmatrix} & \text{if } t \geq 60. \end{cases}$$

Thus, agents 1-4 have very accurate (but not perfect) estimates of their position from 0 – 60 s. After 60 s, the position estimate maintained by agent 4 becomes very inaccurate, which may be due to onboard localization sensor failure, for example. The onboard velocity estimates are similarly affected as $\hat{\dot{x}}_i = \dot{x}_i + \frac{d}{dt}(\Delta x_i)$. The network-wide objective is to track the leader state trajectory, which evolves as $x_L = \begin{bmatrix} \sin(t) \\ 0.5 \cos(t) \end{bmatrix}$.

To demonstrate the benefit of updating the consensus weights based on reputation, consensus weights are updated after the closed-loop system has come to steady-state. The first update occurs at 120 s and the agents' updates are staggered in time in intervals of τ_d . The benefit of the consensus weight updates is shown in the plot of the leader-tracking error in Fig. 5-2, where the leader-tracking error of agent 4 is high due to its very inaccurate state estimate, and is therefore omitted. The tracking error of agent 1 is less affected by the inaccurate position and velocity estimates of agent 4 since agent 1 is directly connected to the leader; however, the effects of agent 4 percolate through the network and severely worsen the tracking performance of agents 2 and 3, as shown in Fig. 5-2. The deleterious effects of agent 4 are mitigated by the trust measurements, neighbor reputations, and consensus weight updates, shown in Fig. 5-3 - 5-5. Upon achieving steady-state using consensus weight updates, the leader-tracking errors return to values similar to those obtained when agent 4 had very accurate position estimates. The RMS leader-tracking performance for agents 1 – 3 is quantified in

Table 5-2 for the steady-state periods of 40 – 60 s, 100 – 120 s, and 160 – 180 s, where $J(t_1, t_2) \triangleq \sum_{i \in \{1,2,3\}} \text{rms}_{[t_1, t_2]} \|x_L - x_i\|$ denotes the sum of the RMS leader-tracking error norms over agents 1 – 3 between the times t_1 and t_2 .

Note that the trust values went below the anticipated lower bound of 0.2, where the lower bound 0.2 was used to compute the update dwell-time. However, the closed-loop system is still stable, which emphasizes the fact that the given conditions are only sufficient, and lower dwell-times than τ_d may also provide stability.

The benefit of weighting the contributions of neighbor recommendations based on their own recommendations, seen by the multiplication by ζ_{in} in (5-6), is demonstrated by performing the simulation again without the multiplicative term ζ_{in} in (5-6). The resulting reputation algorithm that omits ζ_{in} , shown in (5-21), resembles the reputation algorithm proposed in [49], where ζ'_{ij} denotes the alternative reputation measure obtained with the algorithm in (5-21).

$$\dot{\zeta}'_{ij} = \sum_{n \in \mathcal{N}_{\mathcal{F}_i} \cap \mathcal{N}_{\mathcal{F}_j}} \eta_{\zeta_i} (\zeta'_{nj} - \zeta'_{ij}) + \eta_{\sigma_i} (\sigma_{ij} - \zeta'_{ij}) \quad (5-21)$$

Simulation results show that, compared to the results obtained using the reputation algorithm in (5-6), use of the reputation algorithm in (5-21) produces 10.7% worse leader-tracking performance, in terms of the metric $J(160, 180)$ (i.e., steady state, after updates to the consensus weights began). The neighbor reputations for this second simulation are shown in Fig. 5-6, where the reputations of well-localized agents, $\zeta_{21}, \zeta_{32}, \zeta_{13}$, are lower compared to the results produced by the reputation algorithm in (5-6). The reputations are diminished because the recommendation by agent 4 to the reputations of the other agents is not weighted by the reputation of agent 4, unlike in the reputation algorithm in (5-6).

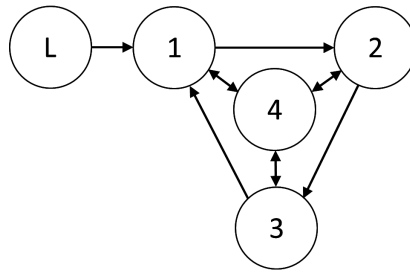


Figure 5-1. Network communication topology.

Agent	1	2	3	4
κ_i	0.3	0.7	0.5	0.9
$v_{1,i}$	5.0	5.5	4.5	4.0
$v_{2,i}$	1.0	0.5	0.7	1.2

Table 5-1. Parameters in dynamics.

$J(40, 60)$	4.64
$J(100, 120)$	8.68
$J(160, 180)$	4.30

Table 5-2. Steady-state RMS leader-tracking performance.

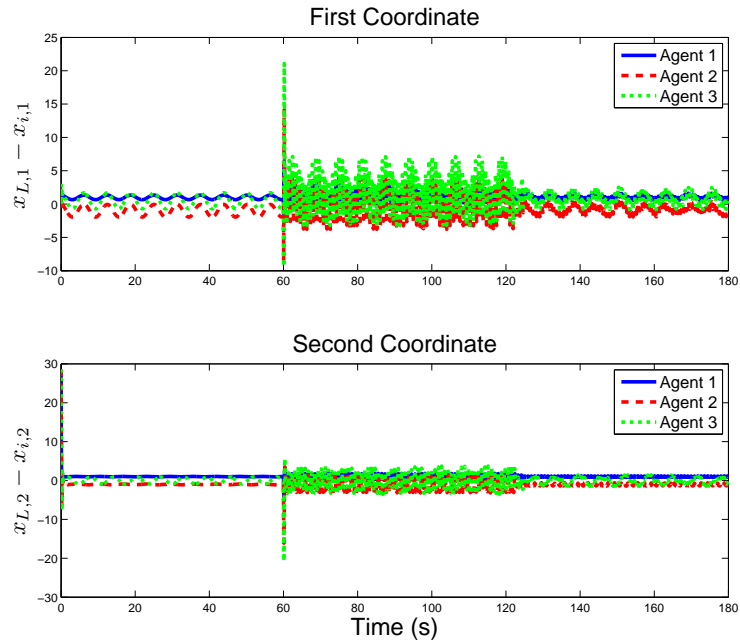


Figure 5-2. Leader-tracking error.

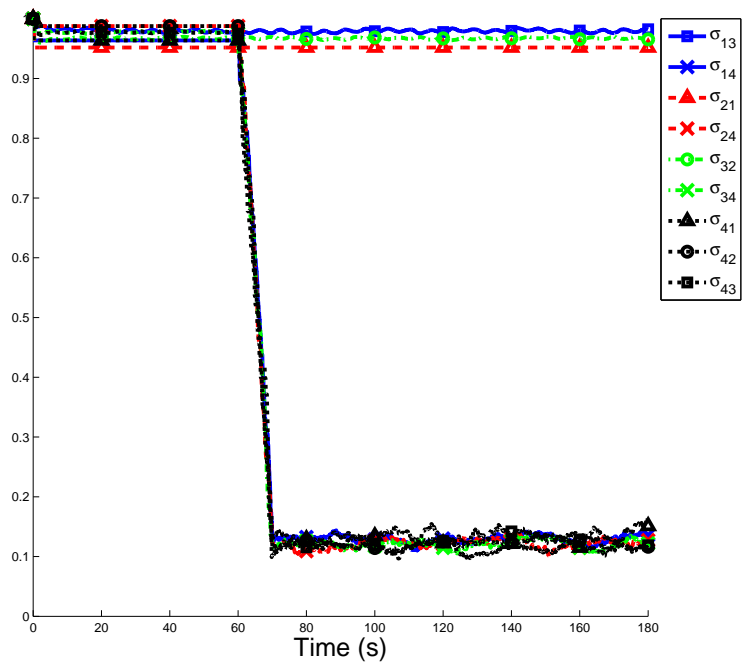


Figure 5-3. Trust measurements.

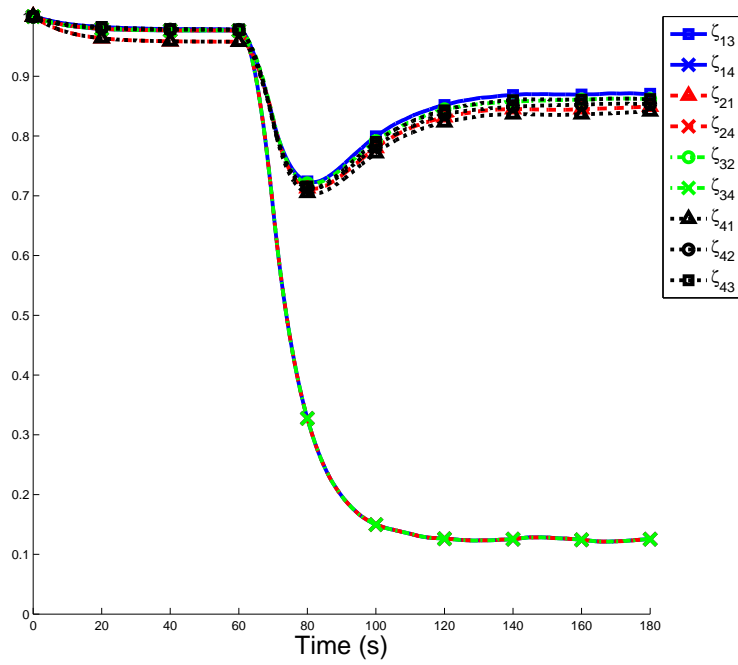


Figure 5-4. Neighbor reputations.

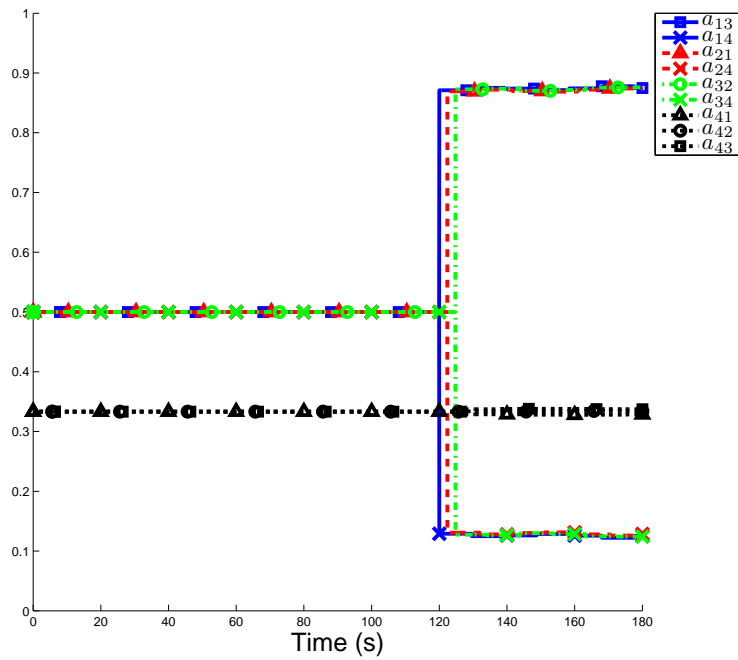


Figure 5-5. Dynamically updated consensus (adjacency) weights.

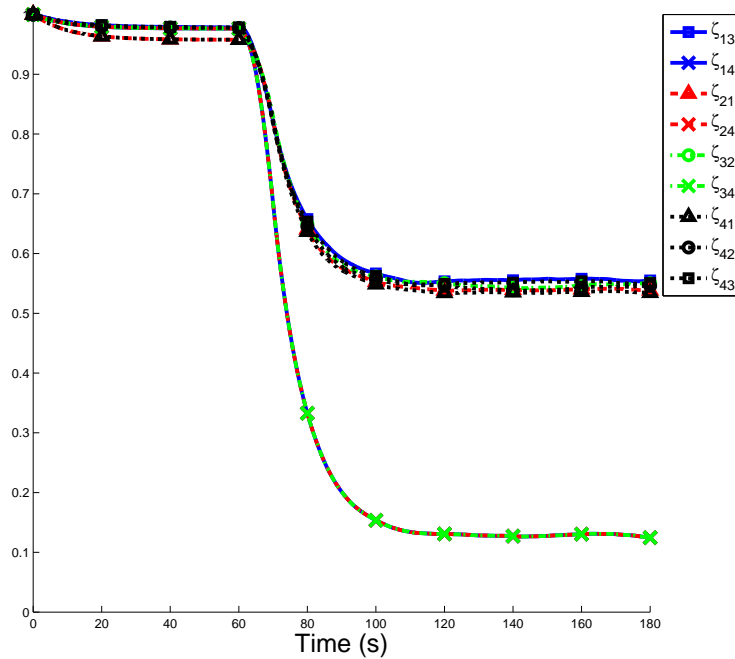


Figure 5-6. Neighbor reputations produced by the alternative reputation algorithm in (5–21).

5.7 Concluding Remarks

A decentralized controller and reputation algorithm which updates consensus weights were developed for approximate synchronization to the leader agent’s state, where the reputation algorithm uses the discrepancy between unreliable communicated information and intermittent sensing data of a neighbor agent in collaboration with mutual neighbors. The leader-follower network topology is modeled as strongly-connected and static, but the updates of consensus weights produce a switched system. Approximate synchronization is ensured through a Lyapunov-based convergence analysis and techniques from switching control theory, which help develop a dwell-time for the follower agents’ consensus weight updates. Whereas most switched control approaches develop a dwell-time based on a finite number of possible structures for the closed-loop dynamics, the dwell-time discussed in this work is based on bounds of the minimum and maximum eigenvalues of the solution to the CALE over a space of Hurwitz

matrices due to the infinite number of possible combinations of the network consensus weights.

CHAPTER 6 CONCLUSIONS AND FUTURE WORK

6.1 Conclusions

Decentralized control is a powerful control technique which provides a means for accomplishing an objective using a disaggregated, cooperating collection of autonomous agents, such as teams of UAVs or AUVs performing reconnaissance, satellites performing collective interferometry, and platoons of ground robots. Delegating a collective task to multiple systems provides benefits in terms of lower communication bandwidth, robustness to hardware failure, increased strategic flexibility, and spatial distribution. However, the benefits of the distribution of mission planning and execution to individual autonomous systems are accompanied by the disadvantage of less situational awareness: the networked systems are only aware of the status of network neighbors in a decentralized communication architecture. Among other consequences, this phenomena makes decentralized multi-agent networks more susceptible to cascading, destabilizing effects caused by exogenous disturbances on an agent's plant or control system, communication delay between network neighbors, and reduced ability to vet the accuracy of communicated information. This dissertation addresses these challenges through the development of novel decentralized control techniques that restrict the propagation of these deleterious effects through the network of autonomous systems.

Chapter 2 details the development of a novel decentralized controller which addresses the challenge of mitigating the effects of exogenous disturbances in a network of autonomous systems while performing synchronization, wherein agents share information with network neighbors in an attempt to collectively drive all agents' states towards that of a network leader. The exogenous disturbances are assumed to be unknown and represent the effects of unmodeled dynamics and external force effects on an agent's dynamics (e.g., a gust of wind causes undesired movement of a UAV). The agents' dynamics are modeled with heterogeneous Euler-Lagrange equations of motion

due to broad applicability to physical systems. Concepts from the RISE control technique and graph theory are leveraged in the development of the decentralized controller and the proof of asymptotic convergence of the agent's states to that of the network leader's. In the proof of convergence, it is demonstrated that the developed controller compensates for the effects of the disturbances of all agents using only relative state information. Simulation results are given which demonstrate the enhanced performance of the developed controller compared to other prominent decentralized controllers. The developed controller is then extended from the synchronization framework to the formation control framework, wherein the agents converge to a geometric configuration specified by desired relative positions between the agents.

The decentralized control technique in Chapter 2 is generalized in Chapter 3 for the objective of containment control. As opposed to synchronization, in which a single leader interacts with the follower agents, the objective of containment control is to have the autonomous follower agents cooperatively interact with multiple leaders and converge to a reasonable linear combination of the leaders' states. For example, a flock of autonomous UAVs may be guided by multiple remotely piloted UAVs in performing a search mission. Specifically, containment control specifies that the follower agents' states converge to the convex hull demarcated by the states of the leaders. Again, concepts from the RISE control technique and graph theory are used to demonstrate convergence of the follower agents' states to the convex hull of the leaders' dynamic states despite the effects of modeling uncertainty and exogenous disturbances.

The developments in Chapter 4 address compensation for the effects of communication delay in a decentralized network in which the agents have heterogeneous, uncertain Euler-Lagrange dynamics and heterogeneous, uncertain communication delays. Communication delay drastically affects performance in accomplishing a network-wide objective, such as synchronization, since the effect of a change in a network leader's state may not impact a follower agent until multiple periods of delay have passed as

the change percolates through the network. In Chapter 4, the notions of self-delayed feedback and feedback without self-delay are introduced: self-delayed feedback signifies the comparison of a neighbor's delayed state with an agent's own manually delayed state, and feedback without self delay signifies the comparison of a neighbor's delayed state with an agent's own current state. The advantages and disadvantages of both feedback types are exemplified in a simulation and a novel decentralized controller is developed which uses both of these types of feedback and estimates of what neighbors' communication delay durations are. A numerical simulation demonstrates that a mixture of these two types of feedback can provide enhanced stability criteria and improved leader-tracking for the synchronization framework.

Chapter 5 addresses the issue of diminished situational awareness in a decentralized interaction environment by developing a control architecture to enhance the robustness of decentralized control to the communication of inaccurate state information. Assuming that communicated information is continuously available, but possibly inaccurate, and that neighbor sensing is intermittent, yet accurate, a trust metric is developed that quantifies the accuracy and reliability of a neighbor's communication. Trust values are shared via a neighborhood-based reputation algorithm, wherein agents collaborate to develop a reputation of a mutual neighbor and reputation recommendations are weighted by the reputation of the recommender. Neighbor reputations are used to weigh the communicated feedback from neighbors in a decentralized control policy by adjusting consensus weights as a function of neighbors' reputations. Although the network connections are modeled as static, updates to the consensus weights introduce discontinuities into the closed-loop system. Notions from switching control theory and the sensitivity of the CALE are used to develop a dwell-time for the follower agents' consensus weight updates through a Lyapunov-based convergence analysis. Simulation results demonstrate that intermittent neighbor sensing can be used

to augment a communication-based control policy by vetting network neighbors in a recommendation-based approach.

6.2 Future Work

The developments given in this dissertation have been shown to theoretically satisfy control objectives and provide comparatively improved performance via Lyapunov-based convergence analyses and numerical simulations. Justifications of these claims could be further established if physical experiments were performed to demonstrate the real-world applicability of the developed techniques. Ground vehicles or quadcopters may be used in the future to demonstrate the efficacy of the control techniques detailed in this dissertation.

Chapters 2-4 assume that the communication topology of the follower agents is undirected. One avenue for extending this work would be to consider a communication topology which is directed, i.e., not all communication links may be bidirectional. An approach similar to that used in Chapter 5 may be used to approach this problem, wherein the sum of the Laplacian matrix corresponding to the follower agent topology and the leader-pinning matrix is used as an input to the Lyapunov equation, the solution of which is a matrix that can be used to generate a candidate Lyapunov function. However, this approach is complicated if considering Euler-Lagrange dynamics, which cause an inertia matrix to be multiplied by the matrix solution of the Lyapunov equation in the feedback expressions of the derivative of the candidate Lyapunov function. Even though the matrix solution of the Lyapunov equation and the inertia matrix are positive definite, it is not necessarily the case that the matrix product is positive definite, which causes the feedback in the derivative of the candidate Lyapunov function to be sign indefinite, and causes analysis with the candidate Lyapunov function to be fruitless. This technical challenge could possibly be addressed by using the inertia matrix in a controller to cancel the respective effects, but such a controller requires exact

model knowledge of the inertia matrix. Further research may provide insight in how to guarantee compensation of dynamics' inertia in general directed networks.

The decentralized controller developed in Chapter 4 addresses compensation of the effects of communication delay by weighting the contributions of self-delayed feedback and feedback without self-delay. This control technique may be enhanced by additions such as developing time-varying feedback weights based on estimates of the current communication delay, weighting feedback more for neighbors which have less communication delay, a protocol which severs a neighbor connection if that neighbor's large communication delay makes its feedback only deleterious, and developing a decentralized estimator of the network leader's state so that the cascading effect of communication delay has less impact.

Some exciting results may be extended from the developments in Chapter 5. In particular, these developments can be extended to devise more sophisticated context-dependent reputation algorithms, an augmentation to the decentralized controller which decides when to sever neighbor connections, and an observer which determines a more accurate estimate of neighbors' states given unreliable communication and intermittent sensing.

APPENDIX A
PROOF THAT P IS NONNEGATIVE (CH 2)

Lemma A.1. *Given the differential equation in (2–23), $P \geq 0$ if, for all $i \in \mathcal{V}_{\mathcal{F}}$, χ_i satisfies*

$$\chi_i > \|\varsigma_{ai}\|_{\infty} + \frac{1}{\alpha_{2,i}} \|\varsigma_{bi}\|_{\infty}. \quad (\text{A-1})$$

Proof. For notational brevity, let an auxiliary signal $\sigma \in \mathbb{R}$ be the negative of the integral of \dot{P} in (2–23) as

$$\begin{aligned} \sigma &= \int_0^t E_2^T(\varepsilon) \Lambda_2(N_d(\varepsilon) - \beta \operatorname{sgn}(E_2(\varepsilon))) d\varepsilon + \int_0^t \frac{\partial E_2^T(\varepsilon)}{\partial \varepsilon} N_d(\varepsilon) d\varepsilon \\ &\quad - \int_0^t \frac{\partial E_2^T(\varepsilon)}{\partial \varepsilon} \beta \operatorname{sgn}(E_2(\varepsilon)) d\varepsilon. \end{aligned} \quad (\text{A-2})$$

Integrating the last two terms in (A–2) yields [58, Lemma 1]

$$\begin{aligned} \sigma &= \int_0^t E_2^T(\varepsilon) \Lambda_2(N_d(\varepsilon) - \beta \operatorname{sgn}(E_2(\varepsilon))) d\varepsilon + \sum_{l=1}^{\mathcal{F}m} E_{2l}(t) N_{d_l}(t) - E_2^T(0) N_d(0) \\ &\quad - \int_0^t E_2^T(\varepsilon) \frac{\partial N_d(\varepsilon)}{\partial \varepsilon} d\varepsilon - \sum_{l=1}^{\mathcal{F}m} |E_{2l}(t)| \beta_{l,l} + \sum_{l=1}^{\mathcal{F}m} |E_{2l}(0)| \beta_{l,l}. \end{aligned} \quad (\text{A-3})$$

The expression in (A–3) may then be expressed as

$$\begin{aligned} \sigma &= \int_0^t \left(\sum_{l=1}^{\mathcal{F}m} E_{2l}(\varepsilon) \Lambda_{2l,l} N_{d_l}(\varepsilon) \right) d\varepsilon - \int_0^t \left(\sum_{l=1}^{\mathcal{F}m} |E_{2l}(\varepsilon)| \Lambda_{2l,l} \beta_{l,l} \right) d\varepsilon \\ &\quad - \int_0^t \left(\sum_{l=1}^{\mathcal{F}m} E_{2l}(\varepsilon) \dot{N}_{d_l}(\varepsilon) \right) d\varepsilon + \sum_{l=1}^{\mathcal{F}m} E_{2l}(t) N_{d_l}(t) - E_2^T(0) N_d(0) \\ &\quad - \sum_{l=1}^{\mathcal{F}m} |E_{2l}(t)| \beta_{l,l} + \sum_{l=1}^{\mathcal{F}m} |E_{2l}(0)| \beta_{l,l}. \end{aligned} \quad (\text{A-4})$$

The upper bounds in (2–20) and (2–21) are then used to upper-bound (A–4) as

$$\begin{aligned} \sigma &\leq \int_0^t \left(\sum_{l=1}^{\mathcal{F}m} |E_{2_l}(\varepsilon)| \Lambda_{2,l} \zeta_{a_l} \right) d\varepsilon - \int_0^t \left(\sum_{l=1}^{\mathcal{F}m} |E_{2_l}(\varepsilon)| \Lambda_{2,l} \beta_{l,l} \right) d\varepsilon \\ &\quad + \int_0^t \left(\sum_{l=1}^{\mathcal{F}m} |E_{2_l}(\varepsilon)| \zeta_{b_l} \right) d\varepsilon + \sum_{l=1}^{\mathcal{F}m} |E_{2_l}(t)| (\zeta_{a_l} - \beta_{l,l}) \\ &\quad - E_2^T(0) N_d(0) + \sum_{l=1}^{\mathcal{F}m} \beta_{l,l} |E_{2_l}(0)|, \end{aligned}$$

where ζ_{a_l} and ζ_{b_l} represent the l^{th} element of ζ_a and ζ_b , respectively. Provided the gain condition for χ_i in (A–1) is satisfied for each $i \in \mathcal{V}_{\mathcal{F}}$ (recall that $\beta \triangleq \text{diag}(\chi_1, \chi_2, \dots, \chi_{\mathcal{F}}) \otimes I_m$ and $\Lambda_2 \triangleq \text{diag}(\alpha_{2,1}, \alpha_{2,2}, \dots, \alpha_{2,\mathcal{F}}) \otimes I_m$), then $\sigma \leq \sum_{l=1}^{\mathcal{F}m} \beta_{l,l} |E_{2_l}(0)| - E_2^T(0) N_d(0)$.

Thus, σ may be upper-bounded as

$$\sigma \leq P(0). \tag{A–5}$$

Integrating both sides of (2–23) yields $P(t) = P(0) - \sigma$, which indicates that $P \geq 0$ from (A–5). □

APPENDIX B
PROOF OF SUPPORTING LEMMA (CH 3)

Proof of Lemma 3.1. Because the eigenvalues of $\mathcal{L}_{\mathcal{F}} + B$ are positive by Assumption 3.5 and [18, Lemma 4.1], the diagonal entries are positive, and the off-diagonal entries are nonpositive, all entries of the matrix $(\mathcal{L}_{\mathcal{F}} + B)^{-1}$ are non-negative [85, Theorem 2.3]. Due to the structure of the Laplacian matrix \mathcal{L} , we have that $\mathcal{L}\mathbf{1}_{\mathcal{F}+L} = \mathbf{0}_{\mathcal{F}+L}$, which implies $(\mathcal{L}_{\mathcal{F}} + B)\mathbf{1}_{\mathcal{F}} + \mathcal{L}_L\mathbf{1}_L = \mathbf{0}_L$. Because $\mathcal{L}_{\mathcal{F}} + B$ is invertible, $\mathbf{1}_{\mathcal{F}} = -(\mathcal{L}_{\mathcal{F}} + B)^{-1}\mathcal{L}_L\mathbf{1}_L$, which implies that row sums of $-(\mathcal{L}_{\mathcal{F}} + B)^{-1}\mathcal{L}_L$ add to one, where each entry of the matrix $-(\mathcal{L}_{\mathcal{F}} + B)^{-1}\mathcal{L}_L$ is nonnegative since $(\mathcal{L}_{\mathcal{F}} + B)^{-1}$ has only nonnegative entries and \mathcal{L}_L has only non-positive entries. Thus, the product $-(((\mathcal{L}_{\mathcal{F}} + B)^{-1}\mathcal{L}_L) \otimes I_m) Q_L$ can be represented as $\left[q_{d1}^T, \dots, q_{d\mathcal{F}}^T \right]^T = -(((\mathcal{L}_{\mathcal{F}} + B)^{-1}\mathcal{L}_L) \otimes I_m) Q_L \in \mathbb{R}^{\mathcal{F}m}$, where $q_{di} \in \mathbb{R}^m$ such that $q_{di} = \sum_{l \in \{1, \dots, L\}} [-(\mathcal{L}_{\mathcal{F}} + B)^{-1}\mathcal{L}_L]_{il} q_l \forall i \in \{1, \dots, \mathcal{F}\}$, where $[\cdot]_{ij}$ denotes the matrix entry of the i^{th} row and j^{th} column, $\sum_{l \in \{1, \dots, L\}} [-(\mathcal{L}_{\mathcal{F}} + B)^{-1}\mathcal{L}_L]_{il} = 1 \forall i \in \{1, \dots, \mathcal{F}\}$, and $[-(\mathcal{L}_{\mathcal{F}} + B)^{-1}\mathcal{L}_L]_{il} \geq 0 \forall i \in \{1, \dots, \mathcal{F}\}, \forall l \in \{1, \dots, L\}$ by the above conclusions. Because the convex hull for the set $S \triangleq \{q_l \mid l \in \mathcal{V}_L\}$ is defined as $\text{Conv}\{S\} \triangleq \{\sum_{l \in \mathcal{V}_L} \alpha_l q_l \mid (\forall l : \mathbb{R} \ni \alpha_l \geq 0) \wedge \sum_{l \in \mathcal{V}_L} \alpha_l = 1\}$ [86], we have that $q_{di} \in \text{Conv}\{q_l \mid l \in \mathcal{V}_L\} \forall i \in \{1, \dots, \mathcal{F}\}$; in other words, the vectors stacked in the product $-(((\mathcal{L}_{\mathcal{F}} + B)^{-1}\mathcal{L}_L) \otimes I_m) Q_L$ are within the convex hull formed with the leader agents' states. Suppose that $\|E_1\| \rightarrow 0$. Then $\|((\mathcal{L}_{\mathcal{F}} + B) \otimes I_m)^{-1} E_1\| \rightarrow 0$, which implies that $\|Q_{\mathcal{F}} + (((\mathcal{L}_{\mathcal{F}} + B)^{-1}\mathcal{L}_L) \otimes I_m) Q_L\| \rightarrow 0$ by (3–4), and thus $Q_{\mathcal{F}} = \left[q_{L+1}^T, \dots, q_{L+\mathcal{F}}^T \right]^T \rightarrow -(((\mathcal{L}_{\mathcal{F}} + B)^{-1}\mathcal{L}_L) \otimes I_m) Q_L = \left[q_{d1}^T, \dots, q_{d\mathcal{F}}^T \right]^T$. Hence, $d(q_i, \text{Conv}\{q_l \mid l \in \mathcal{V}_L\}) \rightarrow 0 \forall i \in \mathcal{V}_{\mathcal{F}}$.

APPENDIX C
DEMONSTRATION OF SUPPORTING INEQUALITY (CH 4)

Consider the inequality $a^T b \leq \frac{1}{2\Phi} a^T a + \frac{\Phi}{2} b^T b$ for any vectors $a, b \in \mathbb{R}^{Fm}$ and any positive scalar $\Phi \in \mathbb{R}_{>0}$. After setting $a^T = kR^T (\kappa_1 \mathcal{A}_{ij} - \kappa_2 \mathcal{L}_{ij})$, $b = \int_{t-\tau_{ji}}^t \dot{R}(\sigma) d\sigma$, and $\Phi = \frac{\phi \iota_2}{\bar{\tau} k^2}$, the scalar $R^T k \sum_{(j,i) \in \mathcal{E}_F} (\kappa_1 \mathcal{A}_{ij} - \kappa_2 \mathcal{L}_{ij}) \int_{t-\tau_{ji}}^t \dot{R}(\sigma) d\sigma$ can be upper-bounded as¹

$$\begin{aligned} \sum_{(j,i) \in \mathcal{E}_F} kR^T (\kappa_1 \mathcal{A}_{ij} - \kappa_2 \mathcal{L}_{ij}) \int_{t-\tau_{ji}}^t \dot{R}(\sigma) d\sigma \leq \\ \sum_{(j,i) \in \mathcal{E}_F} \left(\frac{\bar{\tau} k^2}{2\phi \iota_2} k^2 R^T (\kappa_1 \mathcal{A}_{ij} - \kappa_2 \mathcal{L}_{ij}) (\kappa_1 \mathcal{A}_{ij} - \kappa_2 \mathcal{L}_{ij})^T R \right. \\ \left. + \frac{\phi \iota_2}{2\bar{\tau} k^2} \left(\int_{t-\tau_{ji}}^t \dot{R}^T(\sigma) d\sigma \right) \int_{t-\tau_{ji}}^t \dot{R}(\sigma) d\sigma \right). \quad (\text{C-1}) \end{aligned}$$

By using the Raleigh-Ritz Theorem, (C-1) can be upper-bounded as

$$\begin{aligned} \sum_{(j,i) \in \mathcal{E}_F} kR^T (\kappa_1 \mathcal{A}_{ij} - \kappa_2 \mathcal{L}_{ij}) \int_{t-\tau_{ji}}^t \dot{R}(\sigma) d\sigma \leq \frac{\bar{\tau} k^4}{2\phi} R^T R \\ + \frac{\phi \iota_2}{2\bar{\tau} k^2} \sum_{(j,i) \in \mathcal{E}_F} \left(\int_{t-\tau_{ji}}^t \dot{R}^T(\sigma) d\sigma \right) \int_{t-\tau_{ji}}^t \dot{R}(\sigma) d\sigma. \quad (\text{C-2}) \end{aligned}$$

After using Assumption 4.6 and the inequality $\left(\int_0^b a(s) ds \right)^T \left(\int_0^b a(s) ds \right) \leq b \int_0^b a^T(s) a(s) ds$ for $a \in \mathbb{R}^{Fm}$ and $b \in \mathbb{R}_{>0}$, (C-2) can be upper-bounded as

$$\sum_{(j,i) \in \mathcal{E}_F} kR^T (\kappa_1 \mathcal{A}_{ij} - \kappa_2 \mathcal{L}_{ij}) \int_{t-\tau_{ji}}^t \dot{R}(\sigma) d\sigma \leq \frac{\bar{\tau} k^4}{2\phi} R^T R + \frac{\phi \iota_2 |\mathcal{E}_F|}{2k^2} \int_{t-\bar{\tau}}^t \left\| \dot{R}(\sigma) \right\|^2 d\sigma.$$

¹ Because any matrix product of the form $\Xi \Xi^T$ is positive semi-definite for a square real matrix Ξ , the symmetric matrix $\sum_{(j,i) \in \mathcal{E}_F} (\kappa_1 \mathcal{A}_{ij} - \kappa_2 \mathcal{L}_{ij}) (\kappa_1 \mathcal{A}_{ij} - \kappa_2 \mathcal{L}_{ij})^T$ is positive semi-definite. Additionally, since $\kappa_1 \mathcal{A}_{ij} - \kappa_2 \mathcal{L}_{ij}$ has at least one nonzero entry for every $(j, i) \in \mathcal{E}_F$, $\sum_{(j,i) \in \mathcal{E}_F} (\kappa_1 \mathcal{A}_{ij} - \kappa_2 \mathcal{L}_{ij}) (\kappa_1 \mathcal{A}_{ij} - \kappa_2 \mathcal{L}_{ij})^T$ does not have all zero entries. Since $\sum_{(j,i) \in \mathcal{E}_F} (\kappa_1 \mathcal{A}_{ij} - \kappa_2 \mathcal{L}_{ij}) (\kappa_1 \mathcal{A}_{ij} - \kappa_2 \mathcal{L}_{ij})^T$ is symmetric, positive semi-definite and not the zero matrix, we have that $\iota_2 > 0$.

The procedure for developing the remaining upper bounds given in (4–37) and (4–38) is similar, and therefore omitted.

APPENDIX D
DEMONSTRATION OF REPUTATION BOUND (CH 5)

Let the function $\underline{\zeta} : \mathbb{R} \rightarrow \mathbb{R}$ be defined as

$$\underline{\zeta}(t) \triangleq \min \{ \zeta_{ij}(t) \mid (j, i) \in \mathcal{E}_{\mathcal{F}} \}.$$

Suppose that $(-\infty, \underline{\sigma}^*] \cap \{ \zeta_{ij}(t) \mid t \geq 0 \} \neq \emptyset$ for some $(j, i) \in \mathcal{E}_{\mathcal{F}}$, i.e., a reputation value becomes less than or equal to $\underline{\sigma}^*$ at some time. By continuity of ζ_{ij} , there exists some time $T \in \mathbb{R}_{>0}$ such that $\underline{\zeta}(T) = \underline{\sigma}^* > 0$. Let T_{σ} be defined as $T_{\sigma} \triangleq \min \{ t \in \mathbb{R} \mid \underline{\zeta}(t) = \underline{\sigma}^* \}$. For any $(h, g) \in \mathcal{E}_{\mathcal{F}}$ such that $\zeta_{gh}(T_{\sigma}) = \underline{\sigma}^*$, we have that

$$\dot{\zeta}_{gh}(T_{\sigma}) = \sum_{n \in \mathcal{N}_{\mathcal{F}g} \cap \mathcal{N}_{\mathcal{F}h}} \eta_{\zeta g} \zeta_{gn} (\zeta_{nh} - \underline{\zeta}) + \eta_{\sigma g} (\sigma_{gh} - \underline{\sigma}^*).$$

By the definition of $\underline{\zeta}$, we know that $\sum_{n \in \mathcal{N}_{\mathcal{F}g} \cap \mathcal{N}_{\mathcal{F}h}} \eta_{\zeta g} \zeta_{gn} (\zeta_{nh} - \underline{\zeta}) \geq 0$. Additionally, by the definition of $\underline{\sigma}^*$, we know that $\eta_{\sigma g} (\sigma_{gh} - \underline{\sigma}^*) \geq 0$. Therefore, $\dot{\zeta}_{gh}(T_{\sigma}) \geq 0$ and thus $\zeta_{gh}(T_{\sigma}^+) \geq \underline{\sigma}^*$. By induction, $\zeta_{ij}(t) \geq \underline{\sigma}^*$ for all $(j, i) \in \mathcal{E}_{\mathcal{F}}$ and $t \in \mathbb{R}$.

A similar argument shows that $\zeta_{ij}(t) \leq 1$ for all $(j, i) \in \mathcal{E}_{\mathcal{F}}$ and $t \in \mathbb{R}$ based on the facts that $\zeta_{ij}(0) = 1$ for all $(j, i) \in \mathcal{E}_{\mathcal{F}}$ and $\sigma_{ij} \leq 1$ for all $(j, i) \in \mathcal{E}_{\mathcal{F}}$ and $t \in \mathbb{R}$.

APPENDIX E
PROOF OF SUPPORTING LEMMA (CH 5)

Proof of Lemma 5.1. By Assumption 5.1 and [87, Lemma 4.6], the left eigenvector $p = [p_1, \dots, p_{\mathcal{F}}]^T \in \mathbb{R}^{\mathcal{F}}$ of $\mathcal{L}_{\mathcal{F}}$ associated with the (simple) zero eigenvalue has all positive entries. Let $\xi = [\xi_1, \dots, \xi_{\mathcal{F}}]^T \in \mathbb{R}^{\mathcal{F}} \setminus \{\mathbf{0}_{\mathcal{F}}\}$. Because $p^T \mathcal{L}_{\mathcal{F}} = \mathbf{0}_{\mathcal{F}}$, we have that $p_i d_i = \sum_{j=1}^{\mathcal{F}} p_j a_{ji}$, and hence $\sum_{j=1}^{\mathcal{F}} p_i a_{ij} = \sum_{j=1}^{\mathcal{F}} p_j a_{ji}$ for all $i \in \mathcal{V}_{\mathcal{F}}$, which gives the relation

$$\begin{aligned}
 \sum_{i=1}^{\mathcal{F}} \sum_{j=1}^{\mathcal{F}} p_i a_{ij} \xi_i (\xi_i - \xi_j) &= \sum_{i=1}^{\mathcal{F}} \sum_{j=1}^{\mathcal{F}} p_i a_{ij} \xi_i^2 - \sum_{i=1}^{\mathcal{F}} \sum_{j=1}^{\mathcal{F}} p_i a_{ij} \xi_i \xi_j \\
 &= \sum_{i=1}^{\mathcal{F}} \sum_{j=1}^{\mathcal{F}} p_j a_{ji} \xi_i^2 - \sum_{i=1}^{\mathcal{F}} \sum_{j=1}^{\mathcal{F}} p_i a_{ij} \xi_i \xi_j \\
 &= \sum_{i=1}^{\mathcal{F}} \sum_{j=1}^{\mathcal{F}} p_i a_{ij} \xi_j^2 - \sum_{i=1}^{\mathcal{F}} \sum_{j=1}^{\mathcal{F}} p_i a_{ij} \xi_i \xi_j \\
 &= \sum_{i=1}^{\mathcal{F}} \sum_{j=1}^{\mathcal{F}} p_i a_{ij} \xi_j (\xi_j - \xi_i). \tag{E-1}
 \end{aligned}$$

Let $Q \in \mathbb{R}^{\mathcal{F} \times \mathcal{F}}$ be defined as $Q \triangleq P(\mathcal{L}_{\mathcal{F}} + B) + (\mathcal{L}_{\mathcal{F}} + B)^T P$, where $P \triangleq \text{diag}\{p_1, \dots, p_{\mathcal{F}}\} \in \mathbb{R}^{\mathcal{F} \times \mathcal{F}}$. The relation in (E-1) facilitates the expression of the product $\xi^T Q \xi$ as

$$\begin{aligned}
 \xi^T Q \xi &= \xi^T P \mathcal{L}_{\mathcal{F}} \xi + \xi^T \mathcal{L}_{\mathcal{F}}^T P \xi + \xi^T P B \xi + \xi^T B P \xi \\
 &= 2\xi^T P \mathcal{L}_{\mathcal{F}} \xi + 2\xi^T P B \xi \\
 &= 2 \sum_{i=1}^{\mathcal{F}} \sum_{j=1}^{\mathcal{F}} p_i \xi_i a_{ij} (\xi_i - \xi_j) + 2 \sum_{i=1}^{\mathcal{F}} p_i b_i \xi_i^2 \\
 &= \sum_{i=1}^{\mathcal{F}} \sum_{j=1}^{\mathcal{F}} p_i a_{ij} \xi_i (\xi_i - \xi_j) + \sum_{i=1}^{\mathcal{F}} \sum_{j=1}^{\mathcal{F}} p_i a_{ij} \xi_j (\xi_j - \xi_i) + 2 \sum_{i=1}^{\mathcal{F}} p_i b_i \xi_i^2 \\
 &= \sum_{i=1}^{\mathcal{F}} \sum_{j=1}^{\mathcal{F}} p_i a_{ij} (\xi_j - \xi_i)^2 + 2 \sum_{i=1}^{\mathcal{F}} p_i b_i \xi_i^2.
 \end{aligned}$$

Clearly, $\xi^T Q \xi \geq 0$. Suppose that $\xi^T Q \xi = 0$ for some $\xi \in \mathbb{R}^{\mathcal{F}} \setminus \{\mathbf{0}_{\mathcal{F}}\}$, which requires that $\sum_{i=1}^{\mathcal{F}} \sum_{j=1}^{\mathcal{F}} p_i a_{ij} (\xi_j - \xi_i)^2 = 0$ and $\sum_{i=1}^{\mathcal{F}} p_i b_i \xi_i^2 = 0$. Because $\mathcal{G}_{\mathcal{F}}$ is connected and $\xi \in \mathbb{R}^{\mathcal{F}} \setminus \{\mathbf{0}_{\mathcal{F}}\}$, $\sum_{i=1}^{\mathcal{F}} \sum_{j=1}^{\mathcal{F}} p_i a_{ij} (\xi_j - \xi_i)^2 = 0$ if and only if $\xi = \alpha \mathbf{1}_{\mathcal{F}}$, where

$\alpha \in \mathbb{R} \setminus \{0\}$. However, if at least one follower agent is connected to the leader, then $\sum_{i=1}^{\mathcal{F}} p_i b_i \xi_i^2 > 0$ for all $\xi \in \text{span}\{\mathbf{1}_{\mathcal{F}}\} \setminus \{\mathbf{0}_{\mathcal{F}}\}$, which is a contradiction. Hence, $\xi^T Q \xi > 0$ for all $\xi \in \mathbb{R}^{\mathcal{F}} \setminus \{\mathbf{0}_{\mathcal{F}}\}$, i.e., Q is positive definite. Therefore, because P is positive definite and symmetric and the matrix $P(-\mathcal{L}_{\mathcal{F}} - B) + (-\mathcal{L}_{\mathcal{F}} - B)^T P$ is negative definite by the definition of Q , we have by [88, Theorem 8.2] that $-\mathcal{L}_{\mathcal{F}} - B$ is Hurwitz.

APPENDIX F
PROOF OF SUPPORTING LEMMA (CH 5)

Proof of Lemma 5.2. Because $\sup \{\|\mathcal{P}(M)\| \mid M \in \bar{\mathcal{L}}_B\}$ is bounded, the ball $\Delta(M)$ is non-vanishing for any $M \in \bar{\mathcal{L}}_B$. Additionally, because $\sup \{\|\mathcal{P}(M)\| \mid M \in \bar{\mathcal{L}}_B\}$ is bounded, \mathcal{P} is continuous in the non-vanishing neighborhood $\Delta(M) \cap \bar{\mathcal{L}}_B$ for every $M \in \bar{\mathcal{L}}_B$ by (5–20), which implies that \mathcal{P} is continuous over $\bar{\mathcal{L}}_B$. Hence, because \mathcal{P} is continuous over $\bar{\mathcal{L}}_B$ and $\bar{\mathcal{L}}_B$ is compact, the set $\{\mathcal{P}(M) \mid M \in \bar{\mathcal{L}}_B\}$ is compact, and therefore there exists a matrix $M_0 \in \bar{\mathcal{L}}_B$ such that $\|\mathcal{P}(M)\| \leq \|\mathcal{P}(M_0)\|$ for every $M \in \bar{\mathcal{L}}_B$. Thus, for any finite selection of matrices $\{M_1, \dots, M_w\} \in \bar{\mathcal{L}}_B$ which satisfy $\cup_{n \in \{1, \dots, w\}} \Delta(M_n) \supseteq \bar{\mathcal{L}}_B$, we have that

$$\begin{aligned} \bar{p}^* &\leq \|\mathcal{P}(M_0)\| \\ &\leq \max_{n \in \{1, \dots, w\}} \max_{\Delta M \in \Delta(M_n)} (\|\mathcal{P}(M_n + \Delta M)\|) \\ &= \max_{n \in \{1, \dots, w\}} \max_{\Delta M \in \Delta(M_n)} (\|\mathcal{P}(M_n) + \Delta \mathcal{P}(M_n)\|) \\ &\leq \max_{n \in \{1, \dots, w\}} \frac{1}{1 - \varphi} \|\mathcal{P}(M_n)\| \end{aligned}$$

by the fact that $\mathcal{P} \subset \{\mathcal{P}(M) \mid M \in \bar{\mathcal{L}}_B\}$, the definition of $\Delta(\cdot)$, the upper bound in (5–20), and the triangle inequality. Note that $\|\Delta \mathcal{P}(M_n)\|$ is kept bounded by introducing φ in the definition of Δ to keep the denominator in (5–20) from being arbitrarily close to zero.

REFERENCES

- [1] G. Chen and F. L. Lewis, "Distributed adaptive tracking control for synchronization of unknown networked Lagrangian systems," *IEEE Trans. Syst. Man Cybern.*, vol. 41, no. 3, pp. 805–816, 2011.
- [2] J. Mei and W. Ren, "Distributed coordinated tracking with a dynamic leader for multiple Euler-Lagrange systems," *IEEE Trans. Autom. Control*, vol. 56, no. 6, pp. 1415–1421, 2011.
- [3] E. Nuño, R. Ortega, L. Basañez, and D. Hill, "Synchronization of networks of non-identical Euler-Lagrange systems with uncertain parameters and communication delays," *IEEE Trans. Autom. Control*, vol. 56, no. 4, pp. 935–941, 2011.
- [4] R. Olfati-Saber, J. A. Fax, and R. M. Murray, "Consensus problems in networks of agents with switching topology and time-delays," *IEEE Trans. Autom. Control*, vol. 49, no. 9, pp. 1520–1533, 2004.
- [5] E. Lavretsky, "F/A-18 autonomous formation flight control system design," in *AIAA Conf. Guid., Navig., Control*, 2002.
- [6] J. Ploeg, A. F. Serrarens, and G. J. Heijenk, "Connect & drive: design and evaluation of cooperative adaptive cruise control for congestion reduction," *J. Mod. Transp.*, vol. 19, no. 3, pp. 207–213, 2011.
- [7] W. Ren, "Multi-vehicle consensus with a time-varying reference state," *Syst. Control Lett.*, vol. 56, pp. 474–483, 2007.
- [8] A. Rodriguez-Angeles and H. Nijmeijer, "Mutual synchronization of robots via estimated state feedback: A cooperative approach," *IEEE Trans. Control Syst. Technol.*, vol. 12, no. 4, pp. 542–554, 2004.
- [9] S. Khoo and L. Xie, "Robust finite-time consensus tracking algorithm for multirobot systems," *IEEE/ASME Trans. Mechatron.*, vol. 14, no. 2, pp. 219–228, 2009.
- [10] S.-J. Chung and J.-J. E. Slotine, "Cooperative robot control and concurrent synchronization of Lagrangian systems," *IEEE Trans. on Robot.*, vol. 25, no. 3, pp. 686–700, 2009.
- [11] Y. Hong, J. Hu, and L. Gao, "Tracking control for multi-agent consensus with an active leader and variable topology," *Automatica*, vol. 42, no. 7, pp. 1177–1182, 2006.
- [12] Y. Hong, G. R. Chen, and L. Bushnell, "Distributed observers design for leader following control of multi-agent networks," *Automatica*, vol. 44, no. 3, pp. 846–850, 2008.

- [13] D. V. Dimarogonas and K. H. Johansson, "Stability analysis for multi-agent systems using the incidence matrix: Quantized communication and formation control," *Automatica*, vol. 46, no. 4, pp. 695–700, 2010.
- [14] A. Abdessameud, I. G. Polushin, and A. Tayebi, "Synchronization of multiple Euler-Lagrange systems with communication delays," in *Proc. Am. Control Conf.*, June 2012, pp. 3748–3753.
- [15] Z. Li, W. Ren, X. Liu, and L. Xie, "Distributed consensus of linear multi-agent systems with adaptive dynamic protocols," *Automatica*, vol. 49, no. 7, pp. 1986–1995, 2013.
- [16] H. Wang, "Passivity based synchronization for networked robotic systems with uncertain kinematics and dynamics," *Automatica*, vol. 49, no. 3, pp. 755–761, 2013.
- [17] J. Klotz, Z. Kan, J. M. Shea, E. L. Pasiliao, and W. E. Dixon, "Asymptotic synchronization of leader-follower networks of uncertain Euler-Lagrange systems," in *Proc. IEEE Conf. Decis. Control*, Florence, IT, Dec. 2013, pp. 6536–6541.
- [18] G. Notarstefano, M. Egerstedt, and M. Haque, "Containment in leader-follower networks with switching communication topologies," *Automatica*, vol. 47, no. 5, pp. 1035–1040, 2011.
- [19] D. V. Dimarogonas, P. Tsiotras, and K. J. Kyriakopoulos, "Leader-follower cooperative attitude control of multiple rigid bodies," *Syst. Control Lett.*, vol. 58, pp. 429–435, 2009.
- [20] J. Mei, W. Ren, J. Chen, and G. Ma, "Distributed adaptive coordination for multiple Lagrangian systems under a directed graph without using neighbors' velocity information," *Automatica*, vol. 49, no. 6, pp. 1723–1731, 2013.
- [21] M. Ji, G. Ferrari-Trecate, M. Egerstedt, and A. Buffa, "Containment control in mobile networks," *IEEE Trans. Autom. Control*, vol. 53, no. 8, pp. 1972–1975, 2008.
- [22] Y. Cao, D. Stuart, W. Ren, and Z. Meng, "Distributed containment control for multiple autonomous vehicles with double-integrator dynamics: Algorithms and experiments," *IEEE Trans. Control Syst. Technol.*, vol. 19, no. 4, pp. 929–938, 2011.
- [23] J. Li, W. Ren, and S. Xu, "Distributed containment control with multiple dynamic leaders for double-integrator dynamics using only position measurements," *IEEE Trans. Autom. Control*, vol. 57, no. 6, pp. 1553–1559, 2012.
- [24] Y. Cao, W. Ren, and M. Egerstedt, "Distributed containment control with multiple stationary or dynamic leaders in fixed and switching directed networks," *Automatica*, vol. 48, pp. 1586–1597, 2012.
- [25] Z. Kan, J. Klotz, E. L. Pasiliao, and W. E. Dixon, "Containment control for a directed social network with state-dependent connectivity," in *Proc. Am. Control Conf.*, Washington DC, June 2013, pp. 1953–1958.

- [26] Z. Meng, W. Ren, and Z. You, "Distributed finite-time attitude containment control for multiple rigid bodies," *Automatica*, vol. 46, no. 12, pp. 2092–2099, 2010.
- [27] J. Mei, W. Ren, and G. Ma, "Distributed containment control for Lagrangian networks with parametric uncertainties under a directed graph," *Automatica*, vol. 48, no. 4, pp. 653–659, 2012.
- [28] Z. Meng, D. V. Dimarogonas, and K. H. Johansson, "Zero-error coordinated tracking of multiple Lagrange systems using continuous control," in *Proc. IEEE Conf. Decis. Control*, 2013, pp. 6712–6717.
- [29] A. Abdessameud, I. G. Polushin, and A. Tayebi, "Synchronization of Lagrangian systems with irregular communication delays," *IEEE Trans. Autom. Control*, vol. 59, no. 1, pp. 187–193, 2014.
- [30] A. Abdessameud and A. Tayebi, "Formation control of VTOL unmanned aerial vehicles with communication delays," *Automatica*, vol. 47, pp. 2383–2394, 2011.
- [31] N. Chopra, "Output synchronization on strongly connected graphs," *IEEE Trans. Autom. Control*, vol. 57, no. 11, pp. 2896–2901, 2012.
- [32] H. Li and Y. Shi, "Distributed receding horizon control of large-scale nonlinear systems: Handling communication delays and disturbances," *Automatica*, vol. 50, pp. 1264–1271, 2014.
- [33] U. Münz, A. Papachristodoulou, and F. Allgöwer, "Delay robustness in non-identical multi-agent systems," *IEEE Trans. Autom. Control*, vol. 57, no. 6, pp. 1597–1603, 2012.
- [34] Y.-P. Tian and C.-L. Liu, "Consensus of multi-agent systems with diverse input and communication delays," *IEEE Trans. Autom. Control*, vol. 53, no. 9, pp. 2122–2128, 2008.
- [35] Y.-P. Tian and Y. Zhang, "High-order consensus of heterogeneous multi-agent systems with unknown communication delays," *Automatica*, vol. 48, pp. 1205–1212, 2012.
- [36] X. Wang, A. Saberi, A. A. Stoorvogel, H. F. Grip, and T. Yang, "Consensus in the network with uniform constant communication delay," *Automatica*, vol. 49, pp. 2461–2467, 2013.
- [37] H. Wang, "Consensus of networked mechanical systems with communication delays: A unified framework," *IEEE Trans. Autom. Control*, vol. 59, no. 6, pp. 1571–1576, 2014.
- [38] B. Zhou and Z. Lin, "Consensus of high-order multi-agent systems with large input and communication delays," *Automatica*, vol. 50, pp. 452–464, 2014.

- [39] Y.-C. Liu and N. Chopra, "Synchronization of networked mechanical systems with communication delays and human input," *ASME J. Dyn. Syst., Meas., and Control*, vol. 135, no. 4, 2013.
- [40] A. A. Peters, R. H. Middleton, and O. Mason, "Leader tracking in homogeneous vehicle platoons with broadcast delays," *Automatica*, vol. 50, pp. 64–74, 2014.
- [41] W. Zhu, "Consensus of multiagent systems with switching jointly reachable interconnection and time delays," *IEEE Trans. Syst., Man, Cybern. A, Syst., Hum.*, vol. 42, no. 2, pp. 348–358, 2012.
- [42] S. Liu, L. Xie, and F. L. Lewis, "Synchronization of multi-agent systems with delayed control input information from neighbors," *Automatica*, vol. 47, pp. 2152–2164, 2011.
- [43] K. Peng and Y. Yang, "Leader-following consensus problem with a varying-velocity leader and time-varying delays," *Physica A*, vol. 388, pp. 193–208, 2009.
- [44] Q. Jia, W. K. S. Tang, and W. A. Halang, "Leader following of nonlinear agents with switching connective network and coupling delay," *IEEE Trans. Circuits Syst. I, Reg. Pap.*, vol. 58, no. 10, pp. 2508–2519, 2011.
- [45] X. Liu and J. S. Baras, "Using trust in distributed consensus with adversaries in sensor and other networks," in *Proc. IEEE 17th Int. Conf. Inf. Fusion*, July 2014, pp. 1–7.
- [46] D. G. Mikulski, F. L. Lewis, E. Y. Gu, and G. R. Hudas, "Trust method for multi-agent consensus," in *Proc. SPIE*, vol. 8387, May 2012.
- [47] P. Ballal, F. L. Lewis, and G. R. Hudas, *Recent Advances in Nonlinear Dynamics and Synchronization*. Springer, 2009, ch. Trust-based collaborative control for teams in communication networks, pp. 347–363.
- [48] H. LeBlanc, H. Zhang, S. Sundaram, and X. Koutsoukos, "Consensus of multi-agent networks in the presence of adversaries using only local information," in *Proc. 1st Int. Conf. High Confid. Netw. Syst.*, New York, NY, USA, 2012, pp. 1–10.
- [49] T. Haus, I. Palunko, D. Tolić, S. Bogdan, and F. L. Lewis, "Decentralized trust-based self-organizing cooperative control," in *Proc. IEEE Eur. Control Conf.*, Strasbourg, France, 2014, pp. 1205–1210.
- [50] N. Sharma, S. Bhasin, Q. Wang, and W. E. Dixon, "Predictor-based control for an uncertain Euler-Lagrange system with input delay," in *Proc. Am. Control Conf.*, 2010, pp. 1422–1427.
- [51] P. Patre, W. Mackunis, K. Dupree, and W. E. Dixon, "Modular adaptive control of uncertain Euler-Lagrange systems with additive disturbances," *IEEE Trans. Autom. Control*, vol. 56, no. 1, pp. 155–160, 2011.

- [52] C. Makkar, G. Hu, W. G. Sawyer, and W. E. Dixon, "Lyapunov-based tracking control in the presence of uncertain nonlinear parameterizable friction," *IEEE Trans. Autom. Control*, vol. 52, pp. 1988–1994, 2007.
- [53] V. Stepanyan and A. Kurdila, "Asymptotic tracking of uncertain systems with continuous control using adaptive bounding," *IEEE Trans. Neur. Netw.*, vol. 20, no. 8, pp. 1320–1329, 2009.
- [54] B. Bidikli, E. Tatlicioglu, A. Bayrak, and E. Zergeroglu, "A new Robust 'Integral of Sign of Error' feedback controller with adaptive compensation gain," in *Proc. IEEE Conf. Decis. Control*, 2013, pp. 3782–3787.
- [55] P. Barooah and J. Hespanha, "Graph effective resistance and distributed control: Spectral properties and applications," in *Proc. IEEE Conf. Decis. Control*, 2006, pp. 3479–3485.
- [56] P. M. Patre, W. Mackunis, C. Makkar, and W. E. Dixon, "Asymptotic tracking for systems with structured and unstructured uncertainties," *IEEE Trans. Control Syst. Technol.*, vol. 16, pp. 373–379, 2008.
- [57] B. Xian, D. M. Dawson, M. S. de Queiroz, and J. Chen, "A continuous asymptotic tracking control strategy for uncertain nonlinear systems," *IEEE Trans. Autom. Control*, vol. 49, no. 7, pp. 1206–1211, 2004.
- [58] R. Kamalapurkar, J. A. Rosenfeld, J. Klotz, R. J. Downey, and W. E. Dixon. (2014) Supporting lemmas for RISE-based control methods. arXiv:1306.3432v3.
- [59] D. Shevitz and B. Paden, "Lyapunov stability theory of nonsmooth systems," *IEEE Trans. Autom. Control*, vol. 39 no. 9, pp. 1910–1914, 1994.
- [60] B. E. Paden and S. S. Sastry, "A calculus for computing Filippov's differential inclusion with application to the variable structure control of robot manipulators," *IEEE Trans. Circuits Syst.*, vol. 34, no. 1, pp. 73–82, January 1987.
- [61] N. Fischer, R. Kamalapurkar, and W. E. Dixon, "LaSalle-Yoshizawa corollaries for nonsmooth systems," *IEEE Trans. Autom. Control*, vol. 58, no. 9, pp. 2333–2338, 2013.
- [62] F. H. Clarke, *Optimization and nonsmooth analysis*. SIAM, 1990.
- [63] R. Skjetne, Øyvind Smogeli, and T. I. Fossen, "Modeling, identification, and adaptive maneuvering of Cybership II: A complete design with experiments," in *Proc. IFAC Conf. Control Appl. Marine Syst.*, 2004.
- [64] E. Kyrkjebø and K. Y. Pettersen, "Output synchronization control of Euler-Lagrange systems with nonlinear damping terms," in *Jt. 44th Proc. IEEE Conf. Decis. Control and Eur. Control Conf.*, 2005, pp. 4951–4957.

- [65] N. Chopra, D. M. Stipanović, and M. W. Spong, “On synchronization and collision avoidance for mechanical systems,” in *Proc. Am. Control Conf.*, 2008, pp. 3713–3718.
- [66] T. Presterro, “Verification of a six-degree of freedom simulation model for the REMUS autonomous underwater vehicle,” Master’s thesis, University of California at Davis, 1994.
- [67] T. I. Fossen, *Handbook of Marine Craft Hydrodynamics and Motion Control*. Wiley, 2011.
- [68] A. Hanai, H. T. Choi, S. K. Choi, and J. Yuh, “Experimental study on fine motion control of underwater robots,” *Adv. Robot.*, vol. 18, no. 10, pp. 963–978, 2004.
- [69] N. Fischer, S. Bhasin, and W. E. Dixon, “Nonlinear control of an autonomous underwater vehicle: A RISE-based approach,” in *Proc. Am. Control Conf.*, San Francisco, CA, 2011, pp. 3972–3977.
- [70] N. Fischer, A. Dani, N. Sharma, and W. E. Dixon, “Saturated control of an uncertain nonlinear system with input delay,” *Automatica*, vol. 49, no. 6, pp. 1741–1747, 2013.
- [71] N. Fischer, R. Kamalapurkar, N. Sharma, and W. E. Dixon, “RISE-based control of an uncertain nonlinear system with time-varying state delays,” in *Proc. IEEE Conf. Decis. Control*, Maui, HI, Dec. 2012, pp. 3502–3507.
- [72] R. L. Cruz, “A calculus for network delay, part I: Network elements in isolation,” *IEEE Trans. Inf. Theory*, vol. 37, no. 1, pp. 114–131, 1991.
- [73] —, “A calculus for network delay, part II: Network analysis,” *IEEE Trans. Inf. Theory*, vol. 37, no. 1, pp. 132–141, 1991.
- [74] —, “Quality of service guarantees in virtual circuit switched networks,” *IEEE J. Sel. Areas Commun.*, vol. 13, no. 6, pp. 1048–1056, 1995.
- [75] D. Stiliadis and A. Varma, “Latency-rate servers: A general model for analysis of traffic scheduling algorithms,” *IEEE/ACM Trans. Netw.*, vol. 6, no. 5, pp. 611–624, 1998.
- [76] H. K. Khalil, *Nonlinear Systems*, 3rd ed. Upper Saddle River, NJ, USA: Prentice Hall, 2002.
- [77] J. R. Klotz, Z. Kan, J. M. Shea, E. L. Pasilliao, and W. E. Dixon, “Asymptotic synchronization of a leader-follower network of uncertain Euler-Lagrange systems,” *IEEE Trans. Control Netw. Syst.*, to appear.
- [78] B. Khosravifar, M. Gomrokchi, and J. Bentahar, “Maintenance-based trust for multi-agent systems,” in *Proc. 8th Int. Jt. Conf. Auton. Agents Multiagent Syst.*, vol. 2, Budapest, Hungary, 2009, pp. 1017–1024.

- [79] K. Govindan and P. Mohapatra, "Trust computations and trust dynamics in mobile adhoc networks: A survey," *IEEE Commun. Surv. Tutor.*, vol. 14, no. 2, pp. 279–298, 2012.
- [80] D. Liberzon, *Switching in Systems and Control*. Birkhauser, 2003.
- [81] J. J. Montemayor and B. F. Womack, "Comments on "On the Lyapunov Matrix Equation"," *IEEE Trans. Autom. Control*, vol. 20, no. 6, pp. 814–815, 1975.
- [82] B. N. Datta, *Numerical Methods for Linear Control Systems: Design and Analysis*. London, UK: Elsevier Academic Press, 2004.
- [83] M. Konstantinov, D.-W. Gu, V. Mehrmann, and P. Petkov, *Perturbation Theory for Matrix Equations*, ser. Studies in Computational Mathematics, C. K. Chui, P. Mond, and L. Wuytack, Eds. Elsevier, 2003, vol. 9.
- [84] S.-D. Wang, T.-S. Kuo, and C.-F. Hsu, "Trace bounds on the solution of the algebraic matrix Riccati and Lyapunov equation," *IEEE Trans. Autom. Control*, vol. 31, no. 7, pp. 654–656, 1986.
- [85] A. Berman and R. J. Plemmons, *Nonnegative Matrices in the Mathematical Sciences*, ser. Computer Science and Applied Mathematics. Academic Press, 1979.
- [86] S. Boyd and L. Vandenberghe, *Convex Optimization*. New York, NY, USA: Cambridge University Press, 2004.
- [87] E. Semsar-Kazerooni and K. Khorasani, *Team Cooperation in a Network of Multi-Vehicle Unmanned Systems: Synthesis of Consensus Algorithms*. Springer New York, 2013.
- [88] J. P. Hespanha, *Linear Systems Theory*. Princeton University Press, 2009.

BIOGRAPHICAL SKETCH

Justin Richard Klotz was born in West Palm Beach, Florida. He received the Bachelor of Science degree in mechanical engineering from the University of Florida in 2011. Justin subsequently joined the Nonlinear Controls and Robotics (NCR) research group at the University of Florida in August of 2011 in the pursuit of a Ph.D. under the advisement of Dr. Warren E. Dixon. Funded by the University of Florida's Graduate Student Fellowship, he began research into novel control techniques for networked dynamical systems. Justin was a visiting researcher for the Air Force Research Laboratory at Eglin Air Force Base during the summers of 2012 and 2013, where he collaborated to develop control algorithms for emerging autonomous vehicle applications. He earned a Master of Science degree in mechanical engineering with a focus on dynamics, systems, and control in May of 2013, and was later awarded the Science, Mathematics and Research for Transformation (SMART) Scholarship, sponsored by the Department of Defense, in August of 2013. Justin continued his research with the NCR research group until completing his Ph.D. in mechanical engineering in May of 2015. Justin's research interests include Lyapunov-based nonlinear control, decentralized control, delay-affected control, and reinforcement learning-based control.